

Life Cycle Cost Analysis of a Floating Wind Farm Located in the Norwegian Sea

Candidates:

Fredrik Andersen Bjørni

Sverre Lien

Torjus Aasrum Midtgarden

Supervisor:

Zhiyu Jiang, Associate Professor at the University of Agder

University of Agder, Spring 2023

Faculty of Technology and Science

School of Business and Law

Mandatory Self Declaration

Den enkelte student er selv ansvarlig for å sette seg inn i hva som er lovlige hjelpemidler, retningslinjer for bruk av disse og regler om kildebruk. Erklæringen skal bevisstgjøre studentene på deres ansvar og hvilke konsekvenser fusk kan medføre. Manglende erklæring fritar ikke studentene fra sitt ansvar.

1.	Jeg/vi erklærer herved at min/vår besvarelse er mitt/vårt eget arbeid, og at jeg/vi ikke har brukt andre kilder eller har mottatt annen hjelp enn det som er nevnt i besvarelsen.	<input checked="" type="checkbox"/>
2.	Jeg/vi erklærer videre at denne besvarelsen: ikke har vært brukt til annen eksamen ved annen avdeling/universitet/høgskole innenlands eller utenlands. ikke refererer til andres arbeid uten at det er oppgitt. ikke refererer til eget tidligere arbeid uten at det er oppgitt. har alle referansene oppgitt i litteraturlisten. ikke er en kopi, duplikat eller avskrift av andres arbeid eller besvarelse.	<input checked="" type="checkbox"/>
3.	Jeg/vi er kjent med at brudd på ovennevnte er å betrakte som fusk og kan medføre annullering av eksamen og utestengelse fra universiteter og høgskoler i Norge, jf. Universitets- og høgskoleloven §§4-7 og 4-8 og Forskrift om eksamen §§ 31.	<input checked="" type="checkbox"/>
4.	Jeg/vi er kjent med at alle innleverte oppgaver kan bli plagiattrollert.	<input checked="" type="checkbox"/>
5.	Jeg/vi er kjent med at Universitetet i Agder vil behandle alle saker hvor det forligger mistanke om fusk etter høgskolens retningslinjer for behandling av saker om fusk.	<input checked="" type="checkbox"/>
6.	Jeg/vi har satt oss inn i regler og retningslinjer i bruk av kilder og referanser på biblioteket sine nettsider.	<input checked="" type="checkbox"/>

Publishing Agreement

Fullmakt til elektronisk publisering av oppgaven

Forfatter(ne) har opphavsrett til oppgaven. Det betyr blant annet enerett til å gjøre verket tilgjengelig for allmennheten (Åndsverkloven. §2).

Alle oppgaver som fyller kriteriene vil bli registrert og publisert i Brage Aura og på UiA sine nettsider med forfatter(ne)s godkjenning.

Oppgaver som er unntatt offentlighet eller tausehetsbelagt/konfidensiell vil ikke bli publisert.

Jeg/vi gir herved Universitetet i Agder en vederlagsfri rett til å gjøre oppgaven tilgjengelig for elektronisk publisering:

JA NEI

Er oppgaven båndlagt (konfidensiell)?
(Båndleggingsavtale må fylles ut)

JA NEI

- Hvis ja:

Kan oppgaven publiseres når båndleggingsperioden er over?

JA NEI

Er oppgaven unntatt offentlighet?

JA NEI

(inneholder taushetsbelagt informasjon. Jfr. Offl. §13/Fvl. §13)


Preface

This master's thesis is carried out as a concluding part of the Master's program in Industrial Economics and Technology Management at the University of Agder, Faculty of Engineering and Science. The research project composes of 30 ECTS and was completed in the spring of 2023.


“Life Cycle Cost Analysis of a Floating Wind Farm Located in the Norwegian Sea” is chosen as the title, contemplating the interesting combination of floating wind turbines and their economic aspects. The main purpose is to investigate how the various costs contribute to the levelized cost of energy. Considering the highly relevant subject of floating wind and renewable energy, it is a wish that the content of this report is appealing to the reader and that the research can be of use in the further development of the offshore wind industry.

We want to express our sincere gratitude to our supervisor, Dr. Zhiyu Jiang, Associate Professor at the University of Agder. His exceptional insight, knowledge, and dedication have been instrumental in shaping our research and enabling us to achieve our goals. We would also like to thank our friends and family for supporting us throughout the project.

Finally, we would like to thank our teachers and classmates for their contribution towards making our five years at the University of Agder a great time.


Fredrik Andersen Bjørni


Sverre Lien


Torjus Aasrum Midtgarden

Grimstad, 16.05.2023

Summary

This thesis aims to investigate the levelized cost of energy of an offshore floating wind farm, as well as evaluate its financial feasibility. Thus, the research question is as follows: *How to estimate the life cycle costs of a floating wind farm off the coast of Norway?*

The investigated wind farm is located off the coast of Norway, more specifically in the Troll field area west of Bergen. This area has a water depth of 325 m and a distance to shore of 65 km. The wind farm is set to consist of 50 wind turbines and has a lifespan of 25 years. The OC4 Deepwind semisubmersible floater developed by the National Renewable Energy Laboratory, complemented with a 15 MW turbine, is used as the research model. To find the capital expenditures of the planned wind farm, the Offshore Renewables Balance-of-system and Installation Tool is used, while the operational expenditures are calculated based on the theoretical energy output.

The total levelized cost of energy of the wind farm is calculated to be 100.69 \$/MWh. Capital expenditure is the most prominent cost and constitutes 63.1 % of the total cost, thus, operational expenditures constitute the remaining 36.9 %. Further, sensitivity analyses show that the lifespan, capacity factor, and project discount rate are the factors with the most potential to influence the levelized cost of energy. The financial calculations show that the wind farm is not economically feasible as it has a computed net present value of negative \$ 561 900 000. Finally, novel offshore wind energy solutions involving the utilization of shared substructures and mooring lines have been studied, and the findings suggest the possibility of a diminished levelized cost of energy.

Sammendrag

Denne masteroppgaven har som mål å undersøke energikostnaden over levetiden for en flytende havvindpark, samt evaluere dens økonomiske gjennomførbarhet. Forskningsspørsmålet er derfor som følger: *Hvordan estimere livsløpskostnadene til en flytende vindpark utenfor kysten av Norge?*

Den undersøkte vindparken er lokalisert utenfor kysten av Norge, nærmere bestemt i Troll-feltet vest for Bergen. Dette området har en havdybde på 325 meter og en avstand til land på 65 km. Vindparken er planlagt å bestå av 50 vindturbiner og har en levetid på 25 år. OC4 Deepwind-flyter, utviklet av National Renewable Energy Laboratory, supplert med en 15 MW turbin, blir brukt som forskningsmodell. For å finne investeringskostnadene for den planlagte vindparken blir Offshore Renewables Balance-of-system and Installation Tool benyttet, mens driftskostnadene beregnes basert på den teoretiske energiproduksjonen.

Den totale energikostnaden for vindparkens levetid er beregnet til 100.69 \$/MWh. Investeringskostnadene utgjør den største delen med 63.1 % av de totale kostnadene. Driftskostnader utgjør dermed de gjenværende 36.9 %. Videre viser sensitivitetsanalyser at levetid, kapasitetsfaktor og avkastningskrav er faktorene som har størst potensial til å påvirke energikostnaden. De økonomiske beregningene viser at vindparken ikke er økonomisk levedyktig, da den beregnede netto nåverdien er negativ, med \$ 561 900 000. Til slutt har nyskapende offshore-løsninger som involverer bruk av delte substrukturer og fortøyningsystemer blitt studert, og funnene impliserer muligheter for å redusere energikostnadene over levetiden for vindparken.

Table of Contents

Mandatory Self Declaration	i
Publishing Agreement	ii
Preface	iii
Summary	iv
Sammendrag	v
Table of Contents.....	vi
List of Figures	xi
List of Tables	xiii
List of Abbreviations	xiv
List of Symbols	xv
1. Introduction	1
2. Significance of Offshore Wind	4
3. Theory	7
3.1 Environmental Conditions of an Offshore Site	7
3.1.1 Characteristics of Vertical Wind Speed	7
3.1.2 Wind Speed Distribution	9
3.1.3 Wind Turbulence	10
3.2 Power Performance of an Offshore Wind Farm	11
3.2.1 Wind Farm Layout	11
3.2.2 Wind Turbine Power Curve	12
3.2.3 Capacity Factor	13
3.3 Infrastructure of an Offshore Wind Farm	14
3.3.1 Wind Turbine System	14
3.3.2 Semisubmersible Floating System	15
3.3.3 Mooring Systems for Floating Substructures	16
3.3.4 Electrical Infrastructure for Floating Offshore Wind	17
3.3.5 Inter-Array Power System	18
3.3.6 Offshore Substation	18
3.3.7 Export System	19
3.4 Innovative Offshore Wind Solutions	19
3.4.1 Dual Turbine Platform	19

3.4.2 Shared Mooring for Floating Wind Farms	20
3.5 Life Cycle of an Offshore Wind Farm.....	21
3.5.1 Preliminary Phase.....	22
3.5.2 Engineering & Production Phase	22
3.5.3 Installation of Components of Offshore Floating Wind Farms.....	23
3.5.4 Installation and Assembly of the Complete Floating Structure and Wind Turbine.	23
3.5.5 Mooring System Installation and Hook-Up	24
3.5.6 Installation of Offshore Substations	25
3.5.7 Inter-Array and Export Cable Installation.....	25
3.5.8 Operation and Maintenance.....	27
3.5.9 Decommissioning.....	27
3.6 Financing and Capital Structure	28
3.6.1 Cost of Equity.....	28
3.6.2 Risk-Free Rate.....	28
3.6.3 Market Risk Premium	29
3.6.4 Beta Coefficient.....	29
3.6.5 Tax Shield.....	30
3.6.6 Cost of Debt	30
3.6.7 Weighted Average Cost of Capital	31
3.7 Cost Analysis of Wind Farms.....	31
3.7.1 Life Cycle Cost Analysis.....	31
3.7.2 Cost Breakdown of an Offshore Wind Farm.....	33
3.7.3 Levelized Cost of Energy	33
3.8 Discounted Cash Flows	34
3.8.1 Net Present Value Model.....	34
3.8.2 Internal Rate of Return.....	35
3.9 Existing Literature.....	35
4. Research Question.....	37
5. Case & Materials	38
5.1 System Description	38
5.1.1 System Description of the Semisubmersible Substructure	38
5.1.2 System Description of the Mooring Properties	39
5.1.3 System Description of the Floating Wind Turbines	40

5.2 Description of Site Conditions	41
5.2.1 Geographical Description.....	41
5.2.2 Metocean Conditions.....	42
6. Methodology	44
6.1 Software	45
6.1.1 Microsoft Excel	45
6.1.2 Python.....	45
6.2 ORBIT	45
6.2.1 Primary Parameters	45
6.2.2 Parameters of a Floating System	46
6.2.3 Electric Components	47
6.2.4 Vessels for Installation.....	49
6.2.5 Scour Protection Design.....	50
6.2.6 Indirect Costs.....	51
6.2.7 Transportation, Installation, and Port Specifications.....	51
6.2.8 Cost Categories	54
6.3 Calculation of LCOE.....	55
6.3.1 Calculation of CapEx	55
6.3.2 Calculation of OpEx.....	56
6.2.3 Calculation of FCR.....	56
6.2.4 Annual Energy Production	57
6.4 Financial Modeling	58
6.4.1 Predetermination of Financial Parameters	58
6.4.2 Calculation of Financial Metrics	59
6.5 Calculation of Innovative Solutions	60
6.5.1 Calculation of Adjustment Factor for Shared Substructure	60
6.5.2 Calculation of Reduction Factor for Shared Mooring.....	62
7. Results	63
7.1 Reference Wind Farm.....	63
7.1.1 Definition of Wind Farm Layout.....	63
7.1.2 Initial Calculation for the LCOE	63
7.1.3 Trollvind Total Cost Description	64
7.1.4 Trollvind Detailed Component Cost Description.....	65

7.2 Sensitivity Analyses	68
7.2.1 Project Lifespan.....	68
7.2.2 Effect of the Wind Farm Scale	69
7.2.3 Turbine Power Rating.....	71
7.2.4 Project Discount Rate.....	72
7.2.5 Operational Expenditure	72
7.3 Effect of Metocean Conditions.....	73
7.3.1 Capacity Factor	74
7.3.2 Site Conditions	74
7.3.3 Key Cost Drivers of the LCOE	75
7.4 Financial Modeling	76
7.5 Financial Sensitivity Analyses	78
7.5.1 Project Discount Rate.....	78
7.5.2 Debt Repayment Time.....	79
7.5.3 Electricity Spot Price.....	79
7.6 Innovative Solutions.....	80
7.6.1 Shared Substructure.....	80
7.6.2 Shared Mooring Lines	81
8. Discussion	82
8.1 Baseline Trollvind	82
8.2 Sensitivity Analyses	83
8.2.1 Project Life Span.....	83
8.2.2 Scale Effect.....	83
8.2.3 Turbine Power Rating.....	84
8.2.4 Project Discount Rate.....	84
8.2.5 Operational Expenditure	84
8.3 Metocean Sensitivity Analysis	85
8.3.1 Capacity Factor	85
8.3.2 Site Conditions	85
8.3.3 Key Cost Drivers of the LCOE	85
8.4 Financial Evaluation.....	86
8.5 Financial Sensitivity Analyses	87
8.5.1 Project Discount Rate.....	87

8.5.2 Debt Repayment Time.....	87
8.5.3 Spot Price	87
8.6 Innovative Solutions.....	88
8.7 Limitations	88
9. Conclusion.....	90
10. Suggestion for Further Work.....	91
11. References	92
12. Appendices	100

List of Figures

Figure 1.1	Offshore Wind Installation in Europe, derived from Williams et al. (2022).....	1
Figure 1.2	Fixed and Floating Offshore Structures	2
Figure 2.1	Levelized cost of Energy for Different Energy Sources	5
Figure 2.2	Level of Conflict in the Norwegian Sea for Offshore Wind (Multiconsult, 2023) ..	6
Figure 3.1	Vertical Wind Speed Gradient.....	7
Figure 3.2	Array Schematic of a Wind Farm, derived from Manwell et al. (2009)	12
Figure 3.3	General Power Curve of a Horizontal-axis Wind Turbine.....	13
Figure 3.4	Components of a Floating Wind Turbine.....	14
Figure 3.5	Electrical Components Inside the Nacelle	15
Figure 3.6	Different Semisubmersible Floating Platforms.....	16
Figure 3.7	Different Mooring Line Solutions.....	17
Figure 3.8	Electrical Grid Connection for Offshore Wind	17
Figure 3.9	Technical Layout of an Offshore Substation.....	18
Figure 3.10	Front and Side View of the TwinWind Concept	20
Figure 3.11	Top View of Shared Mooring Systems, derived from Liang et al. (2023)	21
Figure 3.12	Side View of a Shared Mooring System, derived from Liang et al. (2021).....	21
Figure 3.13	Overview of the Life Cycle of an Offshore Wind Farm	22
Figure 3.14	Installation of the Turbine System with Onshore Assembly and Tow-out.....	24
Figure 3.15	Installation of an Offshore Substation on a Jacket Foundation.....	25
Figure 3.16	Power Cable Concepts for Different Offshore Wind Farms	26
Figure 3.17	Burial of a power cable with the use of a plough and a cable-laying vessel	26
Figure 3.18	The Iceberg Analogy of an Offshore Wind Farm.....	32
Figure 3.19	Optimal System Reliability	32
Figure 3.20	Cost Breakdown of an Offshore Wind Farm, derived from Ren et al. (2021).....	33
Figure 5.1	Top and Side View of the Semisubmersible Floater	39
Figure 5.2	Top View of the Mooring Line Structure.....	39
Figure 5.3	Side View of the Floating Wind Turbine System.....	40
Figure 5.4	Geographical Location of Trollvind.....	41
Figure 5.5	Trollvind Conceptual Sketch.....	42
Figure 5.6	Monthly Significant Wave Height at Trollvind, 2013-2022	42
Figure 5.7	Weibull Distribution and Mean Wind Data.....	43
Figure 5.8	Trollvind Wind Rose	43
Figure 6.1	Flowchart of the Work Progress.....	44
Figure 6.2	Overview of the Modeling Performed with ORBIT	54
Figure 6.3	Cost Categories Used for Evaluating Wind Farms	54
Figure 6.4	15 MW Wind Turbine Power Curve, derived from (Gaertner, et al., 2020)	57
Figure 6.5	Power Output Curve and Weibull Distribution of the Wind Speed	58
Figure 7.1	Wind Farm Layout	63
Figure 7.2	Distribution of Costs and Total LCOE for Trollvind	65
Figure 7.3	Duration for Installation Vessels	66
Figure 7.4	Duration for Fabricating and Installing Substructures and Turbines	67

Figure 7.5 Project Lifespan Impact on LCOE.....	68
Figure 7.6 Cost Breakdown for Different Lifespans	69
Figure 7.7 Scale Effect Impact on the LCOE.....	70
Figure 7.8 Cost Breakdown for Different Scale Effects.....	70
Figure 7.9 LCOE for Different Turbine Power Capacity	71
Figure 7.10 Cost Breakdown for Different Turbine Power Ratings at Trollvind.....	71
Figure 7.11 LCOE with Variations in the Project Discount Rate at Trollvind	72
Figure 7.12 LCOE for Different Variations in OpEx Cost for Trollvind	73
Figure 7.13 Cost breakdown for a varying OpEx for Trollvind.....	73
Figure 7.14 Capacity Factor Impact on LCOE.....	74
Figure 7.15 Water Depth Impact on the LCOE	75
Figure 7.16 Distance to Shore Impact on the LCOE.....	75
Figure 7.17 Key Cost Drivers of the LCOE	76
Figure 7.18 Project Discount Rate Impact on Financial Metrics	78
Figure 7.19 Dept Repayment Time Impact on Financial Metrics	79
Figure 7.20 Spot Price Impact on Financial Metrics.....	80

List of Tables

Table 2.1	CO ₂ Equivalents per kWh of Produced Energy for Different Energy Sources.....	4
Table 3.1	Approximate Values for Surface Roughness Length	8
Table 3.2	Wind Turbine Power Curve Applications	12
Table 5.1	Substructure, Based on a Scaling Method of the OC4 Semi-Substructure.....	38
Table 5.2	Mooring for Water Depth 200 m.....	39
Table 5.3	Description of Turbines.....	40
Table 6.1	Primary User-Specified Parameters Utilized	46
Table 6.2	Mooring Line and Semi-submersible Floater Costs	47
Table 6.3	Offshore Substation, Array and Export Cable Costs	49
Table 6.4	Vessel Types Used in the Installation Stage.....	50
Table 6.5	Port and Staging Unit Costs.....	50
Table 6.6	Indirect Costs	51
Table 6.7	Parameters Used for Modeling Costs for Installation.....	53
Table 6.8	Segments Included in the Different Cost Categories	55
Table 6.9	Calculation of CapEx Inflation Adjustment Factors.....	55
Table 6.10	Relationship Between Installation and Decommissioning	59
Table 6.11	Calculation of the Mass and Cost of one TwinWind Substructure	61
Table 6.12	Overview of the Adjustment of Costs for the TwinWind Modeling.....	61
Table 6.13	Modeled Length of Mooring Lines for Shared Mooring Concepts	62
Table 7.1	Distribution of CapEx for Trollvind Wind Farm with 50 Turbines	64
Table 7.2	Parameters for LCOE Calculations for Trollvind	65
Table 7.3	Detailed Component Description and Costs for Trollvind	66
Table 7.4	Detailed Duration for Actions in the Substructure Installation Phase	67
Table 7.5	Percentage Change in LCOE for Trollvind.....	69
Table 7.6	LCOE for Trollvind with Different Capacity Factors.....	74
Table 7.7	Calculation of NPV, IRR, and PP	77
Table 7.8	Calculation of Adjusted Cost for TwinWind.....	81
Table 7.9	Calculation of Adjusted Cost for Shared Mooring Lines Concepts.....	81

List of Abbreviations

AEP	Annual Energy Production
CapEx	Capital Expenditures
CF	Capacity Factor
CCF	Cumulative Cash Flow
DCF	Discounted Cash Flow
DecEx	Decommissioning Expenditures
FCR	Fixed-Charge Rate
FWT	Floating Wind Turbine
HVAC	High-Voltage Alternating Current
HVDC	High-Voltage Direct Current
IRR	Internal Rate of Return
LCC	Life Cycle Costs
LCOE	Levelized Cost of Energy
MW	Megawatt
MWh	Megawatt per hour
kW	Kilowatt
NIBOR	Norwegian Interbank Offered Rate
NPV	Net Present Value
NREL	National Renewable Energy Laboratory
OpEx	Operational Expenditures
ORBIT	Offshore Renewables Balance-of-system and Installation Tool
PPA	Power Purchase Agreement
PPI	Producer Price Index
PP	Payback Period
PV	Present Value
TI	Turbulence Intensity
WACC	Weighted Average Cost of Capital
XLPE	Cross-Linked Polyethylene

List of Symbols

Latin Symbols

A_n	Number of array strings
AS	Substation ancillary system
B_d	Bury depth
B_f	Bury factor
$C_{n,e}$	Number of export cables
CF	Cash flow
C_t	Cash flow in year t
C_r	Cable rating
C_v	Cable voltage
C_p	Cable power capacity
C_l	Array cable length
D	Debt
D_f	Foundation diameter
D_m	Mooring line diameter
d_t	Depth of installed scour protection material
$d_{port-site}$	Distance from the landfall
E	Equity
e_{ext}	Eventual extension
$f(v)$	Probability density function of the wind speed
H_s	Significant wave height
I_{ref}	Factor for IEC61400 – 3 Class
L_m	Mooring line length
L_{C-FB}	Fixed bottom cable length
L_{C-FH}	Catenary free-hanging cable length
$L_{f,c}$	Catenary length factor
$L_{m,f}$	Fixed mooring length at 500 m
$l_{available}$	Available cable length
MPT	Main power transformer
MPT_r	Power rating of transformer
M_{hp}	Mass of the heave plate

$M_{available}$	Available mass of the vessel
M_m	Mooring line mass
$M_{required}$	Required mass of the vessel
M_{sc}	Mass of the stiffened column
M_t	Mass of the trust
N	Number of time steps
n	Number of periods
n_{sets}	Number of sets of transportation
OSS_{cost}	Total cost of offshore substation
$P_{installed}$	Installed capacity
\bar{P}	Theoretical power output
\bar{P}_0	Average output of power
P_c	Plant capacity
P_f	Power factor
p	Pressure
r	Discount rate
r_E	Return on equity
r_F	Risk-free rate
r_L	Levered cost of equity
r_M	Expected return of the market
SG	Substation switchgear
SR	Substation shunt reactor
SD_σ	Standard deviation of σ
$S_{available}$	Available deck space of the vessel
S_d	Scour depth
S_{ext}	Unloaded jacking system speed
S_{lift}	Loaded jacking system speed
S_r	Scour radius
$S_{required}$	Required deck space of the vessel
S_v	Scour volume
S_{vessel}	Speed of the vessel
TS	Substation topside

T_d	Turbine rotor diameter
$T_{n,a}$	Number of turbines per array cable
T_n	Number of turbines
T_p	Wave spectral peak period
T_r	Turbine rating
T_s	Turbine spacing
t	Length of period
$t_{jack-up}$	Jack-up duration
$t_{transit}$	Transit duration
U	Horizontal speed element
$u(z, t)$	Longitudinal component of turbulent wind
V	Mean wind speed
$V(z)$	Wind speed at altitude z
v	Wind speed
v_i	Wind speed at time i
$v(z, t)$	Lateral component of turbulent wind
W_d	Water depth
W_μ	Mean wind speed for marginal distribution
$w(z, t)$	Vertical component of turbulent wind
z	Length of the surface roughness

Greek Symbols

α	Weibull shape parameter
α_r	Power law exponent
β	Weibull scale parameter
β_0	3.75 ms ⁻¹
β_1	Wind turbulence factor of 0.75
β_c	Beta coefficient
β_L	Levered beta coefficient
β_U	Unlevered beta coefficient
λ_{cable}	Linear cable density
ρ	Air density
σ	Standard deviation of mean wind speed
$\bar{\sigma}$	Mean deviation in the probability distribution
σ_{90}	90 th percentile value of σ
τ	Corporate tax rate
τ_{xz}	Perpendicular shear force
τ_0	Shear force
φ	Soil friction angle

Mathematical Operators and Constants

π	The ratio of the circumference to the diameter of a circle
∂	Partial derivative
e	Base of the natural algorithm
ℓ	Mixing length

1. Introduction

The combustion of natural gas, oil, and coal for electricity and heat generation constitutes the most significant contributor to global greenhouse gas emissions, according to Lamb (2021). These emissions contain high concentrations of greenhouse gases that impact the planet's climate and weather systems. The visible effects of global warming have led to significant economic and social impacts on society (Masson-Delmotte, et al., 2018). Moreover, with the projected increase in global energy demand in the coming decades, the pressing need to address these emissions has become more urgent (International Energy Agency, 2020).

Renewable energy is a viable option for mitigating carbon emissions and meeting the rising global demand for energy (International Energy Agency, 2020). Wind energy presents favorable prospects among various alternatives due to its cost-effectiveness, dependability, and lack of emissions during operation. The World Wide Fund for Nature recognizes the offshore wind sector as a crucial component in achieving the objective of 100 % renewable energy by 2050 (World Wide Fund for Nature, 2011). The annual and cumulative offshore wind energy installation in Europe over the past two decades is shown in Figure 1.1. This shows that the industry has experienced significant expansion and is likely to play a central role in future electricity generation.

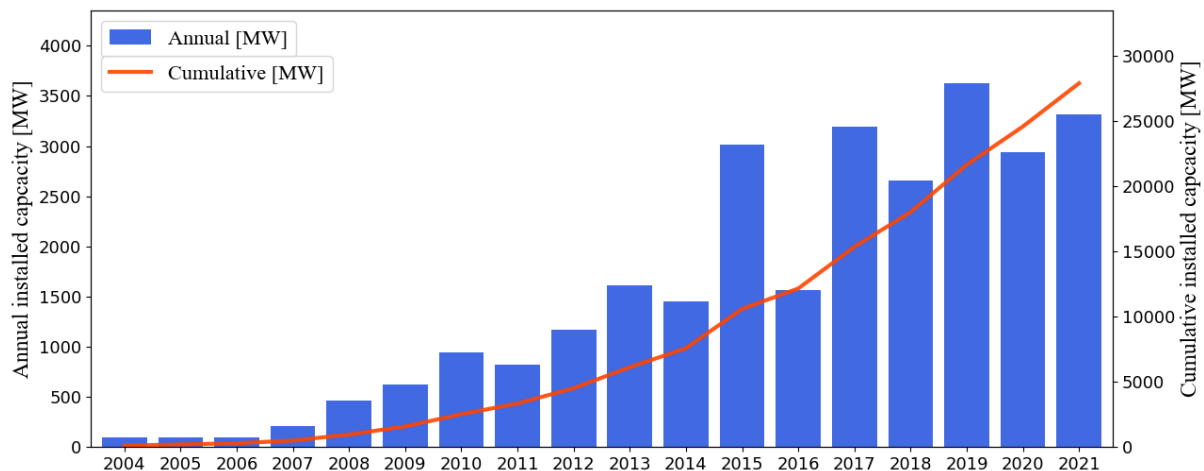


Figure 1.1 Offshore Wind Installation in Europe, derived from Williams et al. (2022)

Various offshore wind turbine designs are currently in operation, and these can be fixed to the seabed and floating (Kreider, Oteri, Robertson, Constant, & Gill, 2022). The selection of a particular design is determined by factors such as seabed characteristics and water depth. Fixed offshore wind turbines are suitable for depths of approximately 60 meters while floating wind turbines have the potential to be utilized in deeper waters. Figure 1.2 illustrates examples of how both the fixed and floating wind turbines may be placed.

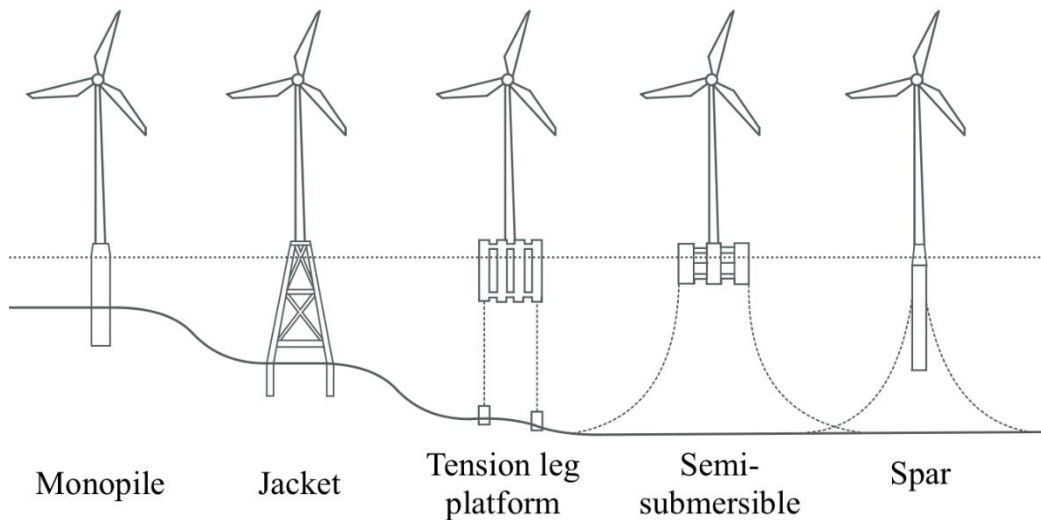


Figure 1.2 Fixed and Floating Offshore Structures

As the figure shows, the industry today uses three main types of floating wind turbines: (1) tension leg platform, (2) semi-submersible, (3) spar buoy, which vary in both types of mooring systems and floating foundations (DNV, 2018).

- (1) Tension Leg Platform: a buoyant structure that is semi-submerged with taut leg mooring lines connected to anchors at the seabed. This restricts the vertical movement of the platform due to waves and helps it to limit the motion and achieve stability.
- (2) Spar-buoy: a sizeable cylindrical buoy that uses ballast to stabilize the wind turbine, with three catenary mooring lines from the buoy to the seabed. Its gravity-based structure requires a large draft to stay stable, which makes it necessary to utilize the structure in water depths of 100 meters or more.
- (3) Semi-submersible: a waterplane area structure with great flexibility. The semi-submersible may be used at both shallow and great water depths and relies on ballasting to achieve stability. It combines the two principles from the spar buoy and the tension leg platform. The foundation is semi-submerged like the tension leg platform; however, it has catenary mooring lines similar to the spar buoy.

Levelized Cost of Energy (LCOE) is a term used to describe the average cost of producing electricity from a particular source throughout its lifetime (Emblemsvåg, 2020). The generated electricity price depends on several factors such as the design of the support structure, grid connection, installation, operation, and maintenance. The application of LCOE is widely incorporated in the policymaking of the world, and it has multiple functional areas for developers and investors (Aldersey-Williams & Rubert, 2019). It can be utilized to evaluate the cost-effectiveness of various electricity-producing methods, e.g., different types of wind farms or solar farms.

The current state of floating wind turbine technology is characterized by low maturity and a lack of commercial-scale projects, resulting in higher costs relative to onshore and bottom-fixed wind turbines, according to Stehly and Duffy (2022). The primary hurdle to making floating wind power commercially viable is the substantial capital investment required, which is notably higher than that for bottom-fixed turbines. This represents the critical challenge of high costs that must be addressed to enable the widespread deployment of floating wind energy systems.

With extensive maritime resources and capabilities from the petroleum sector, Norway is well-positioned for a leading role in floating offshore wind production (DNV, 2020). This thesis aims to investigate the LCOE of an offshore floating wind farm located in the Norwegian Sea. Sensitivity analyses will also be performed to identify key cost drivers of the LCOE, selected key financial metrics will be evaluated, and the LCOE of innovative offshore floating wind solutions will be examined.

2. Significance of Offshore Wind

In recent years the effects of global warming and a sudden energy shortage have become more prominent in society. The confluence of several factors, including Europe's desire to reduce reliance on Russian gas and nuclear energy, as well as a growing aversion to energy sources that harm wildlife and the environment (Pohjolainen, Kukkonen, Jokinen, Poortinga, & Umit, 2018). Hence, presenting a unique opportunity for offshore wind farms to become a major source of clean energy production (Vrana, Kydros, Kotzaivazoglou, & Pechlivanaki, 2023). For offshore floating wind to be a prominent energy source there is a drastic need for technological innovation and scalability to achieve energy security while also ensuring this is a sound economic investment (Barooni, Ashuri, Sogut, Wood, & Taleghani, 2022). With all this in mind, no energy source can be without conflict, this can be avian fauna, ship traffic, marine infrastructure, or close inhabitants (Multiconsult, 2023).

The primary proposed benefit of offshore wind farms is to enhance the capacity of renewable energy sources in mitigating the impact of global warming (European Union, 2020). Offshore wind farms have the potential to generate significant amounts of clean energy with minimal carbon emissions compared to conventional fossil fuel-based power plants (Cranmer & Baker, 2020). Moreover, offshore wind farms provide an opportunity to reduce the reliance on fossil fuels empowering the much-needed energy transition.

While offshore wind consists of enormous components and may encounter downtime, the Intergovernmental Panel on Climate Change still encourages the environmental prospects of offshore wind (IPCC, 2014). In the report, the CO₂ emission per kWh of produced electricity is evaluated for different energy sources. While a floating wind farm will require additional resources, the additional CO₂ should not be too intimidating. This has been studied by Yuan, et al. (2023) for floating deep-sea wind farms which gave a 25.76 g CO₂-eq/kWh. The findings are demonstrated in Table 2.1 and display the prominent need to transition from fossil fuels to renewable energy sources.

Table 2.1 CO₂ Equivalents per kWh of Produced Energy for Different Energy Sources

Energy source	g CO ₂ equivalents per kWh
Coal	820
Natural gas	490
Biomass	230
Solar	41
Hydropower	24
Nuclear	12
Offshore Wind - Bottom-fixed	12
Onshore Wind	11
Offshore Wind - Floating	26

Another important aspect of wind energy is the strong need for enhanced energy security, which has become especially prominent in 2022. In response to the energy scarcity resulting from the Russian invasion of Ukraine, the European Union has formulated a geopolitical energy plan called REPowerEU (European Union, 2022). This plan comprises a range of measures, including energy conservation, diversification of energy sources, and the development of clean energy technologies. Thus, demonstrating the imperative nature of introducing more energy, particularly more renewable energy. By prioritizing renewable energy sources and investing in clean energy technologies, the REPowerEU plan sets a crucial precedent for global efforts to transition towards a more sustainable and enhanced energy security for European citizens.

The expense associated with offshore floating wind power is perceived as higher than that of alternative energy sources (Trinomics, 2020), illustrated in Figure 2.1. The global data is derived from (Martinez & Iglesias, 2022) (Lazard, 2023) (DNV, 2023) (Trinomics, 2020), and Norwegian data from (NVE, 2023) where the lowest estimates resemble NVE prediction of LCOE in 2030. As a result of high LCOE for offshore wind, there is a recognized necessity for the advancement of technology and the execution of scalability in this field (Sintef, 2023). Sintef argues that despite the initial expense associated with such technology, ongoing deployments will result in substantial cost savings, emphasizing the importance of accelerating the construction of floating wind. To render floating wind energy economically feasible, akin to advancements previously made in the field of solar power, it is essential to undertake upscaling and technological innovations (NREL, 2016).

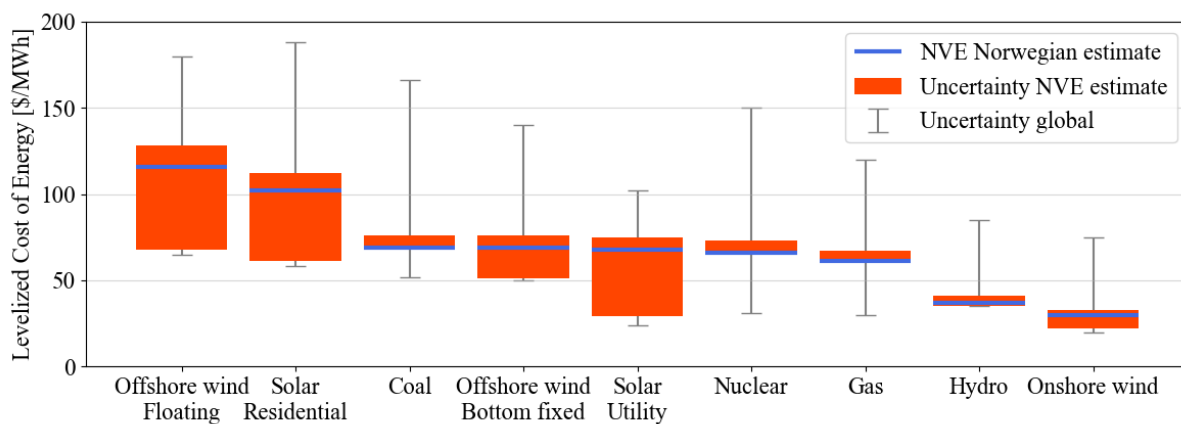


Figure 2.1 Levelized cost of Energy for Different Energy Sources

Offshore wind energy, like all forms of energy production, presents significant challenges in terms of environmental and social impacts. These challenges may take various forms, including conflicts with wildlife, other industries, cultural heritage, citizens, and many others (Multiconsult, 2023). One of the main advantages of offshore wind is the distance from residents, although there may occur disturbances related to noise, visuals, and light pollution the conflict is regarded as less apparent compared to onshore energy (Normann, 2020). Even though offshore wind has been presented as a way to reduce controversy with local inhabitants, moving the turbines offshore cannot be regarded as a quick fix to reduce conflict.

Offshore floating wind turbines are typically located in areas with high wind speeds, which often coincide with important migration routes for birds (Schwemmer, et al., 2022). The rotating blades of wind turbines pose a significant risk to birds, particularly large birds of prey such as eagles and hawks. The risk of collision can lead to injury or death of birds, which can have a significant impact on their populations. This demonstrates the need for evaluating bird migration and living paths to avoid unnecessary incompatibility with the existing avian fauna.

Another significant conflict associated with offshore floating wind is its impact on marine traffic like shipping fleets but also fisheries (Norwegian Environment Agency, 2013). Offshore wind turbines can pose navigational hazards and obstruct shipping lanes. In addition, they can interfere with fishing activities by altering fish habitats or causing physical obstructions, which can lead to conflicts between offshore wind developers and fishing communities (Reckhaus, 2022). This area dispute may also affect other industries such as oil and gas, where further exploration and development may have to be halted due to the presence of existing offshore wind farms (Norwegian Environment Agency, 2013).

Cultural heritage, nature conservation areas, naval operations, and existing sea cables are some additional areas of conflict associated with offshore wind energy development (Multiconsult, 2023). The two first may include particularly valuable areas in terms of natural diversity, shipwrecks, and other conservation areas, while the two last incorporate military activities and existing marine infrastructure. Figure 2.2 illustrates the level of conflict for offshore wind in the Norwegian Sea.

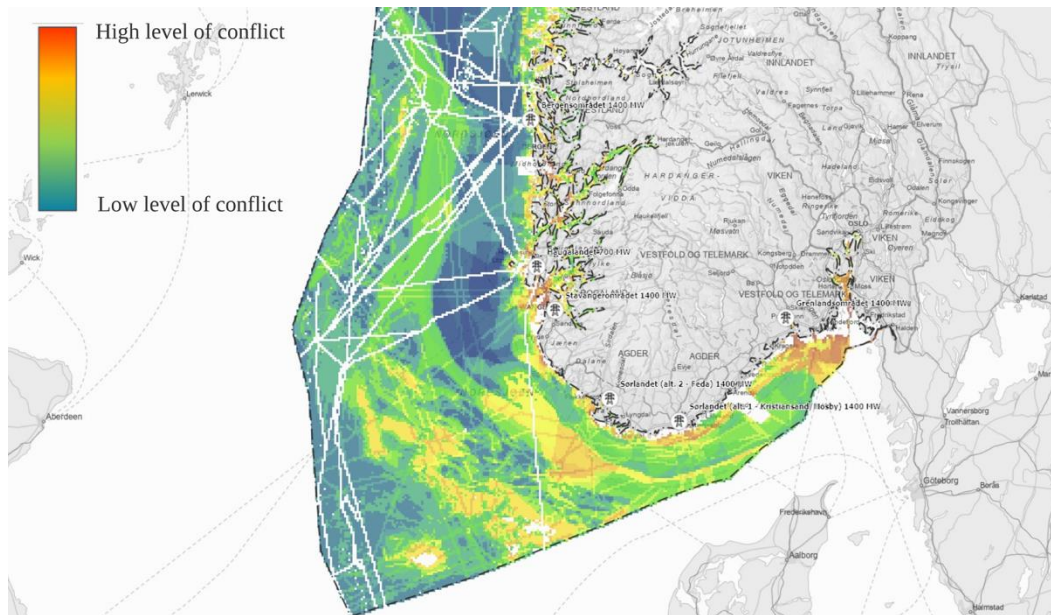


Figure 2.2 Level of Conflict in the Norwegian Sea for Offshore Wind (Multiconsult, 2023)

In conclusion, offshore floating wind has the potential to provide significant benefits in terms of renewable energy, but it also poses significant challenges in terms of environmental and social impacts. The conflict associated with offshore floating wind is complex, and stakeholders must work together to develop solutions that balance the needs of renewable energy production with the needs of the environment and local communities.

3. Theory

3.1 Environmental Conditions of an Offshore Site

3.1.1 Characteristics of Vertical Wind Speed

The change in wind speed with altitude is known as the vertical wind gradient (Ray, Rogers, & McGowan, 2006). Considering it directly affects the power accessible at various hub elevations and significantly affects the periodic stress on the turbine blades, it is crucial to comprehend. It is difficult to accurately characterize wind gradients for offshore site assessments because they depend on many different variables, such as wind speed, height above the ground, surface roughness and variation, and atmospheric stability. At a higher altitude, the wind speed increases until terminal speed is reached, shown in Figure 3.1.

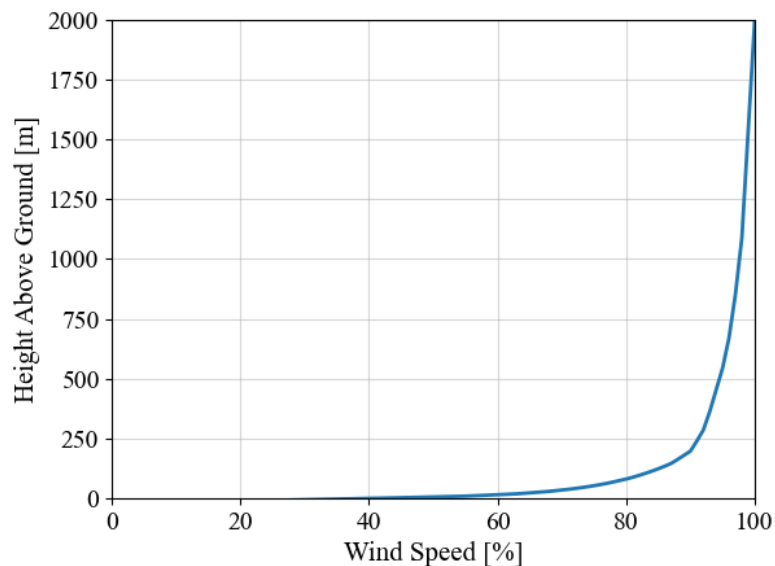


Figure 3.1 Vertical Wind Speed Gradient

In studies on wind energy, the vertical distribution of wind speed across areas of uniform, flat topography has typically been modeled using two mathematical equations (Manwell, McGowan, & Rogers, 2009). The first method, the log law, was developed in the field of hydrodynamics and meteorological research to study the layer of boundary flows. It is supported by both empirical as well as theoretical studies. The power law is the second strategy, which is popular among academics studying energy in the wind. Because turbulent flows are complicated and varied, there is uncertainty with both methods (Hiester & Pennell, 1981).

Wortman (1983) proposed a way of predicting the wind speed gradient in a logarithmic way by conducting a mixing length type analysis. When applied close to the earth's surface, the equation of momentum is reduced to the following:

$$\frac{\partial p}{\partial x} = \frac{\partial}{\partial z} \tau_{xz} \quad (3.1)$$

where z and x represent vertical and horizontal coordinates, p is the pressure, and τ_{xz} is the shear force whose perpendicular corresponds with z in the direction of x . In this area, the pressure is z -independent, thus the integration yields:

$$\tau_{xz} = \tau_0 + z \frac{\partial p}{\partial x} \quad (3.2)$$

where τ_0 is the value of the shear force, near the surface. The gradient of pressure is small close to the surface, resulting in a neglect of the second term on the right side of the equation. By applying the mixing length theory of Prandtl, the shear force can be denoted as (Manwell, McGowan, & Rogers, 2009):

$$\tau_{xz} = \rho \ell^2 + \left(\frac{\partial U}{\partial z} \right)^2 \quad (3.3)$$

where ρ is the air density, U is the horizontal speed element, and ℓ represents the length of the mixing. A combination of Eq. 3.2 and Eq. 3.3 yields:

$$\frac{\partial U}{\partial z} = \frac{1}{\ell} \sqrt{\frac{\tau_0}{\rho}} = \frac{U^*}{\ell} \quad (3.4)$$

where U^* equals $\sqrt{\frac{\tau_0}{\rho}}$, representing the velocity of friction.

Integrating Eq. 3.4 from z_0 to z , where z_0 represents the length of the surface roughness yields the following, denoted as the logarithmic function:

$$U(z) = \frac{U^*}{k} \ln \left(\frac{z}{z_0} \right) \quad (3.5)$$

where k is von Karman's constant. This integration is assuming a completely even surface, and because natural surfaces are not completely smooth, the minimum limit of integration is z_0 . Approximations of the roughness lengths for specific surfaces are displayed in Table 3.1 (Manwell, McGowan, & Rogers, 2009).

Table 3.1 Approximate Values for Surface Roughness Length

Surface	z_0 [m]
Ice	0.01
Open sea, calm	0.20
Open sea, blown	0.50
Snow	3.00
Grass	8.00

The second alternative, the law of power, is a simplified version of the vertical wind speed gradient, denoted by the following equation, proposed by Lamb (1975):

$$V(z) = V(z_r) \left(\frac{z}{z_r} \right)^{\alpha_r} \quad (3.6)$$

where $V(z)$ is the speed of the wind at altitude z , $V(z_r)$ is the reference speed of the wind at altitude z_r , and α_r represents the exponent of the power law. This exponent can be calculated by several methods, such as a function of height and speed, roughness of the surface, or both roughness of the surface and speed (Manwell, McGowan, & Rogers, 2009). A simplification that would apply to most conditions of 0.143 has been proposed by Schlichting (1968), while 0.11 is suggested as a good approximation for sea conditions (Hsu, Meindl, & Gilhousen, 1994).

3.1.2 Wind Speed Distribution

The generated power of wind farms fluctuates significantly because wind power possesses unpredictability, fluctuation, and discontinuous properties (Shi, Dong, Xiao, & Huang, 2021). The amount of wind energy that is accessible and how well the energy conversion system performs depend on the wind speed distribution at a given site. Many probability distribution models have been employed in the evaluation, organizing, layout, development, and operation of wind farms. Therefore, it is essential to precisely comprehend the distribution properties of wind speed to decrease the margin for error of wind energy production estimation.

To estimate the theoretical power output of a wind turbine, the following equation can be applied (Masseran, 2015):

$$\bar{P} = \int_0^{\infty} \frac{1}{2} \rho v^3 f(v) dv \quad (3.7)$$

where \bar{P} is the theoretical power output, v represents the wind speed, and $f(v)$ is the probability density function of wind speed. As a result, \bar{P}_0 , the average output of power, yields:

$$\bar{P}_0 = \frac{1}{2} \rho \bar{v}^3 \quad (3.8)$$

As observed, $f(v)$ is a substantial part of calculating the power output of wind energy, and applying the appropriate probability density function will have a significant impact on the result (Shi, Dong, Xiao, & Huang, 2021).

One of the most widely used statistical distributions in the context of wind resource projects is the Weibull distribution (Masseran, 2015). For instance, Weibull has been utilized extensively for the evaluation of the possibilities for wind power for specific locations. The distribution can determine the amount of wind energy equivalent to the wind turbine capacity factor, and additionally, it has been utilized as an estimating model to assess the effectiveness of the wind

power system. The Weibull probability density function can be denoted as (Jung & Schindler, 2019):

$$F(v) = \frac{\alpha}{\beta} \left(\frac{v}{\beta}\right)^{\alpha-1} \exp\left(-\left(\frac{v}{\beta}\right)^\alpha\right), \alpha > 0, v > 0, \beta > 1 \quad (3.9)$$

where α is the shape parameter, and β represents the scale parameter (ms^{-1}). Through an elementary curve fitting method, the parameters of the Weibull distribution could be approximated with accuracy. A standard approach to fit the Weibull to an observed distribution of wind speed is the method of maximum likelihood. The shape parameter, α , is calculated iteratively (Mahmood, Resen, & Khamees, 2020):

$$\alpha = \left[\frac{\sum_{i=1}^N v_i^\alpha \ln(v_i)}{\sum_{i=1}^N v_i^\alpha} - \frac{\sum_{i=1}^N \ln(v_i)}{N} \right]^{-1} \quad (3.10)$$

where v_i is the wind speed at time i , and N represents the number of time steps. Subsequently, it is possible to calculate the scale parameter:

$$\beta = \left(\frac{\sum_{i=1}^N v_i^k}{N} \right)^{\frac{1}{k}} \quad (3.11)$$

3.1.3 Wind Turbulence

By forming and dissolving successively smaller waves or gusts, the wind's kinetic energy is converted into thermal energy, which is what causes wind turbulence (Manwell, McGowan, & Rogers, 2009). Over time intervals of over an hour, the turbulent wind could have a fairly consistent mean, but over smaller intervals of time, it might be relatively changeable. There are longitudinal, lateral, and vertical components to the turbulent wind (Milan, Morales, Wächter, & Peinke, 2014). The longitudinal component is denoted by the letters $u(z, t)$ in the direction of the predominant wind. The vertical component is $w(z, t)$, and the lateral component is $v(z, t)$, which is perpendicular to u . z represents the altitude, while t denotes the time.

The turbulence intensity (TI) is the most common method to measure turbulence (Manwell, McGowan, & Rogers, 2009). It is determined by dividing the mean wind speed by the wind speed standard deviation. The mean and standard deviation are computed across periods that are larger than those associated with turbulent fluctuations but less time than those connected with different kinds of variations in wind speed. This time interval is typically no longer than an hour, and according to wind energy engineering standards, it is characteristically equivalent to 10 minutes (Wang, Barthelmie, Pryor, & Kim, 2014). In most cases, the sample rate is a minimum of one per second. The TI can be denoted as:

$$TI = \frac{\sigma}{V} \quad (3.12)$$

where σ is the standard deviation of the mean wind speed, V . The International Electrotechnical Commission 61400-3-1:2019, hereby denoted as IEC 61400, assumes a σ that is constant with altitude and distributed log-normally (International Electrotechnical Commission, 2019). The mean, $\bar{\sigma}$, could be defined as:

$$\bar{\sigma} = (\beta_1 I_{ref})V + \beta_0 I_{ref} \quad (3.13)$$

where $\beta_1 = 0.75$, and $\beta_0 = 3.75 \text{ ms}^{-1}$. I_{ref} represents the reference TI , thus the TI at the hub height of a wind turbine with a wind speed equal to 15 ms^{-1} . This varies with the TI classification, as the I_{ref} equals 0.12, 0.14, and 0.16 for low (class C), medium (class B), and high (class A), respectively. This can also be applied to calculate the standard deviation of σ :

$$SD_{\sigma} = (1.44 \text{ m s}^{-1})I_{ref} \quad (3.14)$$

In the process of designing wind turbines, IEC 61400 suggests the appliance of the 90th percentile values of σ . To calculate σ_{90} , which is equivalent to $SD_{\sigma} \times 1.28$ is added to $\bar{\sigma}$, yielding (Wang, Barthelmie, Pryor, & Kim, 2014):

$$\sigma_{90} = I_{ref}(0.75V + 5.6 \text{ m s}^{-1}) \quad (3.15)$$

3.2 Power Performance of an Offshore Wind Farm

The power performance of an offshore wind farm may vary as different conditions and factors affect it. The wind farm layout, wind turbine power curve, and capacity factor are all influential factors.

3.2.1 Wind Farm Layout

The configuration of wind turbines is a significant determinant of the power generation potential of a wind farm (Archer, Mirzaeisefat, & Lee, 2013). The design parameters that delineate the layout of wind turbines in a wind farm encompass the number of turbines deployed, turbine models and diameters, the orientation of rows in relation to the prevalent wind direction, dimensions and geometry of the wind farm, turbine spacing, and turbine alignment. Figure 3.2 illustrates a wind farm array schematic.

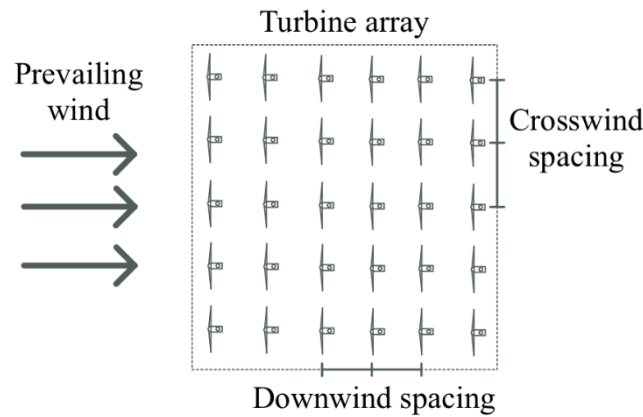


Figure 3.2 Array Schematic of a Wind Farm, derived from Manwell et al. (2009)

The optimization of wind farm layout is a crucial factor in enhancing the power generation potential of wind energy projects (Manwell, McGowan, & Rogers, 2009). The two primary parameters that significantly impact this potential are field geometry and ambient turbulence intensity. By optimizing these parameters, wind farm designers can increase the efficiency of wind turbine operation, improve the farm's overall performance, and achieve higher energy output.

3.2.2 Wind Turbine Power Curve

The power curve of a wind turbine shows the power output of the turbine in relation to the wind speed (Cascianelli, Astolfi, Castellani, Cucchiara, & Fravolini, 2021). Accurate power curve models hold significant importance as they serve as essential instruments for predicting power and enabling real-time monitoring of turbines. Three possible applications of the power curve are described in Table 3.2.

Table 3.2 Wind Turbine Power Curve Applications

Selection of Turbines	The power curve can be utilized in general comparisons between turbine models and can assist in the selection of a suitable turbine from the available options.
Online Monitoring	The power curve can be utilized in assessing a turbine's performance by comparing the actual power curve of the turbine with a benchmark curve that reflects the performance under normal conditions.
Capacity Factor Estimation	The power curve, together with a probability distribution, can be used to estimate the capacity factor of a wind turbine.

Figure 3.3 illustrates a general power curve for a horizontal-axis wind turbine. As seen, it is divided into four phases and has three noticeable wind speeds: (1) cut-in, (2) rated, and (3) cut-out. The cut-in wind speed tells what the minimum wind speed needs to be for a wind turbine to start producing a power output (Sohoni, Gupta, & Nema, 2016). Further, the rated wind speed is where the turbine produces at a maximum of its installed power output, whilst at the cut-out the wind speed is too high, and the wind turbine stops producing.

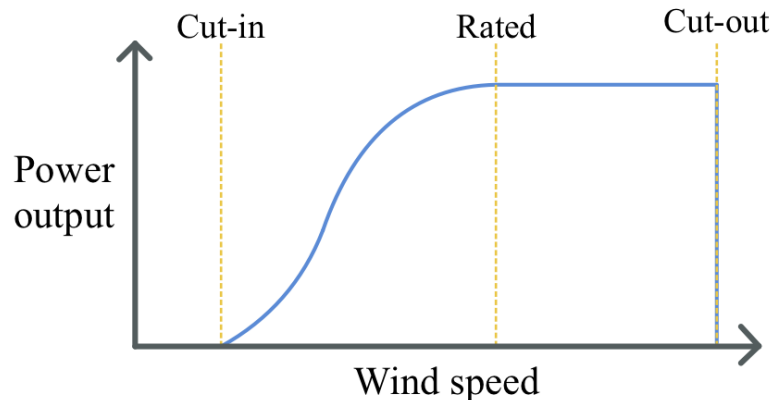


Figure 3.3 General Power Curve of a Horizontal-axis Wind Turbine

The figure shows that the first phase is before the cut-in speed. Here the wind speed is lower than the threshold minimum; thus, no power output is produced. In phase two, which lies between the cut-in and rated wind speed, the power output is increasing rapidly. As the wind speed reaches the rated wind speed, phase three starts and this lasts until the cut-out where phase four follows beyond this.

3.2.3 Capacity Factor

Selecting a suitable site for a wind farm necessitates meticulous consideration to guarantee the identification of the area that exhibits the greatest wind conditions (Abed & El-Mallah, 1997). Accurate assessments of the wind resource characteristics at the proposed location are crucial to avoid discrepancies with the design specifications of the wind turbine, which could lead to lower energy production, i.e., a reduced capacity factor (CF). The CF is determined by the relationship between the wind turbine’s installed capacity ($P_{installed}$) and its annual energy production (AEP) (Abed & El-Mallah, 1997), seen in Eq. (3.16).

$$CF = \frac{AEP}{P_{installed}} \quad (3.16)$$

Although the capacity factor is mainly based on wind conditions, other factors have an influence as well. Grid losses occur due to electrical (heat) losses and happen in inter-array cables, export cables, and substations (Morthorst & Awerbuch, 2009). Further, as the wind farm has downtime by cause of, e.g., maintenance or mechanical failure, the wind farm availability time decreases. Both of these factors will affect the CF.

The wind farm layout will also impact the CF due to aerodynamic array losses (Manwell, McGowan, & Rogers, 2009). These losses can be attributed to the aerodynamic interaction between wind turbines and are mainly a function of wind turbine spacing (crosswind and downwind), wind turbine operating characteristics, number of turbines, and turbulence intensity.

3.3 Infrastructure of an Offshore Wind Farm

3.3.1 Wind Turbine System

A standard wind turbine comprises a rotor, a nacelle, and a tower (Manwell, McGowan, & Rogers, 2009). In offshore turbines, all the components are contained inside a mechanical structure defined as the nacelle. The rotor is attached to an axle that generates electricity via a gearbox. The horizontal configuration, in which the rotor revolves around a horizontal axle, is the most prevalent. The nacelle and rotor together compose what is known as the rotor-nacelle assembly, which is attached to the turbine's tower, illustrated in Figure 3.4.

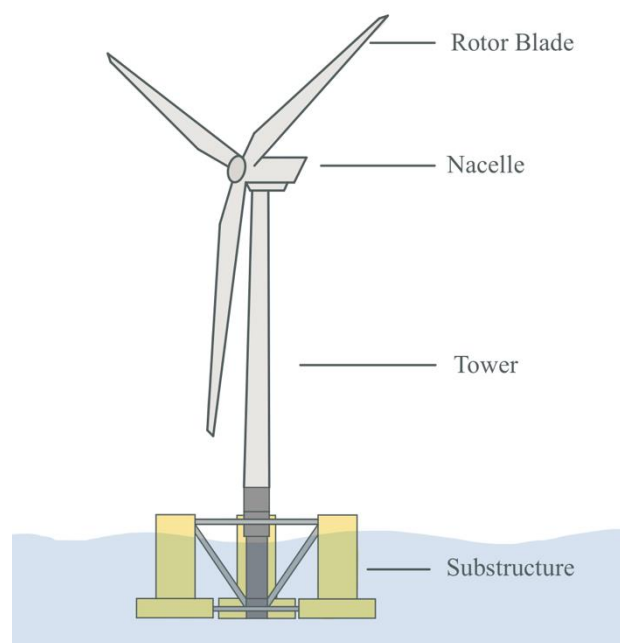


Figure 3.4 Components of a Floating Wind Turbine

The turbine rotor blades turn the nacelle drive axle, which is coupled to a rotor hub and powered by the wind's kinetic energy. While the rotor hub is often composed of cast steel, the rotor blades are primarily made of synthetic composites like glass-reinforced plastics (Greaves, 2016). Both upwind and downwind positions for the rotor are feasible. The risk of the rotating blades colliding with the tower due to being deformed by high wind forces is reduced with an upwind placement of the rotor but is offset by the need for stronger and consequently more costly rotor blades.

The nacelle, which is typically composed of fiberglass, houses important electricity-generating parts such as the brake system, gearbox, generator, and power converter, illustrated in Figure 3.5 (Manwell, McGowan, & Rogers, 2009). Certain parts might also be integrated into the tower of the turbine. Low frequencies are increased in the gearbox to optimally match the power generator used to turn the shaft. To meet grid specifications, direct current is converted to alternating current by a voltage regulator (Islam, Guo, & Zhu, 2013).

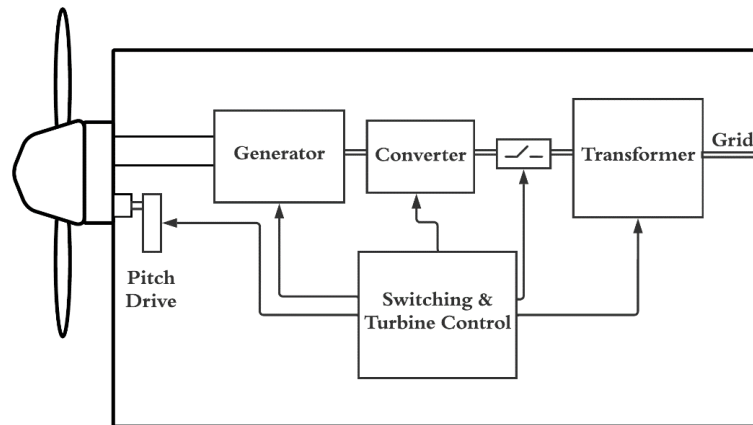


Figure 3.5 Electrical Components Inside the Nacelle

Massive wind turbine towers are often built from rolled steel tube sections that are welded together. The industry is continually innovating for larger rotor blades since the potential energy that may be gathered from the wind increases with greater rotor blade diameters (Greaves, 2016). To reduce the possibility of the rotor being destroyed by waves brought on by severe weather, greater vertical distances between the average seawater level and the rotor blades are preferred for offshore projects. Moreover, higher towers enable the exploitation of more advantageous wind conditions at greater elevations.

3.3.2 Semisubmersible Floating System

The semi-submersible-floating approach was initially used for offshore oil and gas exploration when a wide drill deck was essential (Liu, Li, Yi, & Chen, 2016). The semi-submersible foundation is proposed for supporting offshore wind turbines because of the *wave cancellation effect*, which could enhance wave-induced system dynamics of the offshore structure. The term *wave cancellation effect* describes the phenomenon whereby a phase shift causes the wave pressures acting on submerged objects to cancel each other out. When compared to other types of floating foundations, the hydrodynamic behaviors of a semi-submersible foundation to the wind load excitations are improved. The prolonged natural heave period that occurs as the draft increases are the known explanation (US Patent No. 4850744, 1989).

A full-scale 2 MW turbine from Principle Power's WindFloat technology was effectively installed off the coast of Portugal, for the first time in 2011 (Myhr, Bjerkseter, Nygaard, & Ågotnes, 2014). This platform is one of many forms of the semisubmersible floating system. Marine Innovation & Technology has spent the last years extensively qualifying the hull's technical aspects and optimizing the platform for larger wind turbines.

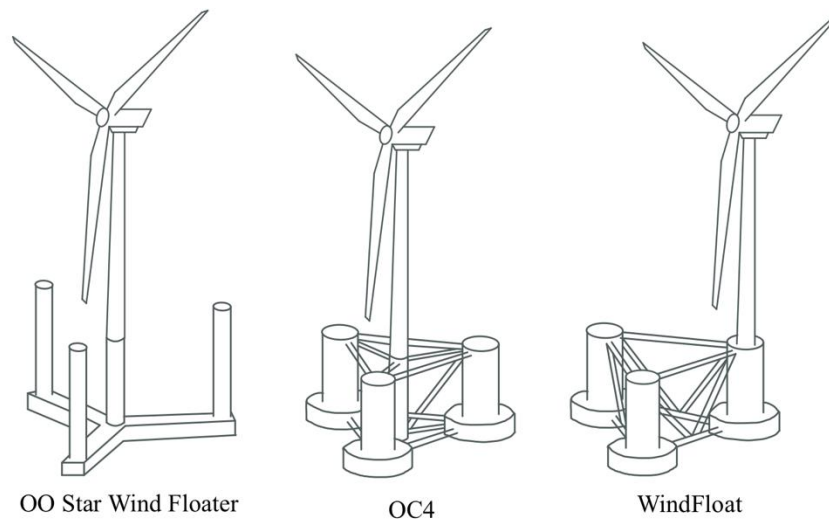


Figure 3.6 Different Semisubmersible Floating Platforms

Commonly for the semisubmersible floaters is that the wind turbine is placed on one of the three columns or as an additional middle column, this is shown in Figure 3.6 (Collu & Borg, 2016). To maximize structural continuity and reduce stress concentration in exposed parts of the construction, the foundation of the tower has equal dimensions to the supporting column. Each column base has a horizontal heave plate added to increase the foundation's hydrodynamic inertia. The plates move a significant amount of water, which optimizes the structure's horizontal dynamic responsiveness. Additionally, the high damping forces caused by the vortices formed at the plates' edges further restrict platform movement.

There are often two separate systems of ballast in the platform, one permanent and one active (Collu & Borg, 2016). Each column is equipped with a permanent ballast at its base, and the purpose is to lower the foundation to its optimal depth. The active ballast system is located directly on top of the permanent water ballast to transport water between columns to lessen the rigid-body effect caused by the mean wind forces impacting the wind turbine. The active ballast system regulates the water distribution across the three active water ballasts to keep the tower of the wind turbine vertical when the wind speed or direction changes, to ensure the wind turbine's operation.

3.3.3 Mooring Systems for Floating Substructures

To keep a vessel or other floating constructions in one position, mooring systems are utilized. Three types of mooring are generally used for floating wind turbine concepts: vertical mooring systems, taut leg mooring systems, and catenary mooring systems, displayed in Figure 3.7 (Myhr, Bjerkseter, Nygaard, & Ågotnes, 2014).

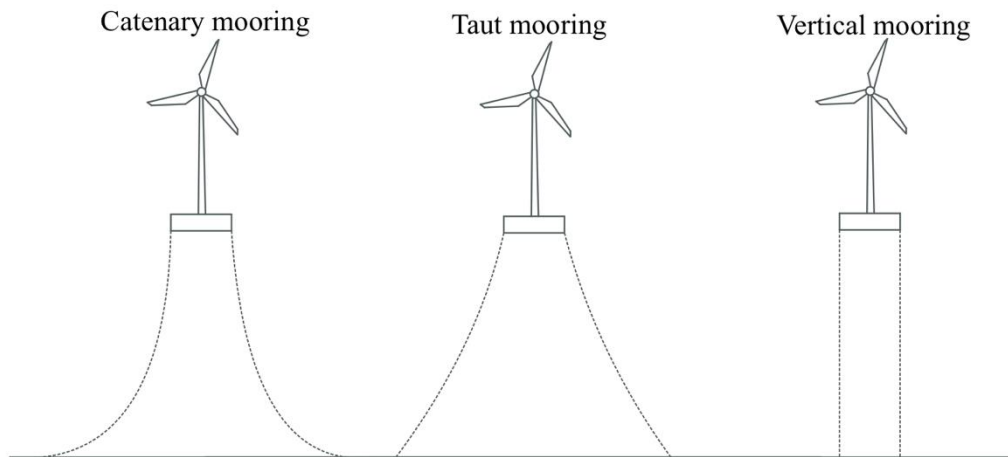


Figure 3.7 Different Mooring Line Solutions

Vertical mooring lines reach the bottom vertically, taut leg mooring lines arrive at the seabed at a pre-defined angle, while catenary lines connect horizontally to the anchor (Ma, Luo, Kwan, & Wu, 2019). The elasticity of the mooring lines produces restoring forces, allowing a taut leg mooring system to resist both vertical as well as horizontal forces. Although horizontal forces are not sustained to the same degree, the vertical mooring method is also able to handle both vertical and horizontal stress. The anchor points only experience horizontal loads during catenary mooring, and the majority of restoring forces are produced by the mass of the mooring line. A mooring line system is primarily made up of an anchor, connectors, and a mooring line (Eriksson & Kullander, 2013). The mooring line, which commonly consists of a chain, synthetic fiber rope, or wire rope, attaches the anchor on the seabed to a floating vessel.

3.3.4 Electrical Infrastructure for Floating Offshore Wind

In the process of transferring the power produced by the wind turbines a complex array system, export facility, and grid connection are necessary (Georgios, 2010). This export system consists of inter-array cables, export cables, offshore substations, onshore substations, and power grid connections (Nunemaker, Shields, Hammond, & Duffy, 2020). All parts of this infrastructure play a crucial role in delivering the produced energy from the offshore wind farm to the onshore electrical grid. In this assessment of the power export system, only the offshore segment is evaluated. An overview of the full structure for exporting power to the electrical grid system can be seen in Figure 3.8.

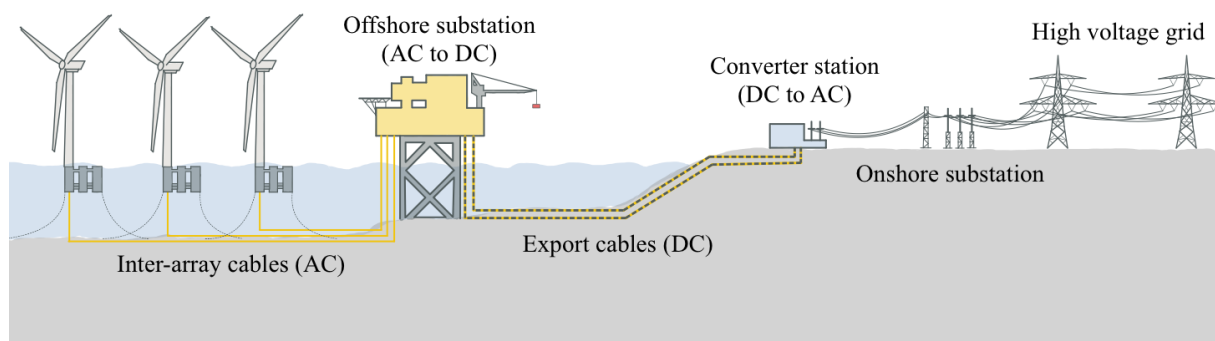


Figure 3.8 Electrical Grid Connection for Offshore Wind

3.3.5 Inter-Array Power System

The inter-array system is responsible for guiding the flow of electricity generated by the turbines to the offshore substation (Nunemaker, Shields, Hammond, & Duffy, 2020). The array system generally consists of strings of medium-voltage cables that are buried in the seabed and connected to all the turbines (Anaya-Lara, 2016). Due to the wake effect phenomenon in wind farms, all turbines must be separated by a specific number of rotor diameters, this leads to large distances and thus long cabling distances. Commonly, the medium voltage inter-array cables are rated as 33 kV with the future potential of developing 66 kV cables. These cables are made with either aluminum or copper as the conductor material and are known as cross-linked polyethylene (XLPE) insulated submarine cables.

The inter-array cables closest to the substation transfer all the power generated by the later string-connected wind turbines (Svendesen, Endegnanew, & Torres-Olguin, 2013). This requires these cables to have a higher current-carrying capacity. Meaning that the maximum current-carrying capacity of the XLPE cables thus sets a limit on the total number of wind turbines that can be connected in series. This results in requiring more expensive cables with a greater capacity closer to the substation.

3.3.6 Offshore Substation

Substations can be placed both onshore and offshore, while projects exceeding 100 MW or with a distance from shore greater than 15 km require an offshore substation (Anaya-Lara, 2016). The substation clusters all the inter-array cables, transforms the voltage, and passes the power onward to the export cable system. The purpose of the substation is to increase the produced energy's voltage (from typically 33 kV to 132 kV). This voltage increase is crucial for reducing the energy losses that occur when transferring electricity over large distances.

A substation's major components consist of three main categories: (1) related to electrical systems, (2) related to facilities, and related to structure (Anaya-Lara, 2016). The electrical system components consist of the transformer, backup power generator, switchgear, converters, and reactive power compensation equipment. Figure 3.9 displays an overview of the general layout and the cable transmission of an offshore substation.

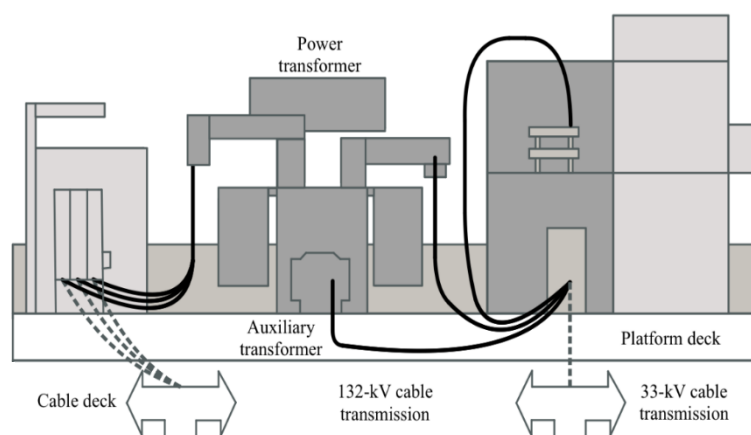


Figure 3.9 Technical Layout of an Offshore Substation

The number and location of the substations are a central cost driver of the grid connection for offshore wind. Preferably, the substation should be located on land, or offshore where the distance for the inter-array cabling is minimized (Anaya-Lara, 2016). The required number of substations is determined by the size of the wind farm (total length of inter-array cabling), voltage level (maximum length of feeder), and the capacity of the wind farm together with the transformer. Wind farms with significant generated power will require an offshore substation based on the considerable power losses from the transmission MW. A limiting factor for the installed power can be the offshore transformer, where the possibility of more than one substation should be studied. With the cost of transformers and the substation's physical size corresponding to their power ratings.

3.3.7 Export System

The export cable is positioned between the offshore substation and the onshore transmission system (Anaya-Lara, 2016). Export cables have the significant purpose of efficiently transmitting electrical power from the wind farm to the landfall with minimal power loss. The cables mainly consist of a conductor in copper or aluminum, an insulator, and a protection layer. Standard offshore export cables are pairs of single-core high-voltage direct current (HVDC) for each platform converter with copper conduction and XLPE insulation. For close-to-shore wind farms, the more cost-effective high-voltage alternative current (HVAC) should also be considered. Depending on seabed conditions and the burial approach, the associated fiberoptic cables and monitoring system cables can be buried as a single unit in the subsea trench. It should be noted that this bundle burial is a cost-effective approach.

3.4 Innovative Offshore Wind Solutions

Researchers and companies have been working on developing innovative solutions that can reduce the LCOE associated with offshore wind energy generation. These solutions include modifications to the design and layout of wind turbines, substructures, mooring, and cabling systems (Catapult, 2022). This focus on innovation has the potential to make offshore wind energy more cost-effective, competitive with other energy sources, and increase its share in the global energy mix.

3.4.1 Dual Turbine Platform

Hexicon, a Swedish renewable energy company, has introduced an innovative concept for offshore wind power known as the TwinWind (Hexicon, 2023). The TwinWind concept comprises two wind turbines mounted on a single tension leg floating platform. A single-point mooring mechanism on TwinWind's downwind semisubmersible platform allows the floating platform to dynamically adjust to the wind direction (Mendoza, Katsidoniotaki, Florentiades, Dot Fraga, & Dyachuk, 2023).

This configuration facilitates the alignment of the foundation with the prevailing wind direction, as opposed to the individual turbine nacelles. The floater features three columns on the vertices and a triangular truss structure. One column houses the mooring attachment with a passive weather-vaning system, while two of the columns hold two inclining towers. The TwinWind concept is illustrated in Figure 3.10.

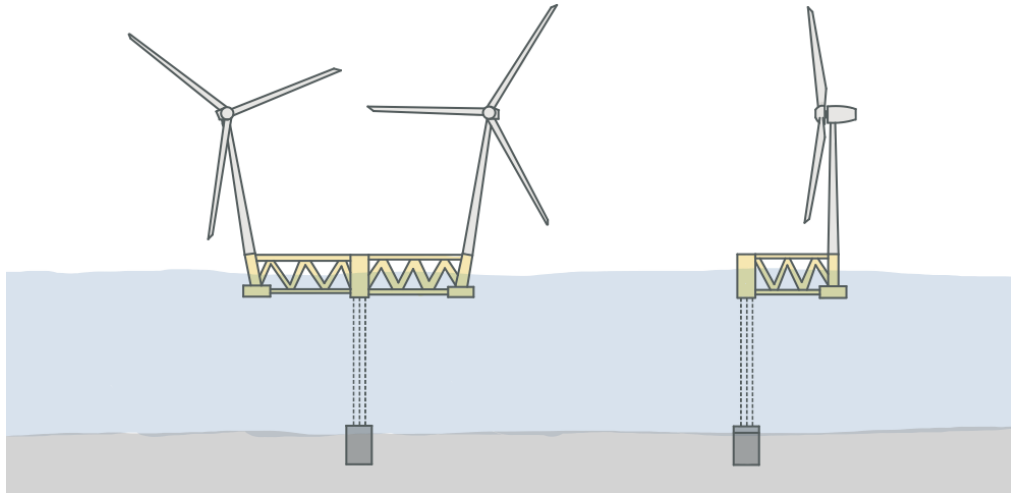


Figure 3.10 Front and Side View of the TwinWind Concept

The proposed design exhibits compatibility with all significant offshore wind turbine designs and can accommodate turbines ranging from 3 MW to 15+ MW in power output (Hexicon, 2023). According to Hexicon, there are three primary drivers toward a lower LCOE. Firstly, TwinWind incorporates a twice-magnified rated capacity compared to a solitary turbine floating foundation while requiring relatively less steel on a per MW basis. Secondly, accommodating a greater number of turbines within a reduced spatial expanse reduces the inter-array cabling requirement for an offshore wind farm by approximately one-third. Thirdly, incorporating two turbines on a singular foundation enables the minimization of installation costs by reducing the number of wet tows and mooring installations required. Furthermore, TwinWind is amenable to onshore and quayside assembly, including turbine installation, which enables the fully commissioned system to be wet towed to the offshore location.

3.4.2 Shared Mooring for Floating Wind Farms

Shared mooring lines are an innovative solution that has been proposed to reduce the cost of mooring in offshore wind (Liang, Jiang, & Merz, 2023). By sharing mooring lines, the number of mooring lines needed for each turbine can be reduced, which leads to a reduced number of anchors as well. This can result in cost savings, as the cost of installing and maintaining mooring lines can be a significant portion of the overall cost of an offshore wind project.

There are different solutions for sharing mooring lines, from the basic of sharing one line for two turbines, all the way to an inter-connected layout of up to ten turbines connected in a net of lines (Hall, Lozon, Housner, & Sirmivas, 2022). A top view of different concepts of shared mooring has been illustrated in Figure 3.11.

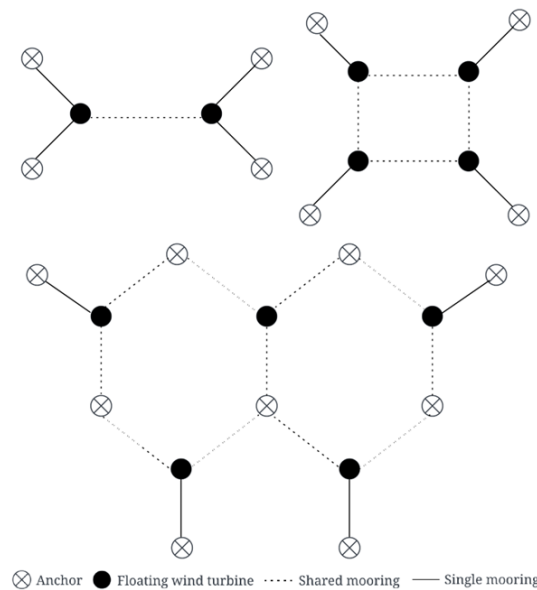


Figure 3.11 Top View of Shared Mooring Systems, derived from Liang et al. (2023)

Liang et al. (2021) and Gözcü et al. (2022) conducted research on the feasibility of a dual-spar floating wind farm with a shared line. In particular, Gözcü et al. (2022) examined the natural frequencies and mode shapes of the system and compared them to those of individual shared mooring turbines. Their investigations revealed that a shared mooring design of a dual-spar wind turbine can exhibit comparable characteristics to those of a single turbine. Figure 3.12 illustrates the shared mooring system.

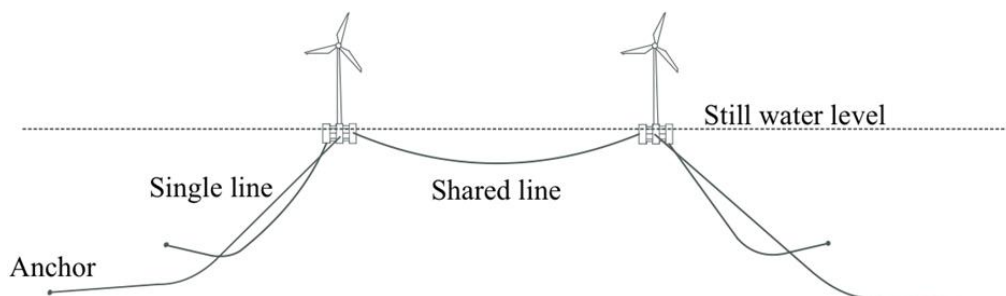


Figure 3.12 Side View of a Shared Mooring System, derived from Liang et al. (2021)

3.5 Life Cycle of an Offshore Wind Farm

The total life cycle of an offshore wind park may stretch well over 30 years from the early concepts to the complete decommissioning (Jiang, 2021) (Accenture, 2017). The life cycle consists of five main phases: (1) early planning and evaluation in the preliminary phase, (2) detailed design and engineering of components, (3) installation of fabricated components, (4) operation and maintenance, and (5) decommissioning. Figure 3.13 provides an overview of the different stages of the life cycle for an offshore wind farm.

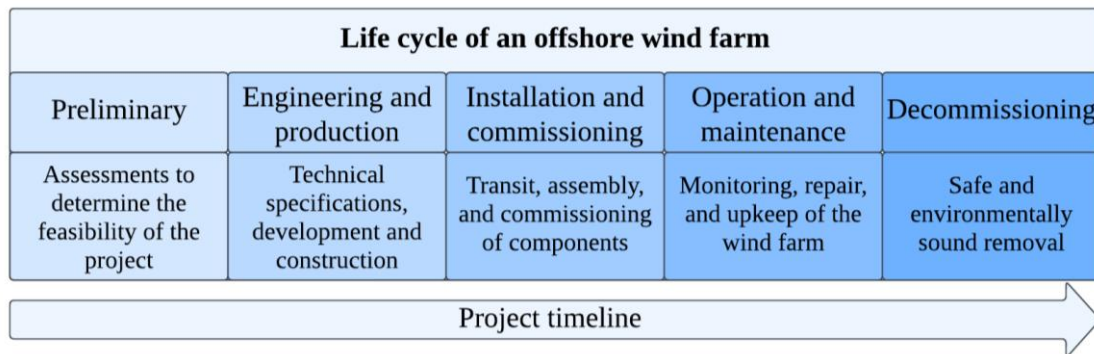


Figure 3.13 Overview of the Life Cycle of an Offshore Wind Farm

3.5.1 Preliminary Phase

Offshore wind projects involve several preliminary steps before their implementation, including site selection, resource assessment, stakeholder engagement, permitting, and feasibility studies (DHI, 2021). Site selection involves analyzing potential offshore sites for wind energy production suitability, accounting for factors such as wind speeds, water depth, seabed conditions, distance to shore, and proximity to existing infrastructure. Resource assessments are conducted to determine the potential wind energy production at each site, involving the deployment of meteorological towers and/or floating LiDAR buoys (DNV, 2023). Stakeholder engagement is important for developers to gather feedback and address any concerns that may arise from local communities, regulators, and other interested parties.

The permitting process involves obtaining various approvals from regulatory agencies before construction can begin, including environmental permits, and permits related to navigation and other maritime activities (DNV, 2022). Finally, feasibility studies are conducted to assess the technical, economic, and environmental viability of the project, including studies related to the design of the wind turbines and support structures, as well as the transmission and grid connection infrastructure required to bring the electricity produced by the project ashore (DNV, 2023). These preliminary steps are essential to ensure the successful design, construction, and operation of offshore wind projects.

3.5.2 Engineering & Production Phase

The engineering and production phase is a crucial stage in the life cycle of an offshore wind farm (Shafiee, Brennan, & Espinosa, 2016). It involves the planning, design, and manufacturing of all components necessary for the construction and installation of the wind farm. This phase occurs after the site selection and permitting phase, where the location for the offshore wind farm already has been identified, and permits have been obtained. This phase of the life cycle includes project management, detailed surveys, detailed engineering, development, and component manufacturing. The phase facilitates a successful installation and further operations of the offshore wind farm.

The survey phase is used to determine the seabed's topography, geology, and environmental conditions (Shafiee, Brennan, & Espinosa, 2016). This information is used to design the foundations, support structures, electrical systems, and other components for the wind turbines. Detailed engineering involves the development of detailed plans and specifications for the wind farm, including the layout of the turbines, the design of the foundations and support structures, and the electrical infrastructure. This stage is crucial to ensure that the wind farm is designed to meet performance requirements, including energy output and durability.

Manufacturing is a critical stage in the engineering and production phase, as it involves the production of all components required for the wind farm's construction (The Federation of Norwegian Industries, 2022). The manufacture of components must be done to the highest quality standards, as any defects or flaws can compromise the performance and safety of the wind farm. In manufacturing an important part is establishing a successful supply chain. This is a complex and highly integrated network of companies, suppliers, and service providers. It is an important component as it plays a crucial role in ensuring that wind farms are designed, manufactured, and installed safely and efficiently. Lastly, the engineering and production phase is a complex and critical stage in the life cycle of an offshore wind farm (Shafiee, Brennan, & Espinosa, 2016). It requires significant planning, coordination, and attention to detail to ensure that the wind farm is designed and constructed to high standards and can deliver reliable and green energy for years to come.

3.5.3 Installation of Components of Offshore Floating Wind Farms

Installation of offshore wind farms is an essential step before commissioning. However, it is often overlooked during project development, leading to risks, financial consequences, and delays (Asgarpour, 2016). The components should be designed, manufactured, delivered to the onshore assembly site, assembled according to the installation strategy, and then transported offshore. The installation involves the assembly of the substructure and its connection to the mooring lines. Followed by the installation of the electrical grid connection, which ensures that the last step of the installation procedure will be achieved (Asgarpour, 2016). This includes the installation of the offshore substation together with the burial and connection of the inter-array and export cables. Large offshore wind farms experience various technical challenges associated with the installation phase.

3.5.4 Installation and Assembly of the Complete Floating Structure and Wind Turbine

There are different installation procedures for different offshore wind systems, and this thesis focuses on the onshore assembly and towing technique of installing the complete substructure-turbine system. One of the main advantages of the semi-submersible platform is its superior towing ability, which provides simpler installation and decommissioning than other concepts (Jiang, 2021). In general, the installation procedure entails onshore assembly of the complete turbine system including the coupled substructure, followed by towing to the offshore site and connection to pre-installed mooring lines. The installation process is illustrated in Figure 3.14.

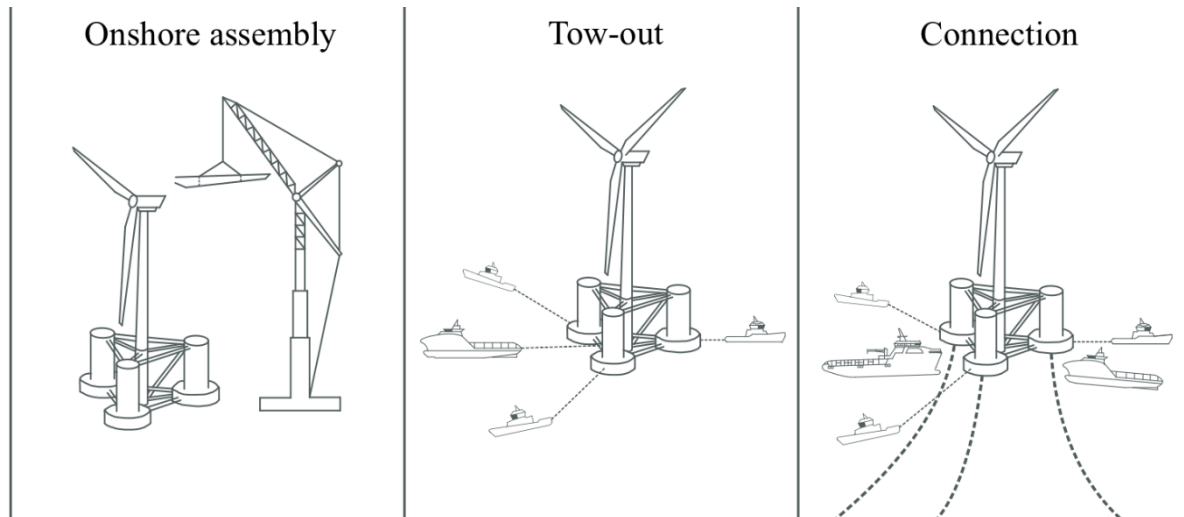


Figure 3.14 Installation of the Turbine System with Onshore Assembly and Tow-out

Onshore assembly consists of the assemblage of the complete substructure together with lifting and fastening the turbine components (Asgarpour, 2016). The turbine installation often consists of five lifts when done onshore for a three-blade turbine: (1) lift and fasten tower section, (2), lift and fasten nacelle, (3-5) and a repeated lifting and fastening of blades (Jiang, 2021). The turbine assembly relies on a completed and prepared substructure and is followed by a mechanical completion and verification before the tow-out of the complete structure. Quality assurance and control onshore are essential factors that significantly contribute to the success of wind farms. Proper implementation of quality measures can ensure the reliability of components, safety of assembly and installation procedures, and thereby prevent costly downtime and repairs of the turbine or substructure.

The tow-out is performed by a group of ballasted towing vessels (towing and station-keeping vessels) dragging the complete structure out to the final site location (Asgarpour, 2016). The tow-out and installation are heavily prone to delay based on weather conditions. Upon arrival at the offshore wind farm site, the completion of the connection to the pre-installed mooring lines is typically performed by the towing group assisted by a multi-purpose support vessel. The mooring lines are subsequently verified to ensure proper installation before commencing the transit back to shore.

3.5.5 Mooring System Installation and Hook-Up

A complete mooring system installation consists of a vessel loadout, transit, survey, and installation of the anchors and the mooring lines (Altuzarra, et al., 2022). The installation of the anchors varies by type, but the drag-embedded anchors are lowered and fastened by dragging them into the seabed. Suction pile anchors are lowered to the seabed before creating a vacuum that fastens the anchor to the seabed by pumping air out of the pile (Myhr, Bjerkseter, Nygaard, & Ågotnes, 2014). After the anchor is installed, the mooring lines can either be fully mounted or a pre-lay of just the bottom chain can be executed. Subsequently, the transit back to shore can begin after the line and anchor have been verified as properly installed.

3.5.6 Installation of Offshore Substations

When assessing the process of installing the substation the type of structural balancing system plays a huge role (Narakorn, 2016). For shallow water, gravity-based or jacket foundations are preferred, while concepts for floating and subsea substations have been proposed for deep-water wind farms (DNV, 2023) (Aker Solutions, 2023). For the floating concepts, the installation process is similar to the installation of floating offshore wind structures (Yoshimoto, Awashima, & Kitakoji, 2013). The construction of the substation is performed onshore before getting tugged out to the pre-installed mooring lines. Further, it is connected to the mooring lines and the riser cable connection. When these steps are completed, the substation can be connected to the grid and final commissioning can be performed.

For the installation of the substation on a gravity-based or jacket foundation the principles are very similar (Asgarpour, 2016). The complete substation is constructed onshore before getting moved onto a heavy-lift vessel. Before finishing the manufacturing of the substation, the offshore foundation has to be installed offshore. Thereby, the substation can be transported by the installation vessel and raised onto the top of the installed foundation, illustrated in Figure 3.15.

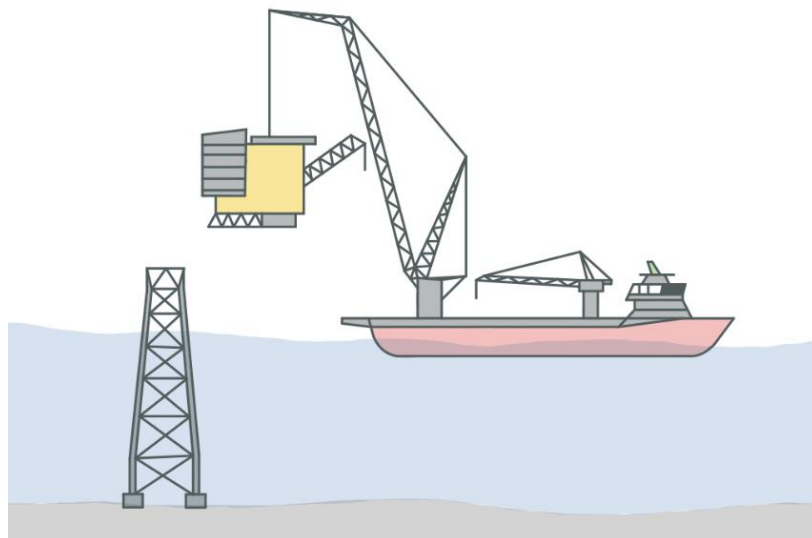


Figure 3.15 Installation of an Offshore Substation on a Jacket Foundation

3.5.7 Inter-Array and Export Cable Installation

Array-cable installation includes diligent preparation and studying to decrease potential risks and understand the technical challenges (Asgarpour, 2016). The installation process includes the main stages of preinstallation surveys, route clearance, cable laying/burial, and post-installation assessment. Based on the type of offshore structure and the seabed conditions, the array-cable installation varies. For monopile foundations, the array cables are dragged through J-tubes before getting connected to the tower bottom, whereas for floating structures, the cables must float down to the seabed (Narakorn, 2016). Thereby the floating cables need to be highly flexible and fatigue resistant. Different array cable installation techniques are displayed in Figure 3.16.

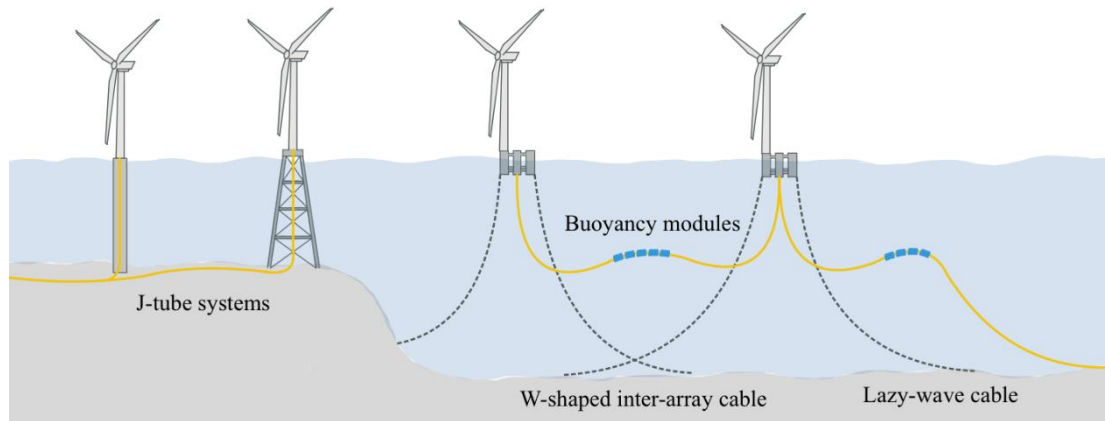


Figure 3.16 Power Cable Concepts for Different Offshore Wind Farms

When the array cable has reached the seabed, the burial method can start (Asgarpour, 2016). The array cables should be positioned 1-2 m under the seabed. This procedure is performed using remotely operated vehicles or a plough supported by an offshore vessel. This procedure is performed between all turbines connected by inter-array, lastly, the final turbine string is linked to the offshore substation. The burial depth and procedure are based on seabed conditions, environmental requirements, and DNV criteria. The process of burying the power cable is illustrated in Figure 3.17.

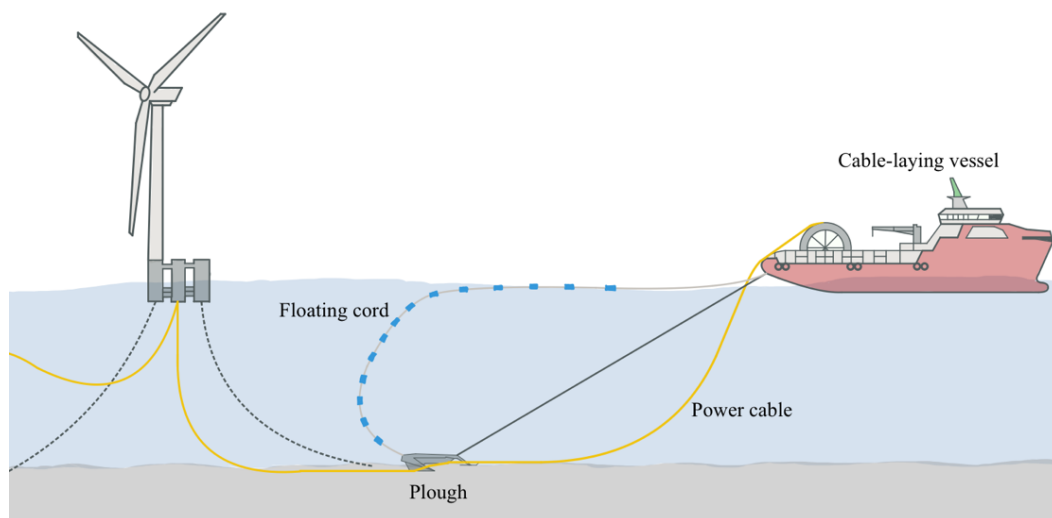


Figure 3.17 Burial of a power cable with the use of a plough and a cable-laying vessel

For the export cables the installation procedure is similar to the inter-array cables (Asgarpour, 2016). Since the export cables are larger than the inter-array cables, the required trenching vehicles and cable-laying vessels are of a larger capacity. In general, the cables near the shoreline ought to be buried deeper in the seabed than those further offshore. After the export cables have been installed, the pre-commissioning tests for the electrical grid system and the total wind farm can be completed.

3.5.8 Operation and Maintenance

The costs associated with operating and maintaining offshore wind farms represent a significant portion of the LCOE of projects (Ren, Verma, Li, Teuwen, & Jiang, 2021). The harsh offshore conditions, coupled with the unpredictable nature of wind, pose challenges for offshore wind farm operation and maintenance, which can be both difficult and costly. To enhance the competitiveness of offshore wind power, it is crucial to minimize the total lifetime expenditure of projects. The duration of downtime throughout the lifespan of an offshore wind farm is significantly impacted by maintenance activities, which in turn contributes substantially to the LCOE. Maintenance involves regular inspections and repairs of engineering structures to rectify failures or replace faulty components.

Effective and reliable maintenance is crucial for the daily operations of offshore wind turbines (Ren, Verma, Li, Teuwen, & Jiang, 2021). However, due to the need for technicians to visit the wind farm from a port, around-the-clock operations without interruptions from on-site maintenance are impossible. To prevent failures, a maintenance team must visit the wind farm frequently, but overly frequent visits are inefficient and costly due to the required maintenance of vessels and personnel. Conversely, a lower visit frequency increases the risk of failures and prolonged downtime. Therefore, maintenance frequency is a trade-off that balances risks, vessel capacities, and human resources (Guachamin-Acero, Jiang, & Li, 2020).

An optimal maintenance strategy aims to maximize economic benefit, extend component lifespans, reduce emergency repairs, decrease overtime labor costs, and minimize the stress of unpredictable equipment failures (Ren, Verma, Li, Teuwen, & Jiang, 2021). The cost of maintenance for offshore wind turbines varies according to the type of foundation and location. This also applies to the maintenance strategy applied, where the most common are reactive, preventative, condition-based, and predictive maintenance.

3.5.9 Decommissioning

Decommissioning is the final stage in the life cycle of an offshore wind project and involves re-doing what has been done in the installation phase (Topham & McMillan, 2017). Topham & McMillan refers to the principle of "the polluter pays" when talking about governing decommissioning and pinpoints the aim of restoring the site to its original condition before the wind farm was deployed. This includes shutting off the turbines, removing electric cables, and scrapping/recycling the leftover materials of the electrical and floating system.

The process of decommissioning can be divided into three primary stages: (1) project management and planning, which involves scheduling while considering the time and cost involved and striving to achieve an efficient and sustainable solution, (2) the removal of the offshore wind farm components, and (3) post-decommissioning activities, such as handling the removed components and monitoring the recovery of the site (Topham & McMillan, 2017).

Decommissioning of offshore wind is complex, and the experience from bottom-fixed projects is that complete removal is challenging (Salahshour, Ong, Skaare, & Jiang, 2022). These methods include cutting, lifting, burying, and other techniques for separating the foundation

from the seabed. Decommissioning is an important step for ensuring that the site is left in a similar condition as it was before the deployment of the project, minimizing the environmental impact and ensuring the safety of marine life and navigation. It also allows for the proper disposal of materials and equipment together with providing opportunities for recycling and repurposing.

3.6 Financing and Capital Structure

3.6.1 Cost of Equity

There are several techniques for calculating the cost of equity, and each model uses a somewhat different methodology to convert investment risk into projected profits (Kolouchova & Novák, 2010). The first strategy uses Gordon's Dividend Growth model, a popular representation of the dividend discount model. According to this idea, the market stock price and the dividend payments determine the investor's necessary rate of return. The Capital Asset Pricing Model (CAPM) represents an alternative method (Zhang, 2017). The Markowitz model for choosing a portfolio serves as the foundation for a series of predictions about the equilibrium anticipated profit on hazardous assets, known as the CAPM. According to this concept, investors select portfolios that 1) reduce portfolio return variance given anticipated return and 2) optimize expected return, considering variance.

The CAPM outlines a linear connection between the investment's projected return and risk. This connection is often referred to as the Security Market Line, and can be denoted as (Bodie, Kane, & Marcus, 2018):

$$r_E = r_F + \beta_C(r_M - r_F) \quad (3.17)$$

where r_E is the return on equity, r_F is the risk-free rate, β_C is the beta coefficient, and r_M represents the expected return of the market. The beta coefficient, β_C , represents the systematic risk of the market segment, thus, a risk that cannot be diversified. As a result, investors only receive compensation for exposure to the market's non-diversifiable systematic risk. According to this connection, every security with an identical beta coefficient contributes equally to risk and return. According to the CAPM technique, previous results are used to determine the cost of equity under the presumption that they would accurately predict future performance.

3.6.2 Risk-Free Rate

The risk-free rate is the return an investor can earn without assuming any risk (Damodaran, 2008). Although the expected return on a zero-beta portfolio would theoretically be the most accurate measure of the risk-free rate, the difficulties and expenses associated with creating such a portfolio lead to the use of government bonds as a proxy for the risk-free rate. The risk-free rate is typically used as a benchmark for determining the expected return of other investments, which carry some level of risk. For investments with higher associated risk, the expected return should be larger to make up for the increased risk that comes with an

investment. Most analysts utilize a single government bond's yield to maturity that most closely fits the examined cash flows. Putting this in a Norwegian perspective, the Norwegian government bond with a 10-year maturity can be reflected to be a suitable risk-free rate (The Central Bank of Norway, 2023).

3.6.3 Market Risk Premium

The market risk premium is a concept used to determine the expected return on investments accounting for the additional risk when investing in equities instead of risk-free investments (Damodaran, 1994). There are various methods for estimating the metric, which is essential when evaluating CAPM, cost of equity, and cash flow analyses. One potential method of deriving the risk premium involves utilizing historical data on stock returns (Damodaran, 2017). This approach operates under the assumption that the risk premium on the market portfolio is stable and normalized, such that the average past risk premium can provide a suitable estimate of the expected future risk premium. However, it is important to note that this methodology may overlook potential changes in market conditions or systemic shifts in the risk premium, and thus it is advisable to consider alternative approaches as well. Other approaches include forward-looking (using current equity prices) and surveying investors' expectations.

3.6.4 Beta Coefficient

In finance, beta is a measure of an investment's volatility connected to the overall market (Fama & French, 2004). Specifically, beta measures the systematic risk of an asset, which is the risk that cannot be diversified away by diversification. The market has a beta of one, and equities that have a beta of more than one are more volatile than the market, while equities with a beta of less than one are less volatile (Jagannathan & Wang, 1996). One widely used approach for calculating beta involves conducting statistical regression analysis on historical data (Scholes & Williams, 1977). This involves regressing the asset returns against a market portfolio index over a specified period. The resulting beta value can be considered an estimate of the asset's systematic risk or sensitivity to market movements. Other less-used methods include the two-pass regression model and the statistical technique of the generalized method of moments.

It is important to note that the CAPM approach necessitates the levered beta (β_L) of the project, which factors in the modified post-tax risk of financial leverage. The unlevered beta (β_U) values represent the inherent business risk of the companies and do not include the impacts of financial leverage. The equation for the levered beta can be observed in Eq. 3.18.

$$\beta_L = \beta_U \times \left(1 + \frac{D}{E}\right) \quad (3.18)$$

where D is debt, and E represents equity.

3.6.5 Tax Shield

Tax shields refer to the reduction in taxable income that arises from taking advantage of tax deductions, credits, or exemptions (Graham & Harvey, 2001). By reducing taxable income, tax shields can lower the amount of tax that a company or individual has to pay, resulting in higher after-tax cash flows. When considering tax shields, the examples of debt interest payments and depreciation expenses are most often relevant. By applying these kinds of tax shields, the after-tax cash flow for a project can increase and affect the value of the investment opportunity. Companies utilizing debt financing may also lower their cost of capital and thereby increase the firm valuation.

3.6.6 Cost of Debt

For the investors that hold the company's debt, the cost of debt represents the opportunity cost of capital (Brealey, Myers, & Allen, Risk and the Cost of Capital, 2011). The cost of debt is less than the cost of capital for the corporation and, as a result, cheaper than the equity cost because debt is safer than assets. The interest rate that creditors demand in exchange for providing the risk of financing a project or business is known as the cost of debt.

The cost of debt is influenced by factors related to the company, such as the size, book-to-market ratio, intangibles, cash flow, and dividend policy (van Binsbergen, Graham, & Yang, 2010). Financial difficulties, individual taxes, debt burdens, and agency fees between various investment groups are also included. Additionally, the default cost of debt (also known as insolvency expenses) accounts for around half of the entire cost, which suggests that the remaining half is made up of agency costs and other non-default costs. Furthermore, the cost of being over-levered is higher than the cost of being under-levered, indicating that a corporation may suffer from having a high debt ratio.

While some businesses have predictable cash flows, others are affected by variables like the cost of commodities and interest rate levels (Brealey, Myers, & Allen, 2011). Likely, these traits do not always produce the intended profile of risk. Interest rate swaps thus offer a practical strategy for protecting against the risk of fluctuating interest rates. The interest on a loan with variable rates is ultimately set at a cost determined by an interest rate reference thanks to an interest rate swap (Lang, Litzenberger, & Liu, 1998). An interest swap contract depends on the borrower and lender exchanging payments. As a supplement to a credit spread, the borrower first makes an annual interest payment based on the reference rate.

By swiftly and inexpensively moving between a fixed-rate or floating-rate profile when the prediction for interest rates changes, these contracts give fixed-income managers a way to control interest rate risk and volatility. Interest rate swaps effectively allow fixed-rate borrowing for borrowers, lowering the uncertainty of upcoming cash flows.

3.6.7 Weighted Average Cost of Capital

The Weighted Average Cost of Capital (WACC) signifies the project discount rate, and it is used to calculate the minimum rate of return a business or project needs to achieve to appease its creditors, investors, and other stakeholders (Stehly, Beiter, & Duffy, 2020). WACC represents the average cost of all capital a company has raised, including debt and equity, and these are weighted by their overall ratio in the capital structure. Thereby, the WACC can be denoted as (Vartiainen, Masson, Breyer, Moser, & Medina, 2019):

$$WACC = \frac{E}{D+E} * r_E + \frac{D}{D+E} * r_D * (1 - \tau) \quad (3.19)$$

where E and D are the value of equity and debt, respectively. r_E is the cost of equity, r_D the cost of debt and τ is the corporate tax rate. Discounting is a method that is used in economic evaluations to account for the time at which costs and benefits arise (Attema, Brouwer, & Claxton, 2018). It is required due to the declining worth of money and is particularly crucial in industries where businesses have a long investment cycle and the time horizon for projects can vary from twenty to thirty years (Lloyd-Smith, Adamowicz, Entem, Fenichel, & Rad, 2021).

3.7 Cost Analysis of Wind Farms

3.7.1 Life Cycle Cost Analysis

A life cycle cost analysis of a product or system is performed to show how different alternatives and their costs compare to each other (Shil & Mahbub, 2007). This analysis calculates the overall cost of purchasing and using the system or product throughout its full life span. Thus, it comprises all expenses incurred from the time a decision has been made to obtain a system until the system is eventually disposed of.

The Life Cycle Costs (LCC) concept can be effectively illustrated by the *Iceberg Analogy*, which highlights the inherent risks associated with undisclosed costs and expenditures (Redman & Crepea, 2006). The analogy suggests that the primary portion of a product's or system's cost is typically concealed beneath the surface, with only a small portion of the overall cost being visible. The visible aspect typically pertains to the acquisition cost of a system or product, whereas the concealed costs relate to maintenance, operation, decommissioning, labor, and other factors that can significantly impact the LCC. Figure 3.18 illustrates the *Iceberg Analogy* of an offshore wind farm.

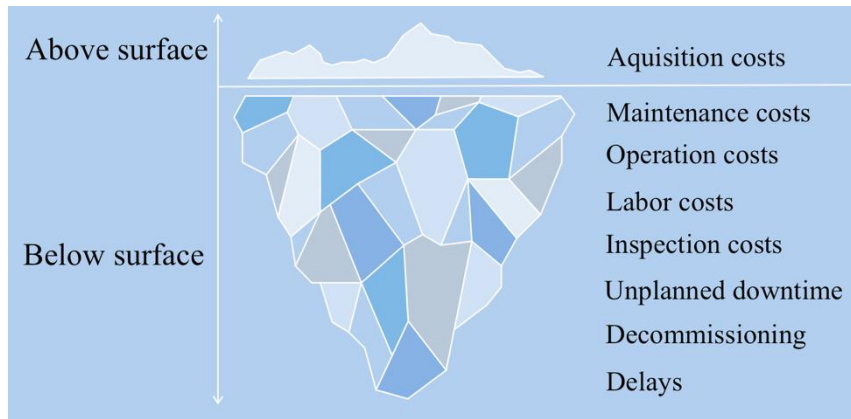


Figure 3.18 The Iceberg Analogy of an Offshore Wind Farm

The LCC may be denoted in various ways, as each system or product may vary concerning what costs are relevant. However, a basic formula for the life cycle cost can be expressed as the sum of acquisition and system utilization costs (Elmakis & Lisnianski, 2006), as shown in Eq. 3.20.

$$LCC = AC + O\&P \quad (3.20)$$

where LCC is the life cycle cost, AC the acquisition cost, and O&P the operation and support cost.

The LCC can be optimized by leveraging the correlation between the acquisition cost and the operation & support cost (Woodward, 1997) (Elmakis & Lisnianski, 2006). The graphs presented in Figure 3.19 postulate that enhanced reliability is associated with an increase in the acquisition cost. As a result, the operation & support costs will fluctuate concerning the acquisition cost. The point of intersection between these two curves, i.e., the acquisition cost and the operation & support cost, represents the point where the costs incurred on enhancing reliability equal the savings realized in operation & support cost. This point of intersection is indicative of the optimal LCC, which is represented on the top curve.

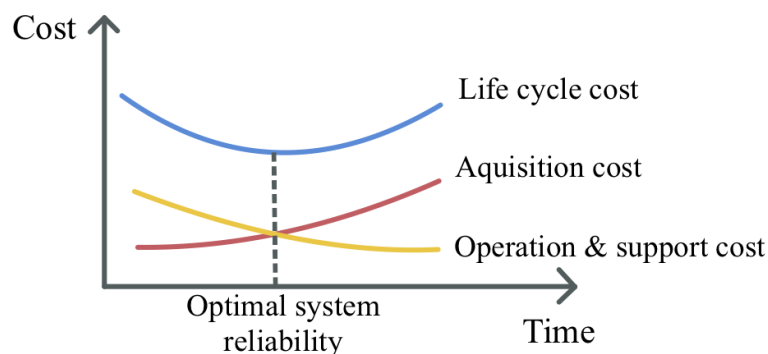


Figure 3.19 Optimal System Reliability

3.7.2 Cost Breakdown of an Offshore Wind Farm

Capital Expenditures (CapEx) represent the sum of the costs for planning, building, and installing a facility or system (Swart, Gaylard, & Mulenga Bwalya, 2022). It pertains to the initial investments involved in the development of a project, encompassing expenses related to its manufacturing, transportation, and installation. According to Maienza et al. (2020), the CapEx constitutes the largest proportion of the total costs for an offshore wind farm.

The system or facility’s day-to-day expenses are categorized as Operational Expenditures (OpEx) (Swart, Gaylard, & Mulenga Bwalya, 2022). As opposed to CapEx, these expenditures are not related to the acquirement of long-term assets and can include e.g. salaries, rent, insurance, maintenance, and repair costs. These costs can be divided into two categories: (1) fixed operation and maintenance and (2) variable operation and maintenance (Stehly, Beiter, & Duffy, 2020). Here, the fixed costs are considered scheduled operation and maintenance or land lease costs, while the variable is unscheduled operation and maintenance costs.

At the end of the wind turbine's lifespan, there is a decommissioning expenditure (DecEx) which includes the decommissioning of the wind turbine itself, as well as clearance of the site. Figure 3.20 shows the cost breakdown for an offshore wind turbine.

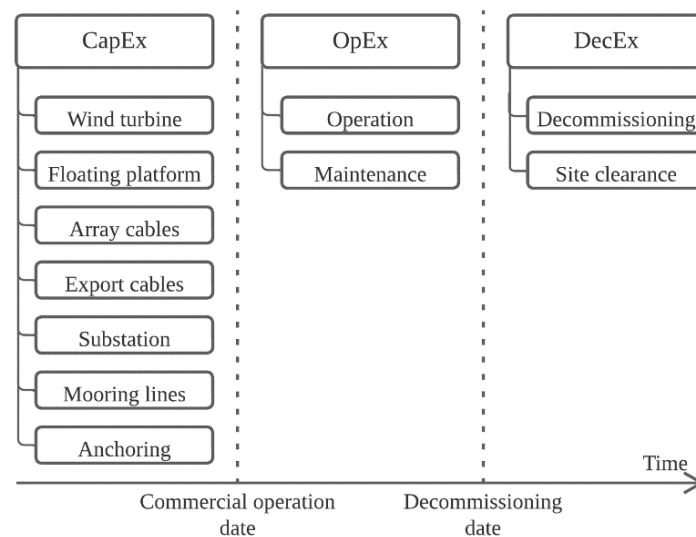


Figure 3.20 Cost Breakdown of an Offshore Wind Farm, derived from Ren et al. (2021)

3.7.3 Levelized Cost of Energy

LCOE is a metric for estimating the average cost of producing electricity from a specific source throughout its lifespan (Emblemsvåg, 2020). The LCOE for an energy project is the quantitative representation of the cost-effectiveness of the project, which can be calculated as the quotient of the total project cost and the cumulative electricity generation over the project's lifespan. Eq. (3.21) shows how the LCOE of a power generation site is computed:

$$LCOE = \frac{(CapEx * FCR) + OpEx}{AEP_{net}} \quad (3.21)$$

where $CapEx$ is the investment expenditures, $OpEx$ is the operations and maintenance costs, FCR is the fixed charge rate, AEP is the annual energy generation. After calculating the LCOE, the generated number is most frequently given in dollars per megawatt-hour [\$/MWh].

The FCR is the percentage of capital costs that needs to be allocated to cover the cost of capital (Bosch, Staffell, & Hawkes, 2019). The equation used to calculate the FCR, Eq. 3.22, encompasses both the interest paid on debt and the return on equity, so $CapEx * FCR$ results in the constant yearly annuity payment. FCR is presented in the following equation:

$$FCR = \frac{WACC}{1 - (WACC + 1)^{-n}} \quad (3.22)$$

where $WACC$ is the weighted average cost of capital and n the economic lifetime of the system.

3.8 Discounted Cash Flows

According to the discounted cash flow (DCF) valuation, the conventional corporate finance method for determining an asset's worth is to estimate its market value (Damodaran, Valuation Approaches and Metrics: A Survey of the Theory and Evidence, 2005). This method states that the fundamental value of an asset is the present value of the asset's anticipated future cash flows, which is discounted at a rate that represents the cash flows' level of risk. The DCF approach is the most extensively used valuation method in business today, as the theoretical foundation enables it to be used to assess a wide range of financial assets, including individual projects, instruments of fixed income, and whole companies (Petersen, Plenborg, & Kinserdal, 2017).

3.8.1 Net Present Value Model

The net present value (NPV) method of economic assessment is likely the most well-liked and developed method (Zizlavsky, 2014). It entails applying a predetermined discount rate to the sum of all future cash flows originating from the potential investment. To estimate the NPV, the initial investment cost, C_0 , is added to the present value (PV) of the future cash flow, yielding (Brealey, Myers, & Allen, 2011):

$$NPV = C_0 + PV = C_0 + \sum_{t=1}^T \frac{C_t}{(1 + r)^t} \quad (3.23)$$

where C_t is the cash flow in year t , and r represents the discount rate.

As a result of the NPV approach, a risk-associated profit tomorrow is less valued than a certain profit today (Gailly, 2011). Therefore, annual discounts are applied to future cash flows. The opportunity cost of the capital estimated is reflected in the discount rate and rises in proportion to the opportunity's projected risks. If the investment is financed with both equity and debt, the discount rate will reflect a combination of the costs, thus, the weighted average cost of capital

(WACC). However, bigger profits are anticipated from riskier projects, indicating that this technique considers the risk, whereas other metrics like return on investment (ROI) or internal rate of return (IRR), do not.

3.8.2 Internal Rate of Return

The IRR is a metric for the return on investment as a percentage (Ruegg & Marshall, 1990). To determine an investment's economic feasibility, the IRR is compared to the investor's discount rate. The investment is profitable if the IRR is higher than the discount rate. If it is less, the investment is not feasible. An investment's savings or returns just match its costs if the IRR is equal to the discount rate, hence the NPV is zero. IRR can be denoted as (Brealey, Myers, & Allen, 2011):

$$NPV = \sum_{t=0}^n \frac{CF_t}{(1 + IRR)^t} = 0 \quad (3.24)$$

where CF represents the cash flow, t is the period, and n is the number of periods.

3.9 Existing Literature

Myhr et al. (2014) conducted an extensive investigation and comparison of the LCOE for solutions for floating wind turbines. The findings suggested that, in comparison to bottom-fixed designs, electricity from floating wind turbines may be produced at an equivalent or reduced LCOE. Several important cost-driving factors were found, and it was feasible to differentiate between characteristics that were not certain and those that were location dependent and thus predictable. Discount rate, distance from the shore, farm size, and depth were the factors that were most sensitive to the LCOE of the predictable factors. Of the less certain factors, the accuracy of the load factor and volatility in steel pricing were two of the key elements that separated the foundation solutions foremost.

Corresponding with Aldersey-Williams et al. (2019) and Myhr et al. (2014), Lerch et al. (2018) identified discount rate and load factor as highly influential parameters on the LCOE. Furthermore, Lerch identified additional significant parameters that exerted a considerable impact on the LCOE and could be crucial for achieving further cost reductions. Specifically, among the parameters examined in the study, the ones that displayed the most substantial variation in LCOE were those associated with manufacturing costs, such as the expenses related to the wind turbine, substructure, and mooring system. Therefore, the study concludes that it is imperative to develop a cost-optimized design that encompasses all the components of a floating offshore wind turbine, which should be taken into account at the initial design phase.

Aldersey-Williams et al. (2019) conducted a study aimed at exploring the implementation of long-term contractual arrangements to lower LCOE for an offshore wind farm. The discount rate, which reflects the investment risk associated with the project, is a critical consideration in this regard. The introduction of contractual agreements of this nature serves to substantially mitigate revenue risk for developers. Bruck et al. (2018) support this assertion, having developed a novel cost model for assessing the LCOE of wind power sourced from a power purchase agreement (PPA). The application of this model demonstrates that the actual LCOE is contingent upon the specific minimum and maximum energy purchase thresholds outlined in the contract. This cost model, as a result, can serve as a valuable framework for establishing appropriate PPA conditions such as pricing schedules and performance metrics.

Castro-Santos et al. (2016) established an approach to assess the viability of a floating offshore wind farm economically. The proposed methodology acknowledges that the life-cycle cost of a floating offshore wind farm encompasses the costs incurred during each phase of its lifespan. Specifically, the methodology identifies six cost categories, including concept and definition cost, design and development cost, manufacturing cost, installation cost, exploitation cost, and dismantling cost. Moreover, these categories are further divided based on their sub-costs and are aligned with the five components that constitute a floating offshore wind farm, which are offshore wind turbine, floating platform, mooring, anchoring, and electric system. The methodology culminates with the computation of economic feasibility indicators, such as internal rate of return, net present value, and pay-back period.

4. Research Question

Floating wind farms are becoming an increasingly popular option for harnessing wind energy in locations where traditional fixed-bottom offshore wind turbines are not feasible. These floating wind turbines can operate in deep water, which opens new possibilities for wind energy development in areas with strong winds and limited shallow water access. Norway is a reasonable location for developing wind farms, with a long coastline and significant wind resources. However, as with any major infrastructure project, it is important to consider the life cycle costs associated with the development and operation of such a project.

Life cycle costs refer to the total costs associated with a project over its entire life cycle, from design and operation to operation and decommissioning. For a floating wind farm, these costs would include the initial capital expenditures for building and installing the turbines and substructures, as well as ongoing operation and maintenance costs, and eventual decommissioning costs. Understanding the life cycle costs of a floating wind farm off the coast of Norway is critical for evaluating the economic feasibility of such a project and for making informed decisions about wind energy development in the region. Additionally, a thorough analysis of these costs can provide valuable insights into ways to optimize the design and operation of floating wind farms to minimize costs and maximize the benefits of this important renewable energy source.

Therefore, the main research question is as follows:

How to estimate the life cycle costs of a floating wind farm off the coast of Norway?

With the partial objectives of:

- 1. Identifying and analyzing key cost drivers throughout the life cycle*
- 2. Understanding how the different input parameters influence the LCOE*
- 3. Assessing the financial metrics of the wind farm investment*

The levelized cost of energy is a common measure for evaluating the price of producing energy, thus, this is the first partial objective of the thesis. Further, the purpose is to determine how the various costs contribute towards the levelized cost of energy, and how the final cost is affected by changes in parameters such as wind farm size, turbine size, and environmental conditions. The third objective is to calculate the economic feasibility of the wind farm, when it is considered as an investment.

5. Case & Materials

5.1 System Description

The system description consists of defining the properties and characteristics of the systems used in the modeling for the cost calculations performed in this thesis. This includes the moored floating substructure with different types of turbine power rating. The system properties used in this thesis are based on the models developed by Jonkman et al. (2014) and Gaertner et al (2020). These system models have been developed to support conceptual studies for evaluating offshore wind technology with the use of representative wind turbines and substructures.

5.1.1 System Description of the Semisubmersible Substructure

The semisubmersible substructure is modeled based on the Offshore Code Comparison Collaboration Continuation (OC4) system developed by the National Renewable Energy Laboratory (NREL) (Nunemaker, Shields, Hammond, & Duffy, 2020). The OC4 Deepwind is a semisubmersible floater involving three offset columns supporting the main tower column in the center (Jonkman, et al., 2014). All of these columns are attached through a set of smaller cross members and pontoons. For the OC4 system, NREL has developed dynamic scaling factors based on earlier research, this means that the system characteristics vary based on the turbine power rating. The significance of this is that the modeled size and weight of the substructure are based on the power rating of the turbines, being a prototypical version of a fully engineered structure. While being based on the OC4 system, the system properties can change centered around alterations of the input parameters. Table 5.1 displays the main characteristics of the OC4 system and based on which input the parameters can get dynamically scaled. Figure 5.1 displays a top and side view of the semisubmersible substructure system.

Table 5.1 Substructure, Based on a Scaling Method of the OC4 Semi-Substructure

Parameter	Value	Unit	Dynamic Scaling
Number of offset columns	3	pcs	N/A
Tower column placement	center	placement	N/A
Depth of platform base below SWL	20	m	Turbine size
Elevation of the main column above SWL	10	m	Turbine size
Elevation of offset columns above SWL	12	m	Turbine size
Spacing between offset columns	50	m	Turbine size
Length of upper columns	26	m	Turbine size
Length of base columns	6	m	Turbine size
Depth to top of base columns below SWL	14	m	Turbine size
Diameter of the main column	6.5	m	Turbine size
Diameter of offset (upper) column	12	m	Turbine size
Diameter of offset (lower) column	24	m	Turbine size
Diameter of pontoons and cross braces	1.6	m	Turbine size

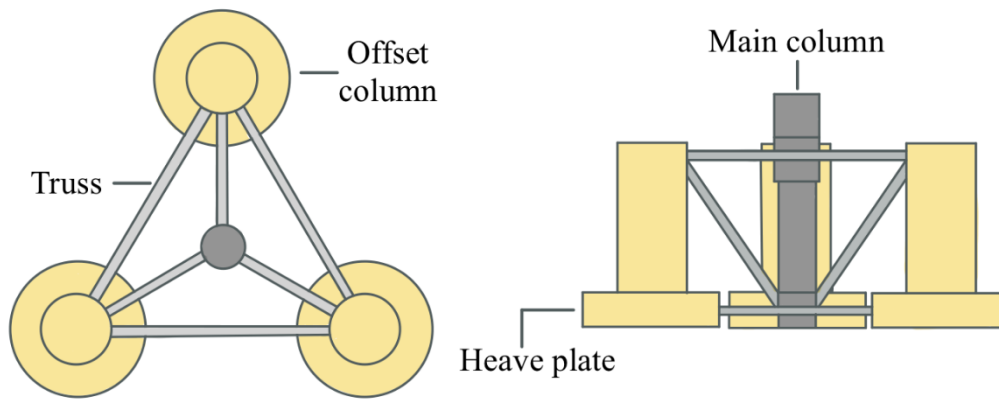


Figure 5.1 Top and Side View of the Semisubmersible Floater

5.1.2 System Description of the Mooring Properties

Coupled with the OC4 substructure three homogenous mooring lines are connected to each of the offset columns (Jonkman, et al., 2014). For the OC4 model, the mooring properties are based on a 5 MW turbine and a water depth of 200 m. In the modeling efforts performed by ORBIT in this thesis these mooring characteristics can get altered based on the water depth and turbine sizes. Table 5.2 displays the key mooring characteristics and how the properties get dynamically scaled based on input considerations, while the mooring line direction can be perceived in Figure 5.2.

Table 5.2 Mooring for Water Depth 200 m

Parameter	Value	Unit	Dynamic Scaling
Number of mooring lines	3	pcs	N/A
Angle between adjacent lines	120	degrees	N/A
Depth to anchors below SWL	200	m	Water depth
Depth to fairleads below SWL	14	m	N/A
Unstretched mooring line length	835.5	m	Water depth
Mooring Line Diameter	0.0766	m	Turbine size

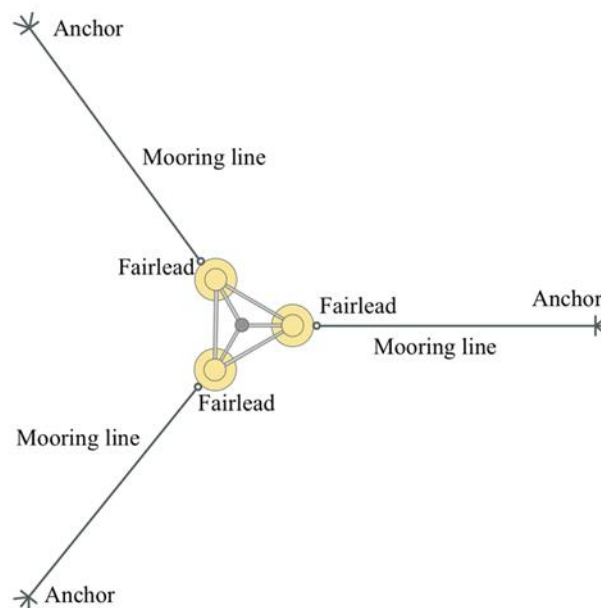


Figure 5.2 Top View of the Mooring Line Structure

5.1.3 System Description of the Floating Wind Turbines

In this thesis there are three wind turbines in use: (1) the 6MW, (2) the 12MW, and (3) the 15MW, where the 15 MW turbine is the most extensively used. All turbine characteristics are either based on the NREL models by Gaertner (2020) or from example models produced by NREL provided in the ORBIT module. All of the wind turbines are conventional three-bladed turbines but have dissimilarities in the tower, nacelle, blade, and wind characteristics. Table 5.3 exhibits the significant turbine system characteristics for each of the three turbines, and Figure 5.3 displays a side view of the full turbine-substructure-mooring system used in this thesis.

Table 5.3 Description of Turbines

Description	Unit	6 MW Turbine	12 MW Turbine	15 MW Turbine
General information				
Power rating	MW	6	12	15
Number of blades	pcs	3	3	3
Rated wind speed	m/s	13	11	10.59
Cut-in	m/s	3	3	3
Cut-out	m/s	25	25	25
Tower				
Area	m ²	36	50.2	78.5
Length	m	110	132	150
Mass	tons	150	399	480
Nacelle				
Area	m ²	200	203	242
Mass	tons	360	604	797
Hub height	m	110	132	150
Blade				
Area	m ²	100	385	480
Length	m	75	107	120
Mass	tons	100	54	72
Rotor diameter	m	154	215	240

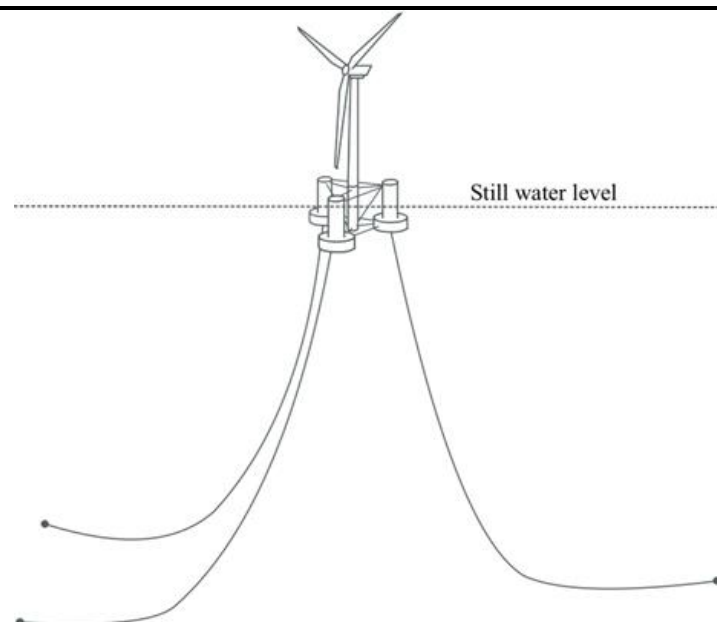


Figure 5.3 Side View of the Floating Wind Turbine System

5.2 Description of Site Conditions

For this study, a conceptual wind farm for a specific location will be assessed. This section will present and define the environmental conditions and boundaries for the location. Equinor has in corporation with Shell, ConocoPhillips, TotalEnergies, and Petoro, initiated a study for evaluating the opportunity of a floating wind farm, hereby denoted as Trollvind (Equinor, 2023). The energy production is planned to begin in 2027, and the purpose of the wind farm is to provide nearby oil platforms with electricity and distribute the surplus to onshore power plants.

5.2.1 Geographical Description

The North Sea is a variation of intermediate and deep water with an average depth of 90 m and a maximum depth of 700 m (European Maritime Spatial Planning Platform, 2022). It is characterized by a varied seabed composition comprising mud, sandy mud, gravel, and sand, with a diverse array of marine landscapes such as sandbanks, bays, and intertidal mudflats (Walday & Kroglund, 2020). Located in temperate latitudes, the North Sea is subject to a climate heavily affected by the inflow of oceanic water from the Atlantic Ocean and the large-scale westerly circulation of air, which regularly includes low-pressure systems. Extreme meteorological conditions exert a direct influence on the hydrography of the region, which is distinguished by the exchange of water with surrounding ocean areas and the impact of strong tides.

The Trollvind wind farm is located in the northern part of the North Sea, along the Norwegian coast, with a water depth of approximately 325 m. (Equinor, 2023). The area has not previously been developed, as the only current floating wind farm in Norway, Hywind Tampen, is located 128 km northwest of the site. The entire Troll field where the wind farm will be located is 750 km² in total and already consists of three oil platforms. Figure 5.4 displays the general geographical location of the Trollvind field.

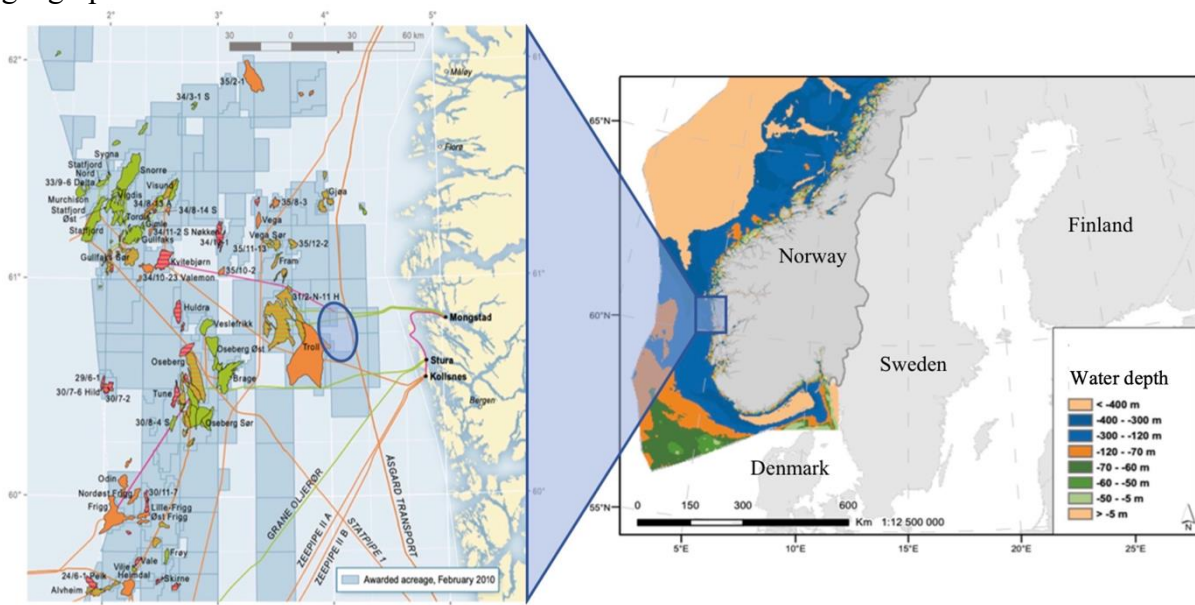


Figure 5.4 Geographical Location of Trollvind

Trollvind is located approx. 65 km west of Kollsnes, where the produced electricity will be transported via export cables. The wind turbines are proposed installed between the three oil platforms Troll A, Troll B, and Troll C. From the wind site, it is 75 km to the nearest harbor applicable for launching the turbines and substructures. Figure 5.5 displays a conceptual sketch of the wind field and the power distribution cables.

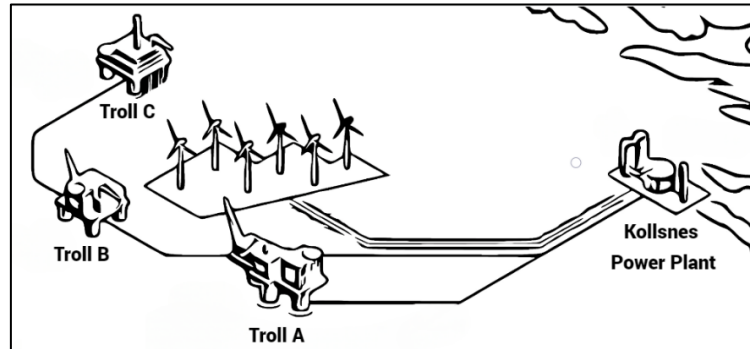


Figure 5.5 Trollvind Conceptual Sketch

5.2.2 Metocean Conditions

According to Johannessen et al. (2002), the weather conditions at an offshore site can be described by three parameters: (1) mean wind speed (W_μ), (2) significant wave height (H_s), and (3) wave spectral peak period (T_p). By fitting analytical distributions to the metocean raw data for an offshore site, it is possible to obtain marginal distributions and joint distributions of the wind and wave conditions (Li, Gao, & Moan, 2023).

When considering a combined approach, the power output from wind turbines and wave energy converters can be estimated using the joint distribution of W_μ , H_s , and T_p . The marginal distributions of both waves and wind are offered for the scenario when wind and wave power are calculated independently. Using the wind turbine's power curve, the marginal distribution of W_μ can be utilized to calculate the wind power. Similar to this, the wave power can be estimated using the wave energy converter's power matrix and the combined distributions of H_s and T_p . Figure 5.6 displays the significant wave height at the location for Trollvind, with data retrieved from Norwegian Centre for Climate Services (2023).

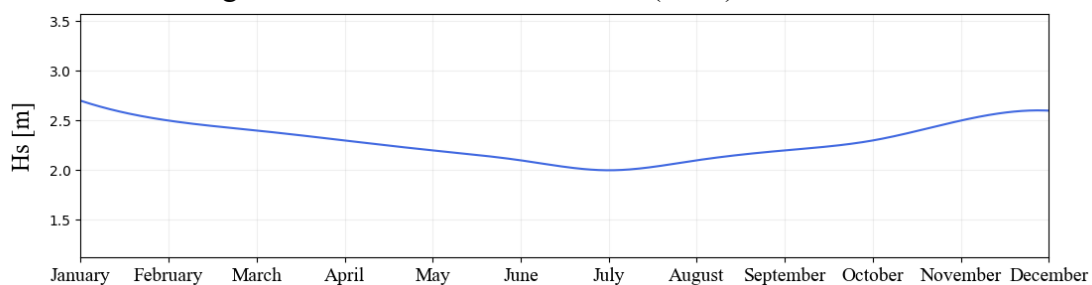


Figure 5.6 Monthly Significant Wave Height at Trollvind, 2013-2022

As to Figure 5.6, the significant wave height is at its lowest during June, July, and August, while the wave height is at its highest in December and January. The wave height, combined with the wind speed are two critical factors when evaluating a location, as it could impact the conditions for operations and maintenance (Ren, Verma, Li, Teuwen, & Jiang, 2021).

To provide a convenient description of the wind speed data for Trollvind, a two-parameter Weibull distribution is created. The distribution, along with the mean wind data is illustrated in Figure 5.7. The shape parameter (α) determines the shape of the distribution curve, while the scale parameter (β) determines the scale or size of the distribution.

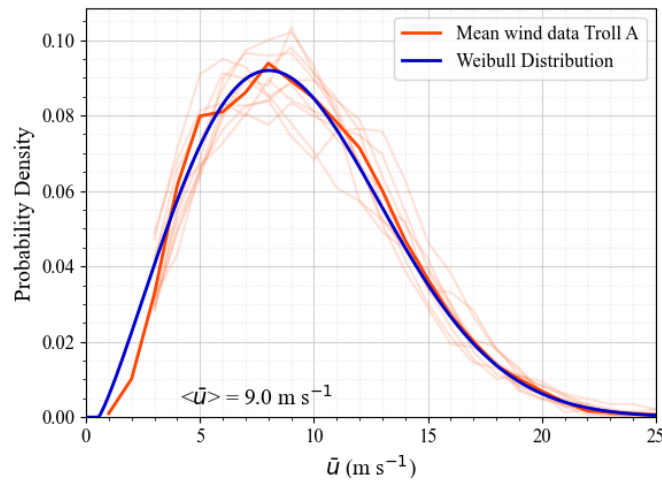


Figure 5.7 Weibull Distribution and Mean Wind Data

The mean wind speed \bar{u} for the period 2013-2022 is 9.0 m s^{-1} , measured at 10 m above sea level (Norwegian Centre for Climate Services, 2023). The shape parameter is calculated to be 9.90, while the scale is 2.18.

To design the wind farm layout, it is vital to evaluate the wind direction in addition to the wind speed. Figure 5.8 illustrates the intensity and direction of the wind conditions in a wind rose. The wind rose is based on data from the Norwegian Centre for Climate Services and displays the percentage distribution in a 360-degree view (2023).

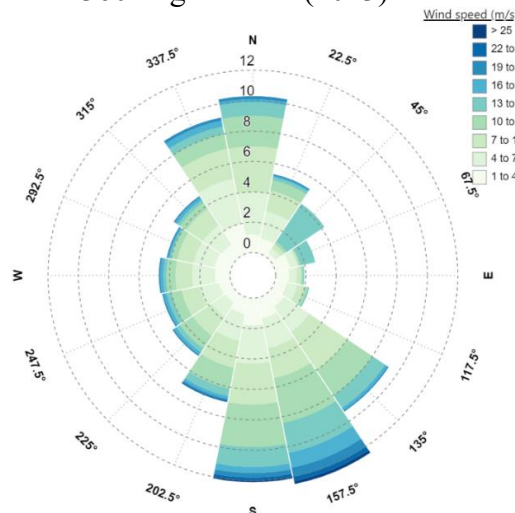


Figure 5.8 Trollvind Wind Rose

Illustrated in the wind rose, the most frequent wind direction is the south/southeast sector with over 35 % of the total wind, followed by north/northwest. Additionally, the south/southeast wind has the most significant wind speeds, thus it is the only direction where wind speeds of over 25 m/s occur. The least frequent wind direction is the east sector, with only 5 % of the wind originating from this sector.

6. Methodology

This section will present the methodological approach of this thesis, where the work can be separated into three primary phases, as shown in Figure 6.1.

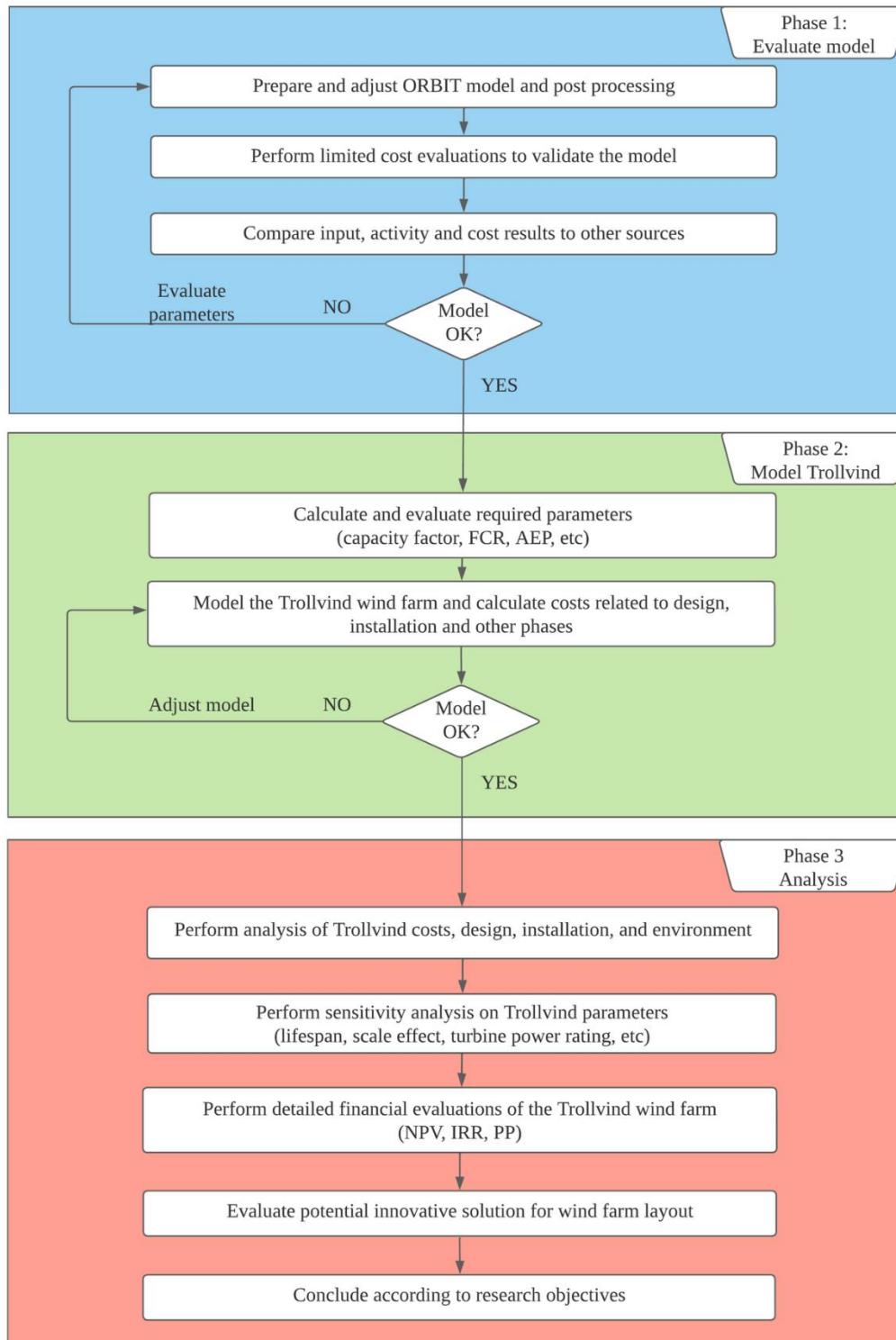


Figure 6.1 Flowchart of the Work Progress

6.1 Software

6.1.1 Microsoft Excel

Microsoft Office Excel is a software application created by Microsoft that employs spreadsheet functionality (Microsoft, 2023). Its wide range of preprogrammed formulas and table creation options make it a versatile tool for data analysis. In this thesis, Excel is mainly used to calculate the LCOE and financial parameters, as well as adjust for inflation and perform other smaller calculations.

6.1.2 Python

Python is an interpreted, object-oriented, and high-level programming language (Rossum, 2007). It is a general-purpose language, i.e., it can be used to create a variety of different programs and it is not specialized for any specific problems. Python is used to illustrate the calculations that are performed in Excel, thus creating all the graphs and figures that are presented in Section 7. Results.

6.2 ORBIT

The Offshore Renewables Balance-of-system and Installation Tool (ORBIT) is a calculation module developed by NREL (Nunemaker, Shields, Hammond, & Duffy, 2020). This module provides modeling of onshore and offshore wind farms and their associated components. Together with the modeling ORBIT provides cost assessments for the capital costs of all components (except for the turbine cost), and costs for installation, project developments, and soft costs. These costs are split into the design phase (detailed engineering, procurement, and construction), the installation phase, and other costs (soft, decommissioning, and project costs). ORBIT is a python based open-source module and NREL (2020) describes the key usage of ORBIT as:

“The model provides a tool for offshore wind industry stakeholders to evaluate the impact of project design decisions and installation strategies on balance-of-systems costs. ORBIT uses simple and scalable representations of major project components. These first-order designs are lower fidelity than those produced by detailed engineering models, but they provide reasonable estimates of component costs, sizes, and masses using a number of user inputs.”

6.2.1 Primary Parameters

ORBIT includes over 100 different parameters that can be user-defined, whereas this section has the purpose of presenting some of the most significant parameters (Nunemaker, Shields, Hammond, & Duffy, 2020). These primary parameters are the central properties of the model and are often required for the model to function. Table 6.1 presents these main user-defined parameters in ORBIT.

Table 6.1 Primary User-Specified Parameters Utilized

Parameter	Unit	Affects
Number of Turbines	[pcs]	All costs and AEP
Turbine Rating	[MW]	All costs and the AEP
Rotor Diameter	[m]	Turbine and array costs
Hub Height	[m]	Turbine costs
Water Depth	[m]	Mooring and array costs
Distance to Shore	[km]	Export system and all installation costs
Distance to Installation Port	[km]	Export system and all installation costs
Substructure/Foundation	[type]	All costs
Array Row Spacing	[rotor width]	Array costs
Array Turbine Spacing	[rotor width]	Array costs
Cable Burial Depth	[m]	Array installation costs
Anchor Type	[type]	Mooring system and installation costs
Number of Anchors	[pcs]	Mooring system and installation costs
Tower Installation Method	[type]	Turbine installation costs
Turbine Installation Method	[type]	Turbine installation costs
Installation Weather Downtime	[weather on/off]	All installation costs
Interconnect Voltage	[type]	Array costs
Array Cable Size #1	[type]	Array costs
Array Cable Size #2	[type]	Array costs
Export Cable Voltage	[type]	Export system costs
Export Cable Size	[type]	Export system costs
Distance to Interconnect	[m]	Export system costs
Turbine Capital Cost	[\$/MW]	Turbine costs
Scrap Value in Decommissioning	[\$/ton]	Development costs

6.2.2 Parameters of a Floating System

Since the floating structural platform is based on numerous parameters some calculations have to be performed. The mass of the semi-submersible platform is based on a curve-fit relationship that scales based on the wind turbine rating (Maness, Maples, & Smith, 2017). For the semi-submersible floater, this relationship affects the mass of the stiffened column (M_{sc}), truss (M_t) and heave plate (M_{hp}), these scaling methods are based on previous NREL modeling and can be seen in Eq 6.1, Eq 6.2, and Eq 6.3.

$$M_{sc} = -0.9571 * T_r^2 + 40.89 * T_r + 802.09 \quad (6.1)$$

$$M_t = 2.7894 * T_r^2 + 15.591 * T_r + 266.03 \quad (6.2)$$

$$M_{hp} = -0.4397 * T_r^2 + 21.545 * T_r + 177.42 \quad (6.3)$$

where T_r is the turbine rating.

For each of the floating structures comes the supporting mooring lines which can differ in weight length and diameter based on specific parameters. The mooring line diameter (D_m), length (L_m), and mass (M_m) and can be calculated using the formulas Eq. 6.4, Eq. 6.5, and Eq. 6.6.

$$D_m = -0.0004 * T_r^2 + 0.0132 * T_r + 0.0536 \quad (6.4)$$

$$L_m = 0.0002 * W_d^2 + 1.264 * W_d + 47.776 + L_{m,f} \quad (6.5)$$

where W_d is the water depth and $L_{m,f}$ being the length of the fixed mooring line which is set to 500 meters.

$$M_m = L_m * Unit\ weight \quad (6.6)$$

From these modeled masses for the substructure and mooring lines the total cost of the floating structure can be calculated. This is performed by using a unit cost for the mooring lines and the steel compartments, presented in Table 6.2.

Table 6.2 Mooring Line and Semi-submersible Floater Costs

Description	Unit	Unit Cost (2017 dollars)
Mooring line 0.09 m	m	\$ 399
Mooring line 0.12 m	m	\$ 721
Mooring line 0.15 m	m	\$ 1088
Stiffened Column	ton	\$ 3120
Truss	ton	\$ 6250
Heave plate	ton	\$ 6250
Outfitting Steel	ton	\$ 7250

6.2.3 Electric Components

When the inter-array grid infrastructure is modeled, some properties must be calculated (Maness, Maples, & Smith, 2017). Initially, the number of array strings, number of turbines per string, and number of turbines per array cable size must be calculated. The number of array strings (A_n) are given by Eq 6.7.

$$A_n = \frac{T_n * T_r}{\sqrt{3} * C_r * C_v * P_f * \frac{(1 - (B_d - 1) * B_f)}{1000}} \quad (6.7)$$

where T_n is the number of turbines, C_r and C_v is the cable rating and voltage, the power factor (P_f) are set to 95 % and B_d and B_f is the bury depth and factor. The number of turbines per array cable ($T_{n,a}$) are given as Eq 6.8, where the scaling connection determines the maximum number of turbines. This can also be written as the relationship between the power capacity of the cables (C_p) and the turbine rating.

$$T_{n,a} = \frac{\sqrt{3} * C_r * C_v * P_f * \frac{(1 - (B_d - 1) * B_f)}{1000}}{T_r} = \frac{C_p}{T_r} \quad (6.8)$$

From Eq 6.8 ORBIT calculates the number of turbines and further defines all cables. Afterward, the last string turbine is assigned to the smallest cable type since it is farthest away from the substation (Maness, Maples, & Smith, 2017). Then the number of turbines for each cable type can be computed accounting for the power produced by the turbines with the smallest cable. For all array strings, the inter-array cables have to be hung under the floating substructure, with a given cable distance between all of the substructures. The catenary free-hanging cable length (L_{C-FH}) can be designed with Eq 6.9, while the fixed bottom cable length (L_{C-FB}) has been given in Eq 6.10.

$$L_{C-FH} = \frac{W_d}{\cos(-0.0047 * W_d + 18.743)} * (L_{f,c} + 1) + 190 \quad (6.9)$$

where the catenary length factor ($L_{f,c}$) is set to 4 %.

$$L_{C-FB} = (T_s * T_d) - (2 * \tan((-0.0047 * W_d + 18.743)W_d) - 70 \quad (6.10)$$

These equations provide the total array cable length, C_l , which can be calculated as:

$$C_l = 2 * W_d + (T_d * T_s) \quad (6.11)$$

where T_d is the turbine rotor diameter and T_s is the turbine spacing.

The export cable modeling follows many of the same principles as the inter-array cables. However, the number of export cables ($C_{n,e}$) must be considered based on the relationship between the rated power of the export cables (C_p) and the plant capacity (P_c). This correlation provides the total number of export cables which can be perceived in Eq 6.12.

$$C_{n,e} = \frac{P_c}{C_p} \quad (6.12)$$

The offshore substation is modeled in ORBIT based on previous developments created by NREL (2020). The substation size is mainly based on the size of the needed main power transformer. The power rating of the power transformer (MPT_r) is given in Eq 6.13, and the total cost of the substation (OSS_{cost}) are given in Eq 6.14 where the other scaling costs are based on the rating of the main power transformer. For more detailed information on the scaling

effect of the offshore substation components the ORBIT description report can be studied (Nunemaker, Shields, Hammond, & Duffy, 2020).

$$MPT_r = \frac{T_n * T_r * 1.15}{T_n * T_r} \quad (6.13)$$

$$OSS_{cost} = MPT + TS + SR + SG + AS + OSS_{assembly} + OSS_{substructure} \quad (6.14)$$

where *MPT* is the main power transformer, *TS* is the substation topside, *SR* is the substation shunt reactor, *SG* is the substation switchgear, and *AS* is the substation ancillary system.

After the full electrical grid with inter-array cables, export cables, and offshore substations have been modeled the total cost of the grid can be calculated. This is performed by using the unit costs for the electrical compartments, these main unit costs are given in Table 6.3.

Table 6.3 Offshore Substation, Array and Export Cable Costs

Description	Unit	Unit Cost (2017 dollars)
XLPE 185mm 66kV	km	\$ 200 000
XLPE 400mm 33kV	km	\$ 300 000
XLPE 500mm 132kV	km	\$ 200 000
XLPE 630mm 33kV	km	\$ 450 000
XLPE 630mm 66kV	km	\$ 400 000
XLPE 1000mm 220kV	km	\$ 850 000
Substation fabrication	ton	\$ 14 500
Substation topside design	pc	\$ 4 500 000
Substation jacket	ton	\$ 6 250
Substation pile/jacket	ton	\$ 2 250
Main power transformer	mega volt ampere	\$ 12 500
Medium voltage switchgear	pc	\$ 950 000
High voltage switchgear	pc	\$ 500 000
Offshore shunt reactors	mega volt ampere	\$ 35 000
Diesel generator backup	pc	\$ 1 000 000
Housings and fire protection	pc	\$ 2 000 000
Other ancillary costs	pc	\$ 3 000 000

6.2.4 Vessels for Installation

For all installation phases, the need for a variety of vessels needs to be considered (Nunemaker, Shields, Hammond, & Duffy, 2020). ORBIT introduces six different types of vessels and five sub-vessels with features like larger docking space, larger lifting capacity, etc. All 11 vessels have different day rates, transit speeds, storage space, crane specs, and so on. Each of the vessels has a different use in the installation process based on the type, size, and depth, while some vessels act as support vessels in the installation process. Table 6.4 provides an overview of some of the main characteristics of the six main vessels.

Table 6.4 Vessel Types Used in the Installation Stage

Description	Heavy Lift	Cable Lay	Support	Tow
Field of application in installation	Heavy lifting	Power cable laying	Support, towing, installation	Towing
Transit speed	7 km/h	11.5 km/h	10 km/h	6 km/h
Cable lay speed	N/A	0.2 km/h	N/A	N/A
Cargo capacity	8 000 t	4 000 t	5 000 t	N/A
Deck space	4 000 m ²	N/A	1 000 m ²	N/A
Mobilization days	7	7	7	0
Day rate (2017 dollars)	\$ 500 000	\$ 120 000	\$ 100 000	\$ 3 000

Together with the day rates of the vessels, the port and staging costs must be evaluated. These costs are associated with all the processes occurring at the port and storage spaces. The cost rates for these practices are presented in Table 6.5.

Table 6.5 Port and Staging Unit Costs

Description	Unit	Unit Cost (2017 dollars)
Vessel entrance and exit	m ² /occurrence	\$ 0.53
Quayside docking	day rate	\$ 3 000
Loading/unloading	ton	\$ 2.8
Open storage	m ²	\$ 0.25
Crane 600-ton capacity	day rate	\$ 5 000
Crane 1000-ton capacity	day rate	\$ 8 000
Crawler crane mobilization	pc	\$ 150 000
Self-propelled transport unit	ton/day	\$ 1.5

6.2.5 Scour Protection Design

All fixed substructures are subject to hydrodynamic scour (Nunemaker, Shields, Hammond, & Duffy, 2020). This development of scour can be limited by installing layers of rocks, sand, or alike materials around the base of the fixed structure (jacket/monopile foundation). ORBIT models this design process based on the DNV-RP-0618, which is performed in a simplified scaling effect since the scour protection represents a minuscule cost of the overall fixed system. The scour depth (S_d), radius (S_r) and volume (S_v) can be calculated with the use of Eq. 6.15, Eq. 6.16, and Eq. 6.17:

$$S_d = 1.3D_f \quad (6.15)$$

$$S_r = \frac{D_f}{2} + \frac{S_d}{\tan(\varphi)} \quad (6.16)$$

$$S_v = \pi d_t S_r^2 \quad (6.17)$$

where D_f is the foundation diameter, φ is the soil friction angle, and d_t is the depth of the scour protection material installed. The cost of the scour protection is \$ 250 000 per ton.

6.2.6 Indirect Costs

Alongside the firm costs of construction and installation some additional expenses must be considered, this includes engineering, management, development, and financial costs (Maness, Maples, & Smith, 2017). The engineering and management cost is related to detailed design engineering for the substructure and other steel compartments (the offshore substation is considered in 6.2.3). While the development costs are all expenses that precede the construction phase, this includes a lot of stages like design studies, environmental studies, pre-studies (physical, biological, socioeconomic, etc.), state leasing process, site assessment, legal processes, etc. These development costs are included in the total project costs. The financial aspect of soft cost includes insurance, project financing, contingency, commissioning, and decommissioning, these costs have been modeled after the cost of energy review presented by Stehly and Beiter (2019). An overview of these unit costs is given in Table 6.6.

Table 6.6 Indirect Costs

Description	Unit	Unit Cost (2017 dollars)
Detailed substructure engineering	pc	\$ 3 000 000
Detailed design of secondary steel	pc	\$ 600 000
Staffing and overhead	kW	\$ 60
Engineering and management	% of installation	% 4
Insurance	kW	\$ 44
Project financing	kW	\$ 183
Contingency	kW	\$ 316
Commissioning	kW	\$ 44
Decommissioning	kW	\$ 58

6.2.7 Transportation, Installation, and Port Specifications

After the design, procurement construction, and so forth have been completed the installation process is impending. This includes procedures like port staging, transit to the site, site preparations, installation, and controlling (Nunemaker, Shields, Hammond, & Duffy, 2020). ORBIT performs comprehensive calculations based on a set of defined durations with dynamic adjustments based on the inputs derived from the design phases. From the primary input parameters in 6.2.1 and the design phase, the complete installation phase gets calculated. This is a scalable and dynamic process that evaluates input and design sizes when estimating port fees, installation time, transit time, vessel types, etc.

After the procurement and port assembly are finished the installation can begin. When evaluating the number of vessels needed a crucial calculation to perform is how much of the material or component can get transported by the vessel in a set (n_{sets}). This calculation is performed by Eq 6.18, and ORBIT is restricted to transporting entire sets instead of taking separate trips.

$$n_{sets} = \min \left(\left\lfloor \frac{M_{available}}{M_{required}} \right\rfloor, \left\lfloor \frac{S_{available}}{S_{required}} \right\rfloor \right) \quad (6.18)$$

where $M_{available}$ is the available mass of the vessel while $M_{required}$ is the required mass of the vessel, and $S_{available}$ is the available deck space of the vessel while $S_{required}$ is the required deck space of the vessel.

When all the material or the components have been loaded onto the deck, the transportation vessel can leave the port and head towards the construction site. The transit duration ($t_{transit}$) are dependent on the speed of the vessel (s_{vessel}) in use and distance from the landfall ($d_{port-site}$), which can be calculated using Eq.6.19.

$$t_{transit} = \frac{d_{port-site}}{s_{vessel}} \quad (6.19)$$

For bottom-fixed and floating structures the need for a jack-up wind turbine installation vessel or a heavy lift vessel is necessary. These vessels are often in use when installing bottom-fixed and floating structures together with turbines and offshore substations. The vessel positions itself at the site before jacking up to a secure position and surveying the seabed using a remotely operated vehicle. The jack-up duration ($t_{jack-up}$) is dynamically calculated using Eq.6.20.

$$t_{jack-up} = \frac{W_d}{s_{ext}} + \frac{e_{ext} - W_d}{s_{lift}} \quad (6.20)$$

where s_{ext} is the speed of the unloaded jacking system, e_{ext} is the eventual extension, and s_{lift} is the speed of the jacking system when lifting a vessel.

When installing inter-array and export cables the transportation loading process differs. Where Eq. 6.18 inspects the available deck space, the cable installation controls for the available cable length that can get loaded onto the cable drum. This relationship for estimating the available cable length $l_{available}$ can be calculated with Eq.6.21.

$$l_{available} = \frac{M_{available}}{\lambda_{cable}} \quad (6.21)$$

where λ_{cable} is the linear density of the cable.

An overview of all the relevant durations and port information for the installation process has been exemplified in Table 6.7. Further, Figure 6.2 displays a top-level overview of the procedures for the installation and design process.

Table 6.7 Parameters Used for Modeling Costs for Installation

Installation Phase	Process	Duration/pcs	Dynamic Duration	
Cables	Array	Lay/bury cable	0.5 km/h	Dynamic based on length
		Position onsite	2 h	N/A
		Prepare cable	1 h	N/A
		Lower cable	1 h	N/A
	Array and export	Pull cable into turbine	5.5 h	N/A
		Test and terminate cable	5.5 h	N/A
		Cable splice	48 h	N/A
	Export	Dig trench	0.1 km/h	Dynamic dist. landfall
		Tow plow	5 km/h	Dynamic dist. landfall
		Pull in winch	5 km/h	Dynamic dist. landfall
Lay/bury cable		0.3 km/h	Dynamic based on length	
Offshore Substation	Port OSS	Fasten foundation	12 h	N/A
		Fasten topside	2 h	N/A
	Vessels OSS transit	Heavy lifting vessel	1 pc	N/A
		Feeder	1 pc	N/A
	Installation	Jacket legs installation	28 h/jacket leg	Based on support
		Jacket other installation	42 h	N/A
		Topside fasten	12 h	N/A
		Topside release	2 h	N/A
		Topside attach	6 h	N/A
	Mooring	Pre-installation	Load mooring	5 h
Mooring site survey			4 h	N/A
Installation		Suction pile install	11 h + 0.005h/m	Dynamic based on depth
		Drag embed install	5 h + 0.005h/m	Dynamic based on depth
		Install mooring line	0.005h/m	Dynamic based on depth
Substructure and Turbine Installation	Port installation	Assembly lines	2 pc	N/A
		Storage	8 pc	N/A
		Turbine assembly crane	2 pc	N/A
		Assembly storage	8 pc	N/A
	Construction on land	Substructure assembly	168 h	N/A
		Prepare for turbine	12 h	N/A
		Lift and fasten tower	12 h * repeat	Repeat if necessary
		Lift and fasten nacelle	7 h	N/A
		Lift and fasten blade	3.5 h * repeat	Repeat if necessary
		Mechanical completion	24 h	N/A
	Tow-out to site	Ballast to towing draft	6 h	N/A
		Tow-out	6 km/h	Dynamic dist. landfall
		Ballast to operational draft	6 h	N/A
	Vessel installation	Connect mooring lines	22 h	N/A
		Control mooring	12 h	N/A
Support vessel		1 pc	N/A	
Towing vessel		1 pc	N/A	
Station keeping vessel		3 pcs	N/A	
Scour Protection	Installation	Load material	4 h	N/A
		Drop material	10 h	N/A

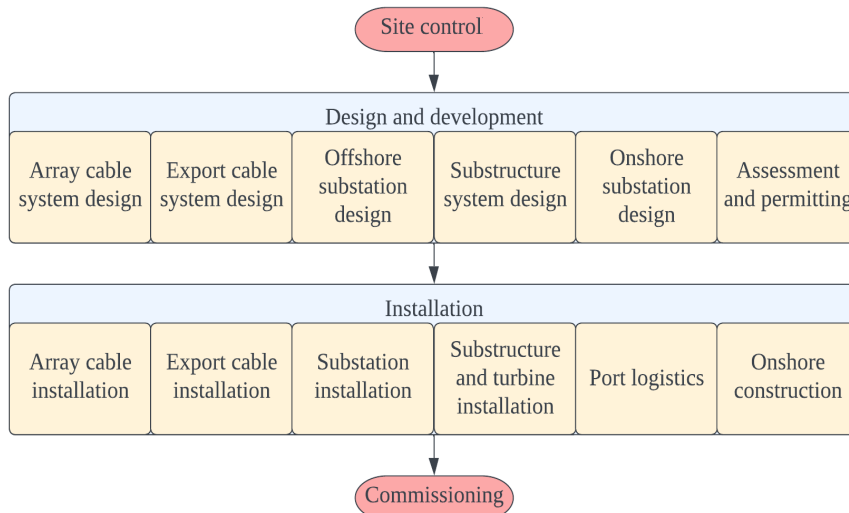


Figure 6.2 Overview of the Modeling Performed with ORBIT

6.2.8 Cost Categories

When all modeling efforts and calculations have been completed the total cost can be calculated. To evaluate the cost distribution in this thesis some sub-sections have been developed. For both the design and installation phases the sub-sections contain the electrical components, turbine, and substructure. The turbine and substructure and turbine installation are combined because of the onshore assembly and tow-out process. While mooring design and installation have been combined since the costs are a small part of the total CapEx. Other sub-costs include all soft costs, project costs, and OpEx. An overview of the cost sub-sections has been illustrated in Figure 6.3, and an outline of what segments each of the sub-cost sections includes has been specified in Table 6.8.

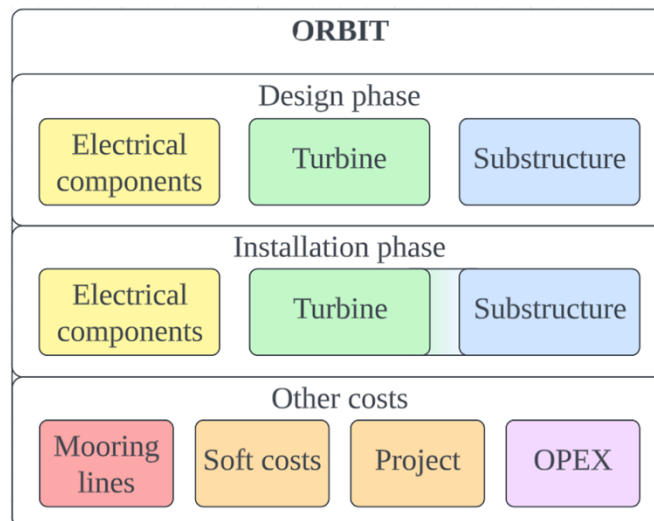


Figure 6.3 Cost Categories Used for Evaluating Wind Farms

Table 6.8 Segments Included in the Different Cost Categories

Cost Category	Includes Segments			
Electrical grid	Inter-array cables	Export cable	Offshore substation	Substation foundation
Turbine	Tower	Nacelle	Rotor blades	Hub
Substructure	Stiffened column	Truss	Heave plate	Secondary steel
Mooring line	Steel chain	Anchor		
Soft	Insurance	Financing	Commissioning	Decommissioning
Project	Site auction	Site assessment	Construction plan	Installation plan
OpEx	Operation	Maintenance		

6.3 Calculation of LCOE

The LCOE is calculated based on Eq. 3.21, and this section will elaborate on each of the variables in the equation and show the necessary calculations for the variables applied in the LCOE calculations.

6.3.1 Calculation of CapEx

The CapEx is calculated with the use of ORBIT, except for the wind turbine. As the ORBIT tool is from 2017, advancements have been made in the field after its release. Therefore, it was considered more accurate to retrieve information regarding this cost from an outside, up-to-date source. Thus, the wind turbine cost is retrieved from an analysis conducted by Rystad (2020). The calculation module provides the capital costs of all other components, and these represent CapEx in Eq. 3.21. From ORBIT, the costs are given in \$ from 2017; thus, it is necessary to adjust for inflation until 2023.

There are two different inflation factors utilized for calculating the adjusted CapEx, the Producer Price Index (PPI), and the steel price. The PPI is applied for all general costs, such as production and installation, while the steel prices are applied for adjusting costs related to steel components, such as the material price of the substructure. Table 6.9 displays the calculation of the factors applied for adjusting the CapEx. All values are retrieved from the Organization for Economic Co-operation and Development (2023).

Table 6.9 Calculation of CapEx Inflation Adjustment Factors

Description	Reference Value	2023 Value	Adjustment Factor
PPI - General	108.9 (2017)	147.8	1.35
PPI - Wind Turbine	128.5 (2020)	147.8	1.15
Steel Price Index	1060.7 (2017)	1845.7	1.74

6.3.2 Calculation of OpEx

The operational expenditures in this thesis will be calculated as a cost per MW per year [\$/MW/yr]. Since the OpEx cost is not calculated in ORBIT, it needs to be set manually. As there are many different types of wind turbines, in terms of size and design, different sources suggest a small variation in OpEx costs. The Danish Ministry of Energy, Utilities and Climate (2018) suggests an OpEx of 93 000 \$/MW/yr in 2020, which after a PPI inflation adjustment from January 2020 to December 2022 would equal an OpEx of 124 400 \$/MW/yr. On the other hand, NREL suggests in their 2021 Cost of Wind Energy Review (2022), which was published in December 2022 and thus is not inflation adjusted, an OpEx cost of 118 000 \$/MW/yr.

With the wind turbine described in Section 5. and the ORBIT calculator originating from NREL, the OpEx from their Cost of Wind Energy Review (Stehly & Duffy, 2022) will be used throughout this thesis. This cost is based on the theoretical energy output, i.e., a wind turbine's capacity factor is not considered when the annual OpEx cost is calculated.

6.2.3 Calculation of FCR

To estimate the FCR applied in the LCOE formula, the WACC is utilized. As described in Section 3.5.7, the WACC represents the average cost of all capital a company has raised. The Cost of Wind Energy Review (2022) implies that the WACC should be provided in nominal value after tax. Thus, Eq. 3.19, which includes tax, is applied for calculating the FCR. Some of the variables in the equation need to be determined, while some need minor calculations.

The Norwegian tax for private limited liability companies is 22 % and will be utilized as a tax rate, τ , for calculating the FCR (The Norwegian Ministry of Finance, 1999). A report by the Norwegian Research Centre (2021) suggests that an unlevered beta of 0.67 and a debt-equity ratio of 0.7 is suitable for wind energy projects. To calculate the levered beta, β_L , the following equation is utilized:

$$\beta_L = 0.67 \times \left(1 + \frac{0.7}{0.3}\right) = 2.22 \quad (6.22)$$

The risk-free rate, r_F , is based on the 3-month Norwegian Interbank Offered Rate (NIBOR), as government bonds are commonly applied as a basis for the risk-free rate (Petersen, Plenborg, & Kinserdal, 2017). As of 15th February 2023, this rate is 3.22 %. r_M , the expected market return, is based on findings by PwC (2022), stating that the median r_M is 5.0 %. With these variables determined, the levered cost of equity, r_L , can be calculated by implementing it in Eq. 3.17:

$$r_L = 3.22 \% + 2.22 \times (5.0 \% - 3.22 \%) = 7.17 \% \quad (6.23)$$

The cost of debt, r_D , is calculated by using the 3-month NIBOR, and adding a risk premium. The risk premium for offshore wind projects has a declining trend in Europe, and the premium

for this thesis is set to 1.5 %, slightly above the trend for 2020 (Brindley & Fraile, 2021). From this, the r_D can be calculated:

$$r_D = 3.22 \% + 1.50 \% = 4.72 \% \quad (6.24)$$

By implementing the parameters in Eq. (3.19), the final term of FCR, after-tax WACC, can be calculated:

$$WACC = \frac{0.3}{0.7 + 0.3} \times 7.17 \% + \frac{0.7}{0.7 + 0.3} \times 4.72 \% \times (1 - 0.22) = 4.73 \% \quad (6.25)$$

6.2.4 Annual Energy Production

To find the annual energy production at Trollvind, the capacity factor for the wind turbines needs to be calculated. To calculate the capacity factor, statistical methods can be used. The method used in this thesis is based on the Weibull distribution for Trollvind, combined with the wind turbine power curve. The Weibull distribution for Trollvind is presented in Section 5., while the wind turbine power curve for the 15 MW turbine is shown in Figure 6.4.

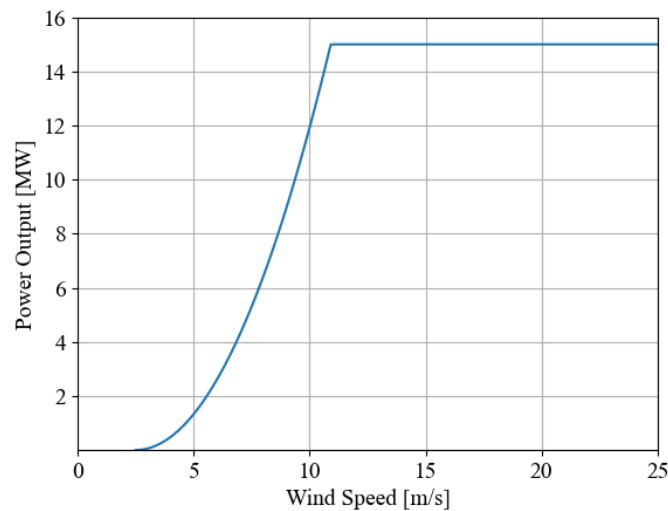


Figure 6.4 15 MW Wind Turbine Power Curve, derived from (Gaertner, et al., 2020)

The figure shows that the 15 MW wind turbine has a cut-in speed of 3 m/s, a rated wind speed of 10.6 m/s, and a cut-out speed of 25 m/s. Figure 6.5 further shows the power curve plotted together with the Weibull distribution. Here, the left y-axis shows the Weibull distribution percentage of wind speed occurrence, while the right y-axis shows the power output where 15 MW is set to be 100 %.

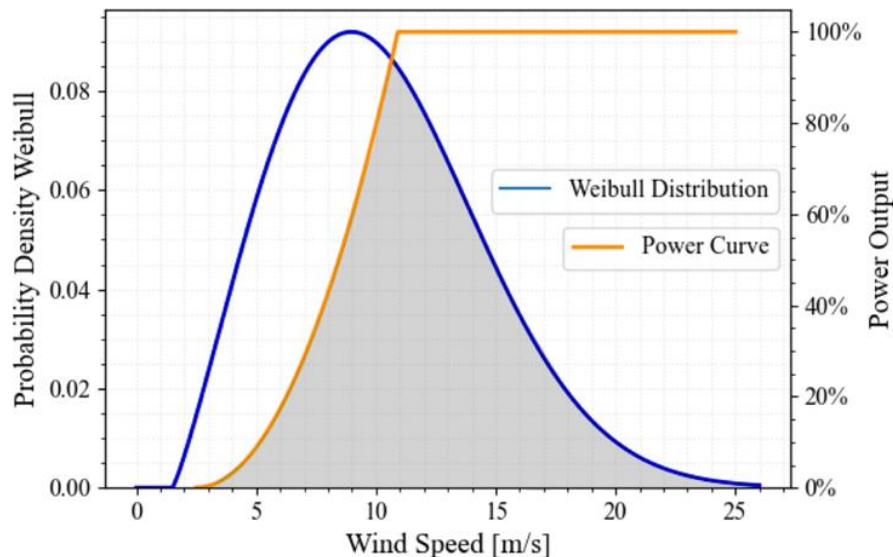


Figure 6.5 Power Output Curve and Weibull Distribution of the Wind Speed

By integrating the Weibull distribution while using the power curve as the upper limit, the capacity factor can be found. This will provide the calculated capacity factor of the 15 MW wind turbine at the Trollvind site. The integration is performed in Python and shows that the calculated capacity factor is 57.75 %. As described in Section. 3.2.3., wind farms experience grid or array losses, as well as downtime. Therefore, it is decided to subtract 5 % from the calculated capacity factor to account for these losses; thus, the capacity factor used for Trollvind is set to 52.75 %.

6.4 Financial Modeling

This section presents the methodology of financial modeling and provides an overview of the calculations and potential simplifications. To provide a full financial evaluation, some technical assumptions need to be made in addition to specifying the financial parameters.

6.4.1 Predetermination of Financial Parameters

All calculations in the financial analysis will be pre-tax, which implies that the pre-tax WACC needs to be calculated since the WACC utilized in LCOE calculations is after-tax. This is achieved by removing the tax term in Eq. 3.19 and recalculating:

$$WACC_{Pre-Tax} = \frac{0.3}{0.7 + 0.3} \times 7.17 \% + \frac{0.7}{0.7 + 0.3} \times 4.72 \% = 5.46 \% \quad (6.26)$$

According to The Norwegian Water Resources and Energy Directorate (2021), the electricity spot price is dependent on many factors and has varied significantly in recent years, which makes it difficult to predict accurately throughout the investment period. Based on this, the actual average price from 2020-2022 is considered representative of future prices, thus the spot price will be 96.2 \$/MWh (Statistics Norway, 2023).

As the ORBIT tool includes DecEx in the CapEx, this cost needs to be separated in the financial calculations. To calculate the cost of decommissioning, a factor relative to the preliminary installation cost is used as a basis, illustrated in Table 6.10 (Myhr, Bjerkseter, Nygaard, & Ågotnes, 2014).

Table 6.10 Relationship Between Installation and Decommissioning

Description	Installation Cost Relationship Factor
Mooring System	0.9
Subsea Cables	0.1
Substation	0.9
Wind Turbine	0.7

Castro-Santos (2016) proposed a simplified average salvage value of 7.5 % of the initial cost for a standard wind turbine, which will be deducted from the decommissioning costs. This percentage will also be utilized for other components comprised of steel.

Straight-line depreciation is the most comprehensive method of depreciation in Norway and implies a fixed depreciation every year (Heskestad, 2002). Thus, the investment will be depreciated according to this method over the 25 years of operation. The debt is assumed raised with a serial loan with a repayment time of 15 years, with the interest rate as calculated in Section 6.2.3.

6.4.2 Calculation of Financial Metrics

To evaluate the economic feasibility of the investment, three metrics will be evaluated: (1) net present value (NPV), (2) internal rate of return (IRR), and (3) payback period (PP). The NPV is calculated by displaying the yearly cash flow series in Excel with the NPV function. The syntax for the NPV function is (Microsoft, 2023):

$$NPV(rate, value1, [value2], ...) \tag{6.27}$$

where *rate* is the discount rate and *value1*, *value2*, etc. are the cash flows.

The same display of the cash flow series can be applied to calculate IRR in Excel. The syntax for the IRR function is (Microsoft, 2023):

$$IRR(values, [guess]) \tag{6.28}$$

where *values* is the range of cash flows, and *guess* is an optional argument that represents a guess for the IRR. If the guess argument is bypassed, Excel will use a default guess of 0.1 (10 %). The function returns the internal rate of return for the cash flows, which is the rate at which the NPV of the cash flows is zero. Excel uses an iterative process to calculate the IRR, which

involves guessing different rates until the NPV is zero. The IRR is the rate at which the NPV is closest to zero.

The PP is estimated by calculating the cumulative cash flow (CCF), and thus identifies how long the investment needs before the CCF becomes positive. By interpolating between the last year of negative CCF and the first year of positive CCF, it is possible to identify the week where the CCF starts being positive.

6.5 Calculation of Innovative Solutions

The following section outlines the modeling of potential new wind farm solutions and offers a comprehensive overview of the calculations and potential simplifications/estimates involved. The methodology incorporates a combination of ORBIT modeling, utilizing previously presented scaling factors, and simplifications to give reasonable estimates for adjusting CapEx components.

6.5.1 Calculation of Adjustment Factor for Shared Substructure

To evaluate the cost of the TwinWind concept, a wind farm with half the number of baseline substructures has been modeled. Further, the cost has been adjusted to compensate for the modification in the number of substructures. Some of the cost components remain the same as those modeled for the Trollvind baseline wind farm (export system, substation, turbine, soft, and project costs), consequently these components will not be subject to evaluation in this section.

For the inter-array cables the number of substructures is halved and thereby the length of the cables is reduced. Since the quantity of power produced on the wind farm is the same, the cost of the cables is adjusted upwards based on the need of higher capacity cables. Switching all cables from XLPE 400 mm 33 kV to XLPE 630 mm 33 kV correlates to a component cost increase of 50 %. Hexicon (2023) implies a reduction in inter-array cable costs of 33 %, which equals an adjustment factor of 1.34. An estimate for adjusting the modeled cost is thereby set to 1.5, to compensate for contingency.

Since the quantity of substructures has been halved, each substructure in this concept must balance and uphold two wind turbines. Hence, the amount of steel used in the substructure is expected to increase significantly. Since the mass of the substructure cannot be acquired, a few assumptions have to be made. Elobeid et al. (2022) modeled a similar concept as TwinWind, which will be supplementary to the original ORBIT scaling method for evaluating an estimate for the steel mass. With the use of Eq. 6.1 to Eq. 6.3, and a turbine rating of 30 MW (two turbines of 15 MW), with additional secondary steel mass of 5 % of the total. These mass and cost calculations are displayed in Table 6.11. Since the scaling factors of the mass may be unfitting because of the turbine rating simplification, an adjustment factor of 1.4 has been added to compensate for the additional costs.

Table 6.11 Calculation of the Mass of one TwinWind Substructure

Substructure	Calculated Mass
Stiffened column	1 166 tons
Truss	3 244 tons
Heave plate	427 tons
Outfitting steel	242 tons
Total	5 079 tons

The conceptual mooring system for the TwinWind consist of anchoring to the seabed with a single point mooring using a catenary anchor system (Hexicon, 2023). This results in difficulties with correctly estimating the mooring cost for the solution. Thereby, the mooring cost are seen as an approximation as modeling is difficult, and tension leg mooring are not assessed as ideal for water depths of over 300 m (Nygaard & Myhr, 2014). Thus, an adjustment factor of 1.6 based on the modeled mooring cost for the substructures has been applied for the total mooring system.

To estimate the installation cost, adjustment-based assumptions have been made. All the three affected costs are adjusted based on the same assumptions explained in the paragraphs above, and a reasoning is shown in Table 6.12. For the array installation, this includes shorter but larger cables (Hexicon, 2023). Further, the substructures are larger, while the quantity is halved.

The OpEx is not adjusted, as the cost is based on the theoretical power output. Mendoza et al. (2023) performed an aerodynamical performance review of the dual turbine concept, they estimated the increased performance of the dual concept to be in the range of 2-3 %. Thereby, an increase of 2.5 % in AEP has been considered in this evaluation. Additionally, there are other factors in the AEP aspect that have not been considered, this may include increased downtime as maintenance of one turbine requires the other turbine to be shut off and other hard to estimate situations. Table 6.12 provides an overview of the adjustment of modeled costs for the affected components.

Table 6.12 Overview of the Adjustment of Costs for the TwinWind Modeling

Description	Adjustment Factor	Reasoning
Array System	1.5	Decreased length, increased cable size
Substructure	1.4	Decreased quantity, increased size
Mooring System	1.6	Shorter but larger lines
Array System Installation	1.2	Fewer but larger cables
Substructure Installation	1.7	Decreased quantity, increased size
Mooring System Installation	1.6	Shorter lines, tension leg installation
OpEx	1.0	Same theoretical power output
AEP	1.025	Aligns with wind

6.5.2 Calculation of Reduction Factor for Shared Mooring

In order to assess the cost savings associated with shared mooring, the overall mooring length of various innovative concepts have been estimated. This includes two turbines with shared mooring, four turbines with shared mooring (squared), and conceptual hexagon mooring systems. To evaluate the mooring length reduction, the ORBIT mooring scaling factor have been utilized together with shared line properties from Liang et al. (2023). The findings indicate that a single catenary mooring line spans 979 m, while a shared mooring line extends to a length of 989 m. For the hexagon concept, the shared mooring lines are estimated to be approximately 1/3 of an original shared mooring line. The modeled length of the mooring lines for the different innovative concepts are presented in Table 6.13.

Table 6.13 Modeled Length of Mooring Lines for Shared Mooring Concepts

Description	Modeled Length of Mooring [m]	Reduction Factor
Single turbine		
Catenary Mooring	2 939	
Length of mooring per turbine [1 turbine]	2 939	1.0
Two turbines with shared line		
Catenary mooring	3 919	
Shared mooring	989	
Length of mooring per turbine [2 turbines]	2 454	0.83
Four turbines with shared lines (squared)		
Catenary mooring	3 919	
Shared mooring	3 956	
Length of mooring per turbine [4 turbines]	1 969	0.67
Multiple hexagon concept		
Catenary mooring	4 899	
Shared mooring	13 516	
Tension leg mooring	5 200	
Length of mooring per turbine [16 turbines]	1 476	0.50

Regarding the installation phase aspect of the innovative concepts, cost adjustments have been exclusively implemented. These adjustments have been made under the assumption that the reduction factor of quantity and length also applies to installation costs. Another assumption is that the dimensions of anchors are unchanged.

7. Results

7.1 Reference Wind Farm

7.1.1 Definition of Wind Farm Layout

The baseline wind farm in this thesis is set to consist of 50 turbines with 15 MW rated power, resulting in a theoretical capacity of 750 MW. Figure 7.1 displays the layout of the Trollvind baseline wind farm.

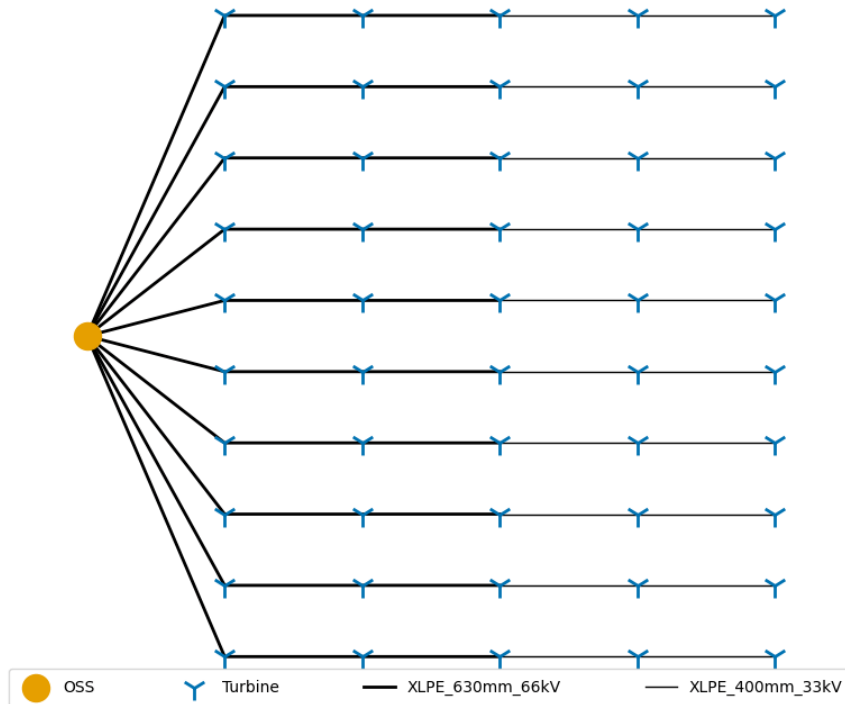


Figure 7.1 Wind Farm Layout

As displayed in the figure, the wind turbines are arranged in a 10 by 5 array. There are 10 cables connected to the offshore substation (OSS), where the cables increase in voltage and radius closer to the OSS, to sufficiently transport the electricity and minimize the array loss. The spacing between the turbines is set to 8 times the rotor diameter in the wind direction and 4 times the rotor diameter perpendicular to the wind direction.

7.1.2 Initial Calculation for the LCOE

Based on the approach presented in Section 6., the components not evaluated in ORBIT can be calculated as:

$$FCR = \frac{4.73 \%}{1 - (4.73 \% + 1)^{-25}} = 6.9 \% \quad (7.1)$$

$$OpEx_{annual} = \$ 118\,000/MW/yr * 15MW * 1yr * 50 turbines = \$ 88.5M \quad (7.2)$$

$$AEP = 15MW * 50 turbines * 52.75 \% * 8760 hr/yr = 3\,465\,675 MWh \quad (7.3)$$

7.1.3 Trollvind Total Cost Description

To establish a baseline LCOE for the sensitivity analyses, calculations were conducted for the Trollvind wind farm. The baseline is important for evaluating how the LCOE is impacted by variations in different parameters. This section will present the benchmark LCOE and illustrate all drivers of cost for Trollvind.

Table 7.1 shows the CapEx distribution for Trollvind. The electrical grid is the array system, the export system, and the offshore substation combined, while the other costs are defined in Section 6. Methodology.

Table 7.1 Distribution of CapEx for Trollvind Wind Farm with 50 Turbines

Description	Cost	Percentage of CapEx
Electrical Grid	\$ 384 363 000	10.2 %
Electrical Grid Installation	\$ 221 400 000	5.9 %
Turbine	\$ 759 000 000	20.1 %
Substructure	\$ 1 275 740 000	33.8 %
Substructure Installation	\$ 56 700 000	1.5 %
Mooring Line (Inc. Installation)	\$ 218 120 000	5.8 %
Soft	\$ 653 400 000	17.3 %
Project	\$ 203 850 000	5.4 %
Total	\$ 3 772 572 000	100 %

As of Table 7.1, the total investment for manufacturing and installing an offshore wind park of 50 wind turbines at Trollvind is \$ 3 772 572 000, which implies a cost for each installed turbine including all components of over \$ 75 000 000. With a theoretical capacity of 15 MW per turbine, each MW costs over \$ 5 000 000 to install.

According to the table, the substructure represents the largest portion of CapEx at 33.8 %, followed by the turbine at 20.1 %, and the electrical grid at 10.2 %. The mooring system, including installation costs, accounts for 5.8 % of the total CapEx, while soft costs represent 17.3 % of the total. Project costs are the smallest isolated cost driver and account for 5.4 % of the total CapEx.

Table 7.2 displays several key financial and technical parameters applied for the LCOE calculations, along with the computed LCOE for Trollvind.

Table 7.2 Parameters for LCOE Calculations for Trollvind

Description	Trollvind
CapEx	\$ 3 772 572 000
OpEx (annual)	\$ 88 500 000
AEP	3 465 575 MWh
FCR	6.9 %
Lifespan	25 years
LCOE	100.69 \$/MWh

According to the table, the AEP is estimated to be 3 465 575 MWh, while the yearly OpEx is \$ 88 500 000. The final LCOE of the Trollvind wind farm is 100.69 \$/MWh, given production over 25 years before decommissioning. To evaluate which components make up the largest cost proportion of the LCOE, all costs related to energy production are displayed in Figure 7.2.

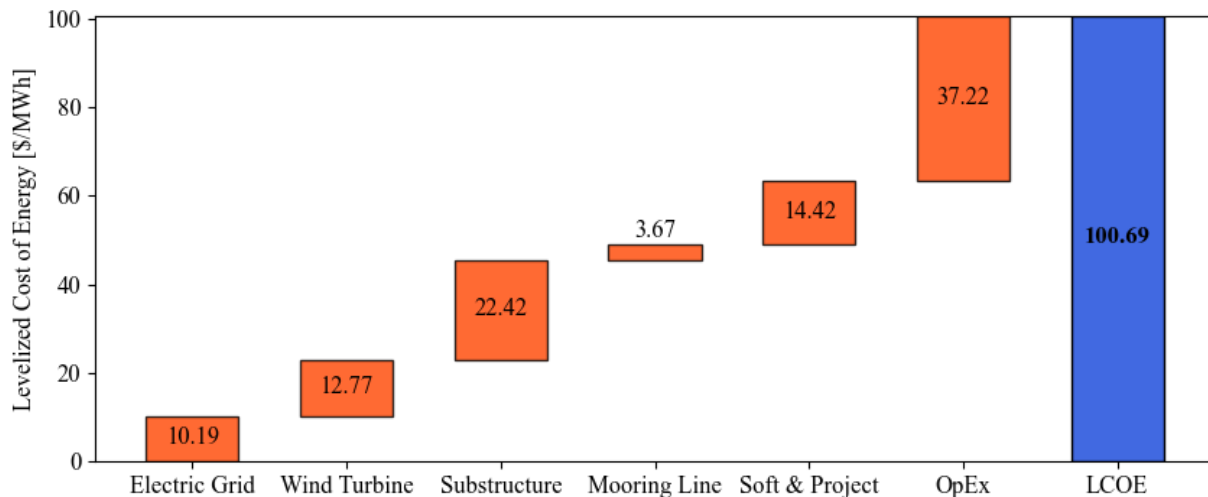


Figure 7.2 Distribution of Costs and Total LCOE for Trollvind

In Figure 7.2, the costs of installation have been included in the total cost of components. The mooring line is the smallest cost with a total of 3.67 \$/MWh, while the largest LCOE contributor is OpEx, with a cost of 37.22 \$/MWh. The cost related to operation and maintenance accounts for around 37 % of the LCOE over the 25 years of production, hence it is the most significant individual cost driver. However, the combined costs of CapEx are greater than the OpEx and make up the largest part of the LCOE.

7.1.4 Trollvind Detailed Component Cost Description

For further evaluating the cost components of the Trollvind wind farm, the procurement and manufacturing costs have been evaluated in sum for each of the main design components. Table 7.3 provides a more thorough description of the component's dimensions and the total cost of the design phase.

Table 7.3 Detailed Component Description and Costs for Trollvind

Component	Dimensions	Description	Cost
Inter-array cables	10 strings of 5 array cables, total length of 124.7 km	33 km of XLPE 400 mm 33 kV cables	\$ 13 365 000
		89.7 km of XLPE 630 mm 66 kV cables	\$ 48 438 000
Export system	6 cables with a total length of 409.5 km	XLPE 500 mm 132 kV cables	\$ 110 576 799
Substations	Substations with 220 main power transmission rating and a jacket foundation	Topside	\$ 44 813 925
		Jacket foundation	\$ 6 679 530
		MPT	\$ 7 425 000
		Switchgear	\$ 391 500
		Shunt reactors	\$ 10 395 000
		Ancillary system	\$ 8 100 000
Mooring	3 lines of 479.7 m + $L_{m,f}$ per substructure	Steel mooring line with diameter 0.15 m	\$ 905 886
	3 anchors per substructure	Suction pile anchor	\$ 331 434
Substructures	50 semisubmersible substructures with a total mass of 29 121 tons	Stiffened column	\$ 6 497 742
		Truss	\$ 12 231 369
		Heave plate	\$ 4 357 284
		Secondary steel	\$ 2 416 282
Turbine	15 MW wind turbine	Complete turbine system	\$ 15 180 000

It should be noted that the mooring, anchor, and substructure component costs are given for each system. The overview displays how the largest electrical grid costs are related to the three export cables, the 66 kV inter-array cables, and the top side of the substations. The mooring system consists of three lines of 479.7 m of 15 mm steel chain connected to a suction anchor. For each complete line, the total costs are around \$ 1 230 000. For the substructure, the truss elements amount to around 50 % of the total component cost. The turbine is calculated independently as a complete system, shown in Section 6. Methodology.

Additionally, the installation phase and vessel usage have been studied. This has been reviewed by examining all the vessel actions together with the durations and cost aspects. For presenting the results only the vessel installation duration will be presented, while the cost aspect can be comprehended by matching the day rates for each vessel given in the methodology section. Figure 7.3 displays the duration for each installation phase (except for substructure installation) with the associated vessels.

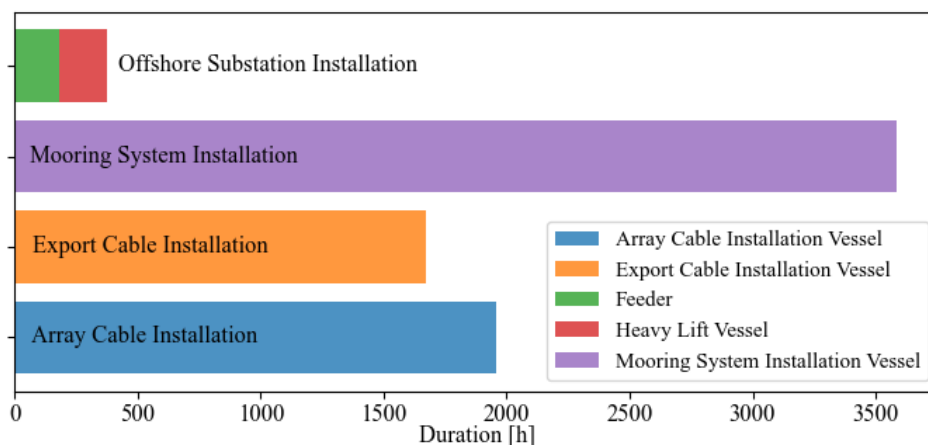


Figure 7.3 Duration for Installation Vessels

The figure exhibits the distribution of time used in the installation phases and shows that for a large array of wind farms, a lot of time must be used in finalizing mooring and cabling, with 4 746 hours used to survey, install anchors, and connect mooring lines. For the electrical segments, 5 203 hours were used in total for preparing, testing, terminating, and laying of cable together with the tow-out, installation, and testing of the offshore substation. Subsequently, since the substructure and turbine installation comprise approximately 70 % of the installation duration, this has been examined separately as shown in Figure 7.4. Further, Table 7.4 presents the detailed duration for all activities in the substation installation phase.

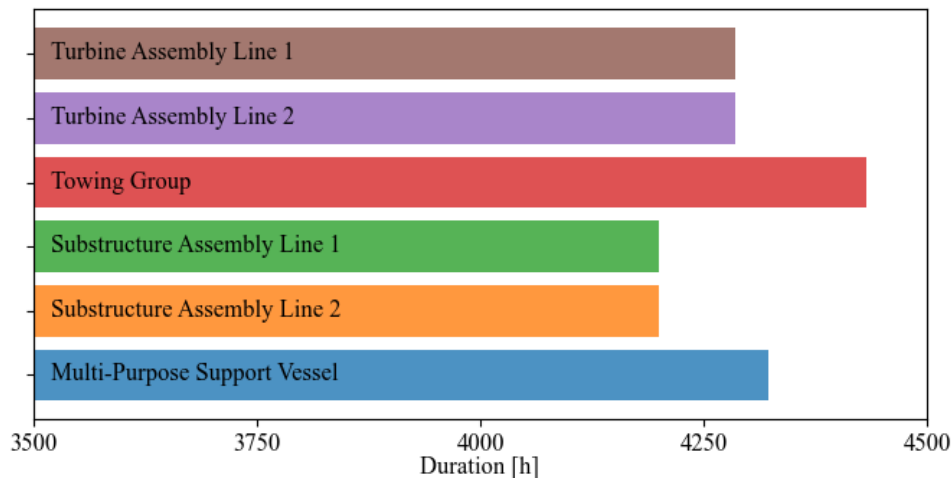


Figure 7.4 Duration for Fabricating and Installing Substructures and Turbines

Table 7.4 Detailed Duration for Actions in the Substructure Installation Phase

Process	Duration [h]
Ballast to Operational Draft	304
Ballast to Towing Draft	304
Check Mooring Lines	598
Connect Mooring Lines	1107
Delay: At the Construction Site	2039
Delay: No Completed Assemblies Available	774
Lift and Attach Blade	525
Lift and Attach Nacelle	350
Lift and Attach Tower Section	1203
Mechanical Completion	1192
Mobilize	168
Move Substructure	408
Position Substructure	96
Positioning Support	2108
Prepare for Turbine Assembly	612
Substructure Assembly	8387
Tow Substructure	624
Transit	640

In this examination of the substructure installation, the segment of onshore construction of the substructures and the turbine assembly have been included. Including the construction and assembly, this amounts to 21 429 hours used for the installation. The towing group amounted to 4 431 hours, and the support vessel for 4 323 hours. Additionally, approximately 8 400 hours were used in substructure construction and 8 571 hours for the turbine assembly. In the installation phase, the positioning and mooring line connection is a large portion with 2 108 and 1 100 hours needed in total. Other time use includes tow/transit of 1 265 hours and delays of over 2 800 because of construction buffers and on-site time wastes.

Other associated costs like soft costs are not thoroughly modeled, but rather based on \$/kW quantities specified by NREL. Amounting to a total of \$ 653 million, divided into construction insurance (7 %), construction financing (28 %), contingency (49 %), commissioning (7 %), and decommissioning (9 %).

7.2 Sensitivity Analyses

In this section, several sensitivity analyses will be performed for Trollvind. This will illustrate how the LCOE varies with the different inputs. Thus, providing an insight into which factors have the highest impact on the LCOE for Trollvind.

7.2.1 Project Lifespan

As established in Section 6. Methodology, the baseline lifespan in this thesis is set to 25 years. It is expected that the LCOE will vary with different project lifespans. In this analysis, the CapEx costs will remain constant despite varying lifespans. Thereby, it is anticipated that the LCOE will be reduced as the lifespan increases since the CapEx will be discounted over more years. Figure 7.5 shows how the LCOE varies with different lifespans for Utsira.

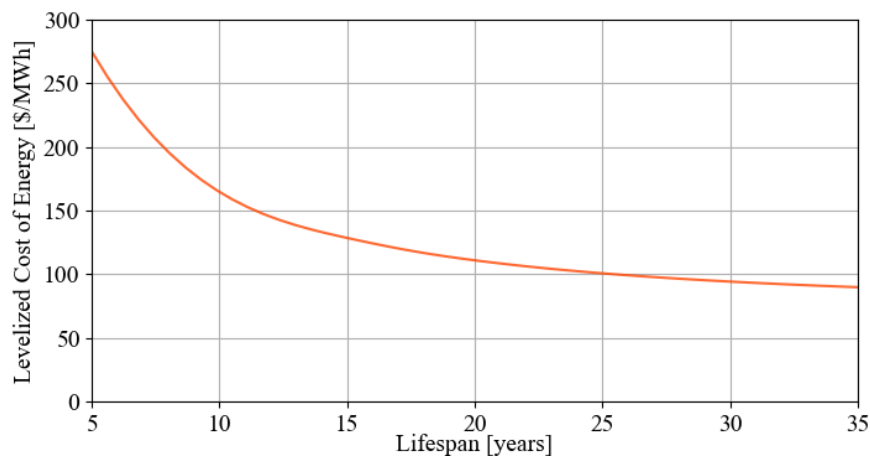


Figure 7.5 Project Lifespan Impact on LCOE

The figure shows that the LCOE is reduced as the project's lifespan increases. 275.1 \$/MWh is the LCOE at a five-year lifespan, and it is reduced to 89.8 \$/MWh for a 35-year lifespan, which is a reduction of 67.3 %. It further shows that the LCOE is not reduced linearly, but more significantly at the start of the lifespan.

Table 7.5 shows the percentage change in LCOE between the different lifespans at Trollvind. As displayed in Table 7.5 and seen in Figure 7.5, the decline in LCOE and the percentage decreases as the lifespan increases.

Table 7.5 Percentage Change in LCOE for Trollvind

	Lifespan [years]						
	5	10	15	20	25	30	35
LCOE [\$/MWh]	275.1	164.7	128.5	110.9	100.7	94.2	89.8
Difference [%]	40.1	22.0	13.7	9.2	6.5	4.7	

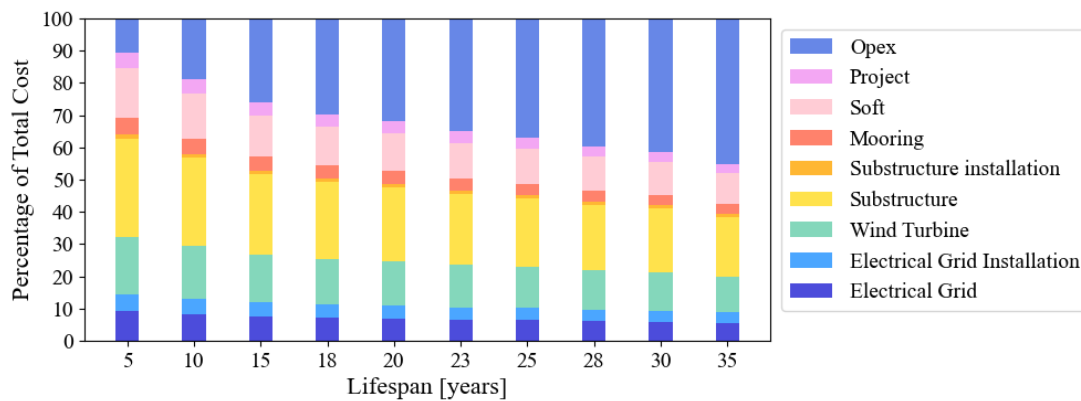


Figure 7.6 Cost Breakdown for Different Lifespans

Figure 7.6 illustrates the cost breakdown at each lifespan. As expected, with an increased lifespan it is seen that the OpEx cost makes up a larger part of the total cost. Further, the OpEx cost is the most prominent, constituting 37.0 % of the total cost at a 25-year lifespan. The wind turbine, together with its substructure and installation, almost equals the same percentage as the OpEx cost at 36.0 %. The project cost is seen to be very little prominent, with only representing 4.8 % and 3.0 % of the total at a five-year and 35-year lifespan, respectively. On the other hand, the electrical grid with installation represents 14.4 % at a five-year lifespan and 8.8 % at a 35-year lifespan.

7.2.2 Effect of the Wind Farm Scale

The scale effect may lead to a reduced LCOE as the energy output will increase with the number of wind turbines. However, both the CapEx and OpEx will also increase following the installation of more turbines. Thus, examining how the scale of the wind farm impacts the LCOE is of interest. Figure 7.7 shows how the LCOE varies concerning the scale of the wind farm at Trollvind.

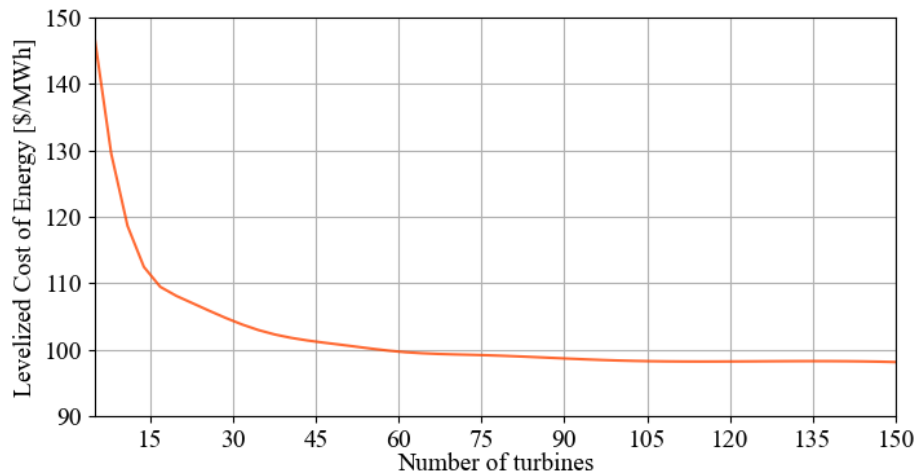


Figure 7.7 Scale Effect Impact on the LCOE

Figure 7.7 shows that the LCOE drops drastically from five to twenty turbines, after this, the graph flattens out. The drop from five to 20 turbines is from 146.7 \$/MWh to 108.0 \$/MWh which is a 26.4 % decrease. However, from 20 to 150 wind turbines the decrease is only 9.2 %. The results show that the LCOE decreases slightly from 100.7 \$/MWh at the baseline of 50 turbines to 98.1 \$/MWh at 150 turbines, only a 2.6 % difference. Figure 7.8 presents the cost breakdown at different scales of the wind farm.

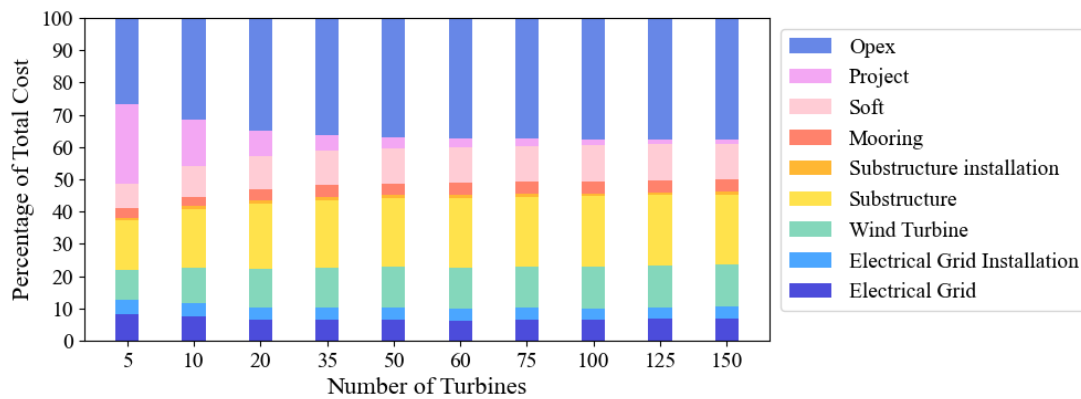


Figure 7.8 Cost Breakdown for Different Scale Effects

The figure illustrates that the costs start to normalize when the scale of the wind farm increases. This can be exemplified by the OpEx cost. At five turbines it makes up 26.7 % of the total, however, when it comes to 35 turbines it constitutes 36.3 %, and at 150 turbines 37.8 %. The most prominent change can be seen in the project cost. It decreases from 24.6 % of the total cost to 1.2 % for a five-turbine wind farm to a 150-turbine wind farm, respectively. As seen, the electrical grid with installation drops from making up 12.7 % at five turbines to 10.1 % at 50 turbines, before it increases to 10.5 % at 150 turbines.

7.2.3 Turbine Power Rating

With an increase in turbine power rating, the energy output will be higher. This will affect the denominator in the calculation of the LCOE, seen in Eq. 3.23. A higher turbine power rating will also increase the CapEx and OpEx, thus it is of interest to examine how the turbine power rating influences the LCOE. Figure 7.9 illustrates the LCOE for Trollvind as wind turbines of 6 MW, 12 MW, and 15 MW are placed.

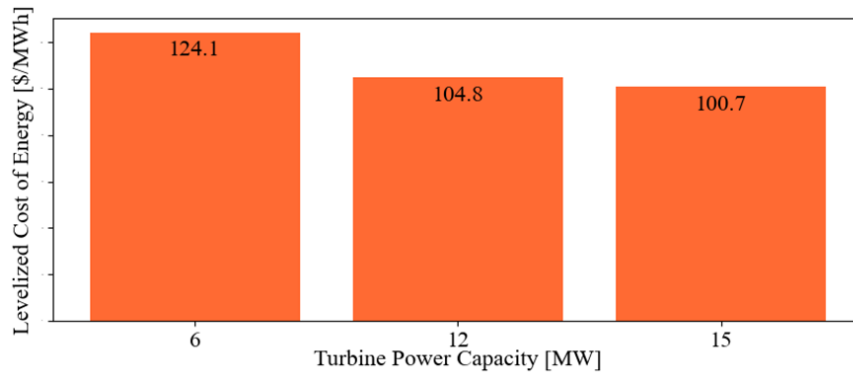


Figure 7.9 LCOE for Different Turbine Power Capacity

With the annual OpEx cost being determined by the annual energy production, it rises linearly with the power rating. However, the CapEx increases by 60.9 % from the 6 MW turbine to the 12 MW, and from 12 MW to 15 MW the increase is at 18.6 %. In opposition to the OpEx, these numbers show that although the power rating doubles from 6 MW to 12 MW, the CapEx does not follow this linearly. Figure 7.8 shows that the 15 MW wind turbine results in the lowest LCOE, with an LCOE of 100.7 \$/MWh. The LCOE decreases from 124.1 \$/MWh for a 6 MW turbine, to 104.8 \$/MWh for a 12 MW turbine. This gives a decrease in LCOE from 6 MW to 12 MW at 15.6 %, which equals a 2.6 % decrease in LCOE per MW. However, from 12 MW to 15 MW the decrease in LCOE is only 1.3 % per MW. Figure 7.10 shows the cost breakdown for each turbine power rating.

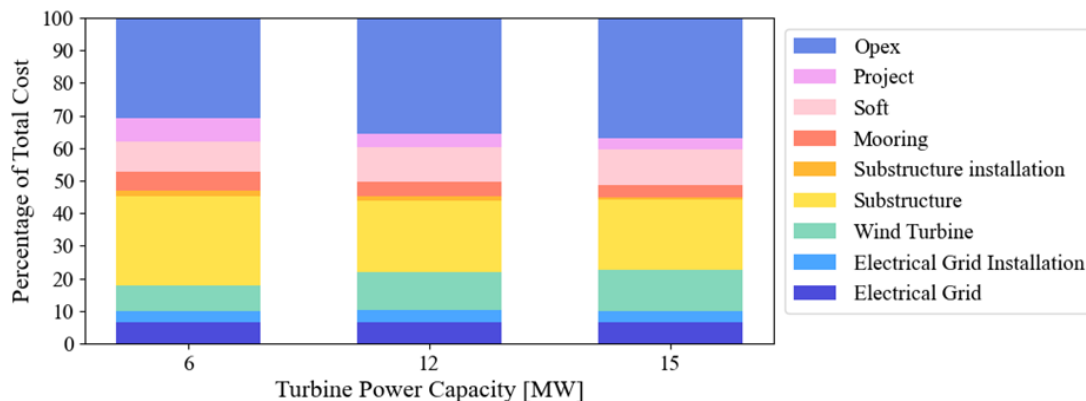


Figure 7.10 Cost Breakdown for Different Turbine Power Capacity

The OpEx cost is increasingly more prominent in the total cost from 6 MW to 15 MW. From 6 MW to 12 MW, it increases from 31.0 % to 37.0 % of the total cost, which is a 2.0 % increase per MW. From 12 MW to 15 MW the increase is at 0.4 % per MW. The wind turbine with its substructure, as well as the installation, constitute almost an equal proportion of the total with 35.0 %, 34.9 %, and 37.0 % for the 6 MW, 12 MW, and 15 MW turbines, respectively.

7.2.4 Project Discount Rate

The project discount rate influences the FCR, which is used in the calculations of LCOE, shown in Eq. 3.22. As presented in Section 3. Theory the WACC represents the project discount rate which is used to calculate the FCR. The WACC is sensible to change as factors such as the equity-to-debt ratio of a project, the corporate tax, the cost of equity, and the cost of debt may all vary. Therefore, it is of high relevance to investigate how the LCOE is affected when the WACC varies. Figure 7.11 illustrates the change in LCOE as the WACC varies for Trollvind.

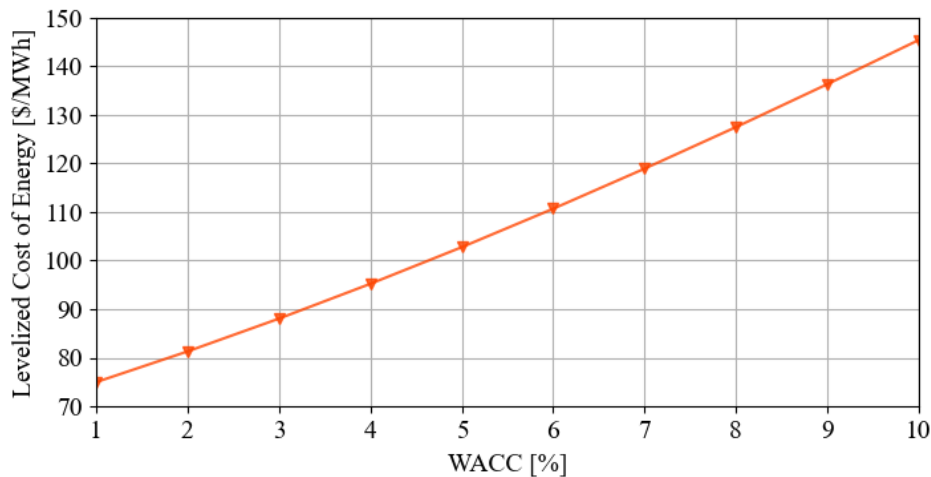


Figure 7.11 Project Discount Rate Impact on LCOE

The figure shows that the LCOE is vastly impacted by the changes in WACC as it increases from 75.0 \$/MWh for a 1 % WACC, to 145.5 \$/MWh at a 10 % WACC. This is an increase of 94.0 %. The result shows that if the project discount rate fluctuates only one percent from the original of 4.73 %, the LCOE would be increased by 7.9 \$/MWh or decreased by 7.4 \$/MWh. As the graph and previous calculation show, the LCOE is not increasing exactly linearly, even though it does not have a significant curve. If the graph were seen to be increasing linearly, it would on average increase by 7.7 % for each percentage point that the WACC fluctuates. As the WACC impacts the LCOE equation and not the individual costs, the cost breakdown will not be affected from the baseline.

7.2.5 Operational Expenditure

The operational expenditures constitute 35.5 % of the baseline LCOE at Trollvind. Estimating the OpEx cost can be challenging due to its possible variability, thus a sensitivity analysis is performed to show how the LCOE is affected when the OpEx cost varies. The analysis will be based on the baseline OpEx for Trollvind, which is 88 500 000 \$/year. From the baseline, the OpEx cost will vary from ± 50 %, i.e., from 44 250 000 \$/year to 132 750 000 \$/year. The results are presented in Figure 7.12.

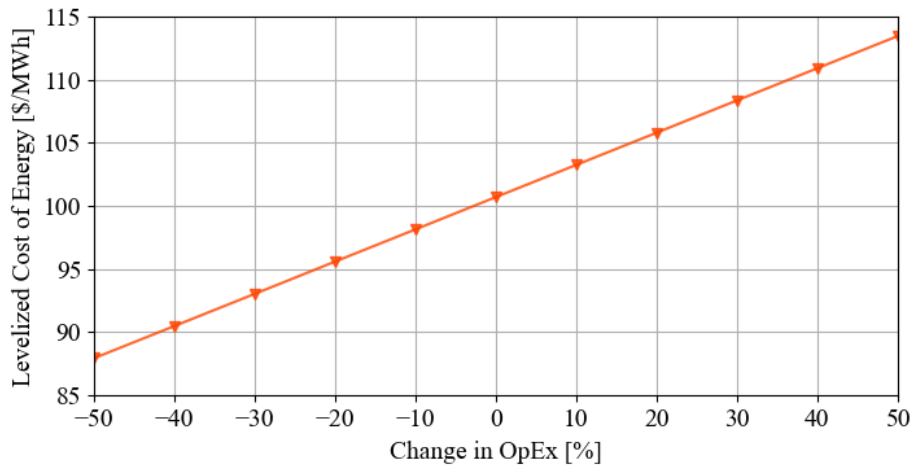


Figure 7.12 OpEx Impact on LCOE

With the OpEx cost being the only variable that is affected, the LCOE changes linearly. It goes from an LCOE of 87.9 \$/MWh at -50 %, to 113.5 \$/MWh at +50 %. This gives a decrease or increase in LCOE of 12.7 % from the baseline. The graph has a slope of 2.6 \$/MWh, which tells that for every ten percentage points that the OpEx fluctuates the LCOE increases or decreases by 2.6 \$/MWh.

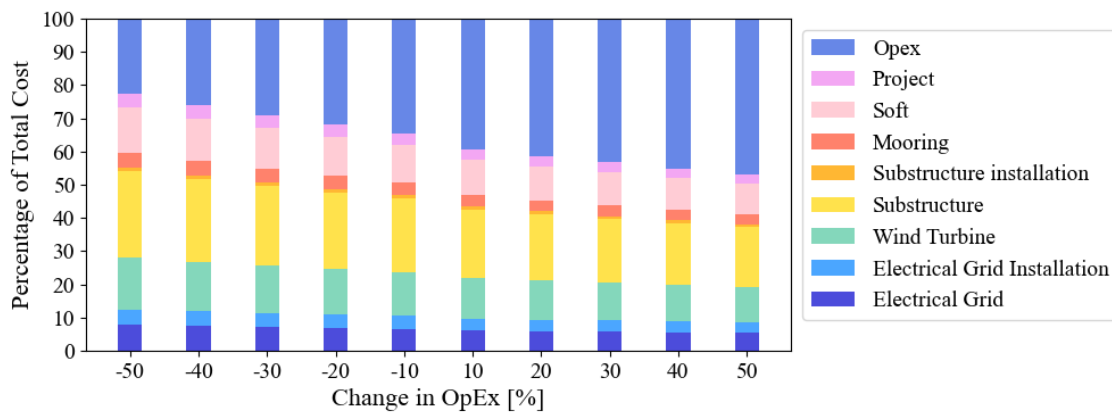


Figure 7.13 Cost breakdown for a varying OpEx for Trollvind

Figure 7.13 shows that the OpEx cost can be highly influential on the total cost. At a 50 % increase in OpEx, it accounts for almost half of the total cost at 46.8 %, and at a -50 % in OpEx cost it still makes up 22.7 %

7.3 Effect of Metocean Conditions

In this section, there will be performed sensitivity analyses on the metocean conditions. The evaluated parameters are the capacity factor, water depth, and distance to shore and the baseline conditions are equal to the Trollvind wind farm.

7.3.1 Capacity Factor

As seen in Section 6. Methodology, the calculated capacity factor for Trollvind is 52.8 %. The capacity factor may vary based on several different factors, such as different wind turbines or wind conditions. As the capacity factor influences the energy output, it directly impacts the calculation of the LCOE. Therefore, it is of interest to see how the LCOE is affected based on variations in the capacity factor, this is illustrated in Figure 7.14.

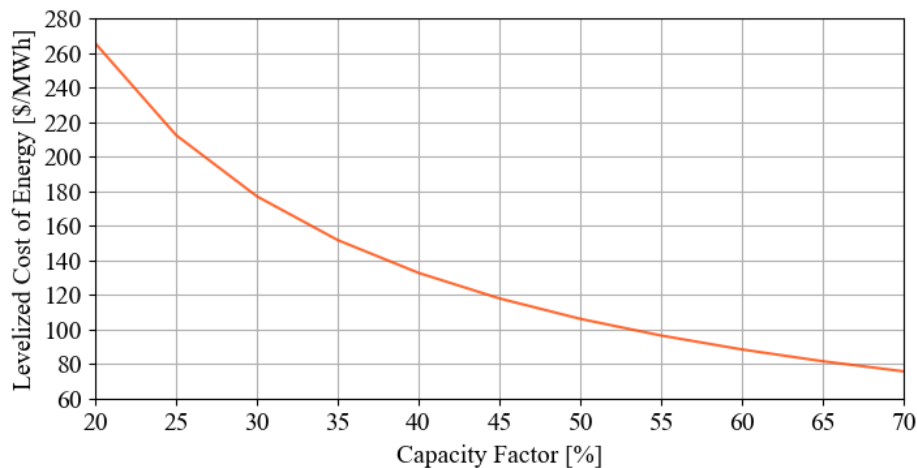


Figure 7.14 Capacity Factor Impact on LCOE

The figure shows that capacity factor has a more imminent effect on the LCOE at lower factors, as it does not decrease linearly. From a capacity factor of 30 % to 40 %, the LCOE is reduced from 177.1 \$/MWh to 132.8 \$/MWh, which is a 25.0 % reduction. However, from a capacity factor of 50 % to 60 %, the reduction is 16.7 %, from 106.2 \$/MWh to 88.5 \$/MWh. Table 7.6 shows the percentage change in LCOE between the different capacity factors. As the table displays, the LCOE decreases as the capacity factor increases.

Table 7.6 LCOE for Trollvind with Different Capacity Factors

	Capacity Factor [%]					
	20	30	40	50	60	70
LCOE [\$/MWh]	265.6	177.1	132.8	106.2	88.5	75.9
Difference [%]	33.3	25.0	20.0	16.7	14.2	

7.3.2 Site Conditions

At various offshore sites, the water depth and distance to shore can vary; thus, it is of interest to see how they influence the LCOE. Figure 7.15 illustrates the change in LCOE as the water depth varies from 100 to 700 meters, while Figure 7.16 shows the variation in LCOE as the distance to shore varies from 50 to 400 km.

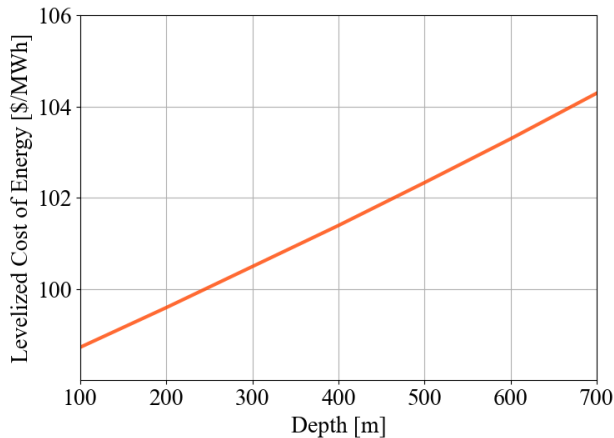


Figure 7.15 Water Depth Impact on the LCOE

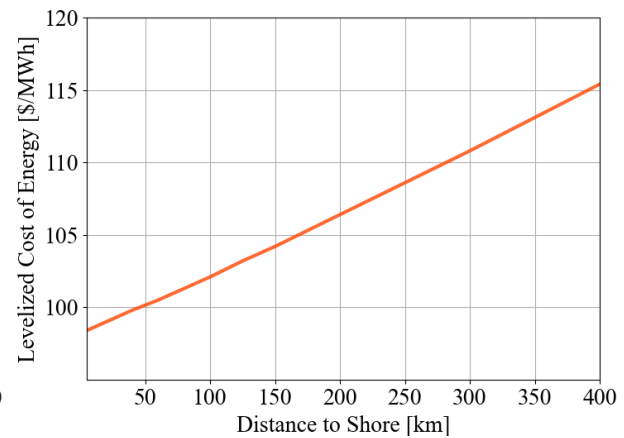


Figure 7.16 Distance to Shore Impact on the LCOE

Although the LCOE has some changes as the water depth and distance to shore vary, it does not have a very notable impact. The water depth graph develops close to linearly with a slope of 0.93 \$/MWh per 100-meter increase in water depth. Further, the LCOE for the distance to shore increases almost linearly as well, and it increases by 0.80 \$/MWh for every 20 km the distance increases.

As the LCOE does not vary a lot for either the water depth or the distance to shore, the cost breakdown will be close to similar for all inputs; however, there are a few small changes. For the water depth, the mooring cost is the most affected. It increases from 2.1 % of the total to 6.1 % at 100 m and 700 m, respectively. The only other cost that is affected by the water depth is the electrical grid with installation, although its total change is only by 0.2 %. The electrical grid is the only affected cost when the distance to shore varies. and it increases from 8.4 % to 18.8 % of the total cost at 5 km to 400 km, respectively.

7.3.3 Key Cost Drivers of the LCOE

The key cost drivers of the LCOE will be presented in a tornado diagram that shows which factors are the most prominent on the LCOE, and how it changes when the cost drivers fluctuate. The baseline LCOE for Trollvind, which is 100.7 \$/MWh, is set as zero. From this baseline, the diagram shows how much the LCOE is affected by different cost drivers.

In this diagram, the sensitivity analyses that have been performed will be presented. Further, a variation in the turbine spacing, steel price, and contingency will also be included. The turbine spacing is set to vary from 3 rotor diameters to 12 rotor diameters. The steel price is another highly variable factor, thus it is an element to consider when evaluating the LCOE of a wind farm. The contingency is also taken into consideration as there will always be some uncertainty around different projects. The steel price is set to affect the wind turbine, substructure, mooring system, and offshore substation. These costs will vary $\pm 50\%$ from the baseline steel price. Meanwhile, the contingency is affecting the total CapEx cost. This is set to vary $\pm 15\%$ from the baseline CapEx. Figure 7.17 illustrates the key cost drivers in a tornado diagram.

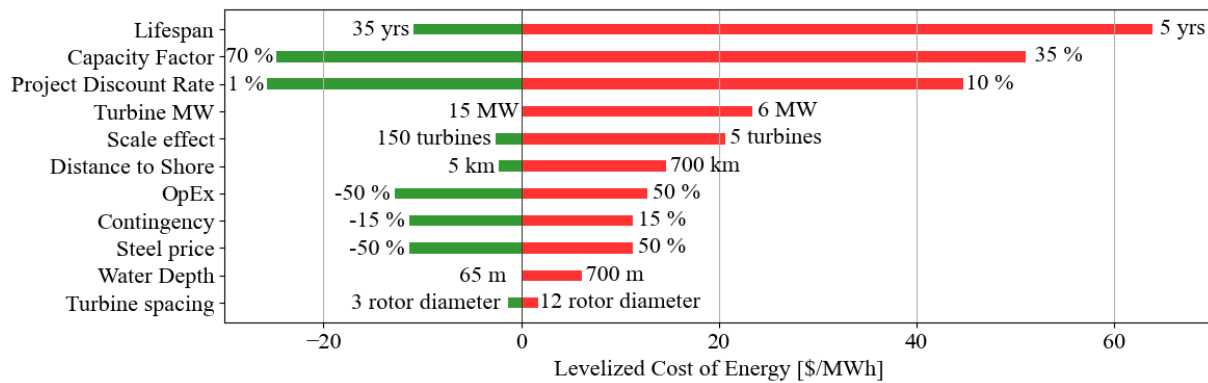


Figure 7.17 Key Cost Drivers of the LCOE

The diagram shows that the lifespan, capacity factor, and project discount rate have the highest impact on the LCOE. From the baseline, all have the potential to influence and increase the LCOE by a significant amount. A lifespan of 10 years will have an increased LCOE of 64.0 \$/MWh, a capacity factor of 35 % increases it by 51.1 \$/MWh, and a project discount rate of 10 % raises it by 44.8 \$/MWh from the baseline. On the other hand, it is also possible that they may contribute to a reduced LCOE by -10.9 \$/MWh, -24.8 \$/MWh, and -25.7 \$/MWh for the lifespan, capacity factor, and project discount rate, respectively.

The contingency and steel price are equal in their possible influence on the LCOE, ranging from ± 11.3 \$/MWh. Almost similar to these are the variations in OpEx. It varies only slightly more in LCOE at ± 12.8 \$/MWh. A reduction in the number of turbines increases the LCOE significantly, while an increase slightly reduces the LCOE. As it increases the LCOE by 20.7 \$/MWh at 10 turbines, even though the LCOE only decreases by 2.6 \$/MWh at 150 turbines. This applies to the distance to shore as well as it only has the potential to reduce the LCOE by -2.3 \$/MWh, while it can increase it by 14.7 \$/MWh at 700 km from shore. The increase in water depth is expected to result in a rise of 6.2 \$/MWh in the LCOE at a depth of 700 m. Impacts of turbine spacing on LCOE may range from -1.3 \$/MWh when spaced at 3 rotor diameters to +1.7 \$/MWh when spaced at 12 rotor diameters.

7.4 Financial Modeling

For evaluating the economic potential of the wind farm, selected financial calculations have been conducted. First, the net present value, (NPV), internal rate of return (IRR), and payback period (PP) are calculated and set as the financial baseline. Furthermore, sensitivity analyses of the various parameters are computed and displayed to examine how it affects the initial investment.

The financial modeling has been conducted with the same baseline parameters as Section 7.1. The economic feasibility of the wind farm is calculated based on a cash flow analysis, displayed in Table 7.7. As elaborated in Section 6. Methodology, the project discount rate is equal to the pre-tax WACC of 5.46 %.

Table 7.7 Calculation of NPV, IRR, and PP

<i>USDm</i>	2024	2025	2026	2027	2028	2029	2030	2031	2032
Total Revenue	-	333.2	333.2	333.2	333.2	333.2	333.2	333.2	333.2
(-) CapEx	3 571.0	-	-	-	-	-	-	-	-
(-) OpEx	-	88.5	88.5	88.5	88.5	88.5	88.5	88.5	88.5
(-) DecEx	-	-	-	-	-	-	-	-	-
(+) Depreciation	-	142.8	142.8	142.8	142.8	142.8	142.8	142.8	142.8
(-) Principal Payment	-	166.6	166.6	166.6	166.6	166.6	166.6	166.6	166.6
(-) Interest Payment	-	118.0	110.1	102.3	94.4	86.5	78.7	70.8	62.9
(+) Interest Tax Deduction	-	26.0	24.2	22.5	20.8	19.0	17.3	15.6	13.8
Cash Flow	- 3 571.0	128.9	135.0	141.2	147.3	153.4	159.6	165.7	171.8
Cumulative Cash Flow	- 3 571.0	- 3 442.1	- 3 307.1	- 3 165.9	- 3 018.6	- 2 865.1	- 2 705.6	- 2 539.8	- 2 368.0

<i>USDm</i>	2033	2034	2035	2036	2037	2038	2039	2040	2041
Total Revenue	333.2	333.2	333.2	333.2	333.2	333.2	333.2	333.2	333.2
(-) CapEx	-	-	-	-	-	-	-	-	-
(-) OpEx	88.5	88.5	88.5	88.5	88.5	88.5	88.5	88.5	88.5
(-) DecEx	-	-	-	-	-	-	-	-	-
(+) Depreciation	142.8	142.8	142.8	142.8	142.8	142.8	142.8	142.8	142.8
(-) Principal Payment	166.6	166.6	166.6	166.6	166.6	166.6	166.6	-	-
(-) Interest Payment	55.1	47.2	39.3	31.5	23.6	15.7	7.9	-	-
(+) Interest Tax Deduction	12.1	10.4	8.7	6.9	5.2	3.5	1.7	-	-
Cash Flow	178.0	184.1	190.3	196.4	202.5	208.7	214.8	387.6	387.6
Cumulative Cash Flow	- 2 190.0	- 2 005.9	- 1 815.6	- 1 619.2	- 1 416.7	- 1 208.1	- 993.3	- 605.7	- 218.1

<i>USDm</i>	2042	2043	2044	2045	2046	2047	2048	2049	2050
Total Revenue	333.2	333.2	333.2	333.2	333.2	333.2	333.2	333.2	-
(-) CapEx	-	-	-	-	-	-	-	-	-
(-) OpEx	88.5	88.5	88.5	88.5	88.5	88.5	88.5	88.5	-
(-) DecEx	-	-	-	-	-	-	-	-	36.0
(+) Depreciation	142.8	142.8	142.8	142.8	142.8	142.8	142.8	142.8	-
(-) Principal Payment	-	-	-	-	-	-	-	-	-
(-) Interest Payment	-	-	-	-	-	-	-	-	-
(+) Interest Tax Deduction	-	-	-	-	-	-	-	-	-
Cash Flow	387.6	387.6	387.6	387.6	387.6	387.6	387.6	387.6	36.0
Cumulative Cash Flow	169.5	557.0	944.6	1 332.2	1 719.8	2 107.4	2 494.9	2 882.5	2 846.5

Disc. Rate	5.46 %	NPV	- 561.9 <i>USDm</i>	IRR	4.0 %	PP	18 years, 30 weeks
-------------------	--------	------------	---------------------	------------	-------	-----------	--------------------

Based on an estimated spot price of 96.15 \$/MWh, the wind farm is expected to generate a total of \$ 333 200 000 in revenue each year until 2049. The investment cost in 2024 is estimated to be \$ 3 571 000 000 and is depreciated linearly through the entire period, thus resulting in \$ 142 800 000 over 25 years. Decommissioning costs are \$ 36 000 000 after subtracting the scrap value of the components. Due to the loan being a 15-year serial, the principal payments are \$ 166 600 000 each year until the loan is repaid in 2039. The interest payments decrease along with the loan being repaid, and at the final term, the total interest cost is \$ 943 900 000. The tax shield reduces the interest costs by 22 % a year, which implies a reduction of \$ 207 660 000.

Based on the results from Table 7.4 the Trollvind wind farm NPV is negative \$ 561 900 000, implying a non-profitable scenario for the baseline investment. The corresponding IRR is 4.0 %, thus smaller than the opportunity cost (WACC). As long as the wind farm is operating, the cash flow is positive. The PP is 18 years and 30 weeks, which means the investment will have a cumulative cash flow of zero in Medio 2042.

7.5 Financial Sensitivity Analyses

For evaluating how susceptible the financial model of the wind park is to specific parameters, several sensitivity analyses have been conducted. These include financial metrics such as the project discount rate, repayment time, and investment period. The analyses will be performed to identify how the parameters affect three indicators: NPV, IRR, and PP.

7.5.1 Project Discount Rate

The rate at which the wind farm investment is discounted is set to 5.46 % as the baseline, and it is of interest to evaluate how the discount rate impacts the NPV. As the discount rate changes, the IRR and PP are expected to not change, due to the discount rate not impacting the nominal cash flow. Figure 7.18 displays how the NPV is affected by a variation of the discount rate from 1-10 %.

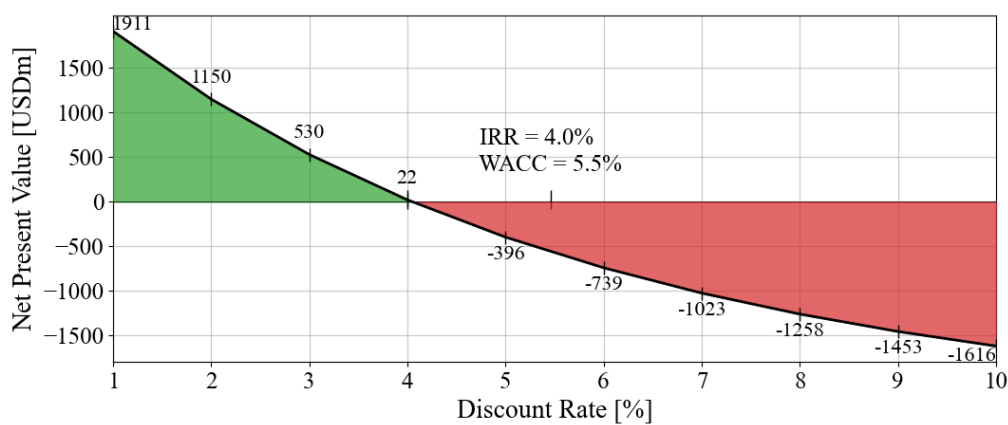


Figure 7.18 Project Discount Rate Impact on Financial Metrics

As expected, PP and IRR are not impacted by the variation in the discount rate and are therefore still 18 years and 30 weeks, and 4.0 %, respectively. The NPV changes from a positive value to a negative value at the point where the discount rate equals the IRR, 4.0 %. For a discount rate of 1 %, the NPV is estimated to be \$ 1 910 900 000, which is the maximum value of the analysis. The NPV is also positive for values of 2-4 %, but corresponding with the IRR at 4 %, NPVs for discount rates over this point are negative.

As the discount rate increases, the NPV decreases to a negative NPV of \$ 1 615 600 000 for a discount rate of 10 %. The NPV tendency line is steepest in the interval of 1-4 %, thus the difference between the NPVs is more significant in this interval. From 4-10 %, the line is flatter, hence the values have a less significant spread. The total difference in NPV between a rate of 1 % and a rate of 10 % is \$ 3 526 500 000, almost equivalent to the initial investment cost.

7.5.2 Debt Repayment Time

The baseline investment is calculated with a 15-year serial loan, which resulted in a negative NPV. For optimizing the time estimated to repay the loan, a sensitivity of the total debt repayment time is conducted. Figure 7.19 illustrates the difference in NPV for debt repayment times of 10-20 years.

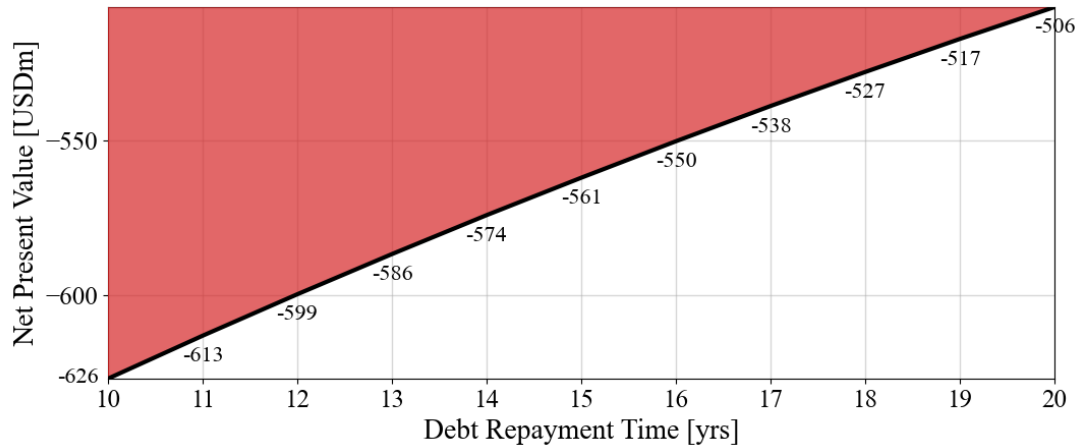


Figure 7.19 Debt Repayment Time Impact on Financial Metrics

As displayed in the figure, the NPV is negative \$ 626 900 000 for a repayment time of 10 years, which is also the minimum NPV. The tendency is that NPV increases along with the repayment time, with a minor variation in the slope. By increasing the repayment time from 10 to 15 years, the NPV increases from negative \$ 626 900 000 to negative \$ 561 900 000, hence a total increase of \$ 65 000 000. From 15 to 20 years, the difference is only \$ 55 200 000, implying a more rapid increase of NPV in the interval of 10-15 years, compared to 15-20 years.

The greatest NPV is achieved by a debt repayment time of 20 years, as the NPV is negative \$ 506 200 000. From the minimum value at 10 years to the maximum value at 20 years, the total difference is \$ 120 200 000, hence a 19.2 % reduction of the deficit. The PP is 17 years and 51 weeks for 10 years of repayment time, which is the earliest PP for all variations. As the repayment time increases, the PP is delayed by 6-7 weeks for each extra year, until the trend changes direction and the PP is expedited for years 19 and 20.

7.5.3 Electricity Spot Price

As the electricity spot price is a parameter with significant fluctuations and contains several uncertainties, it is of interest to evaluate how the changes impact the profitability of the investment. It is expected that variations in the spot price will affect the total revenue, and thus have a significant impact on the NPV, IRR, and PP. Figure 7.20 displays the results from the sensitivity analysis of variations in the spot price. The columns represent the NPV, while the black line illustrates the trend of IRR.

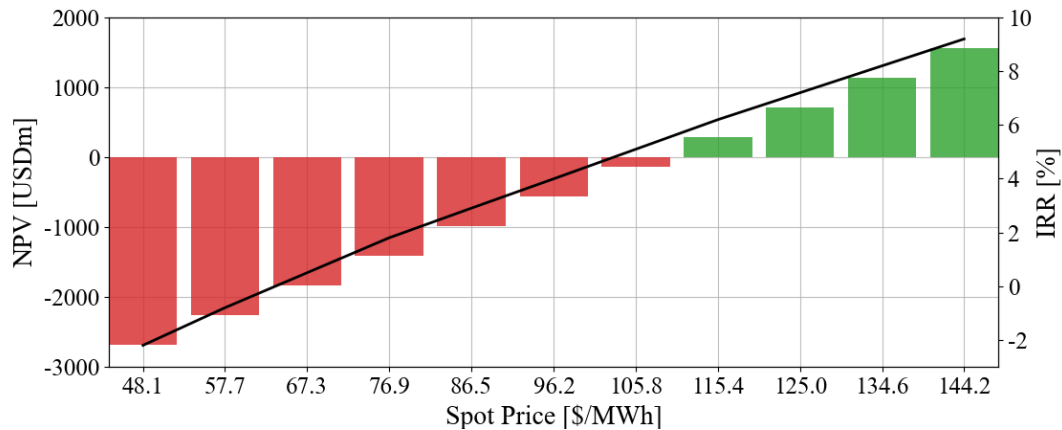


Figure 7.20 Spot Price Impact on Financial Metrics

As of Figure 7.20, spot price fluctuations can lead to great variations in NPV and IRR. If the price is reduced by 50 % from the baseline of 96.2 \$/MWh, the resulting NPV is negative \$ 2 689 500 000. At this level of spot price, the IRR is negative 2.2 %, and the PP will never end, as the cumulative cash flow is negative at the end of the investment period. At a 30 % reduction, which implies a spot price of 67.3 \$/MWh, the NPV is negative \$ 1 838 400 000, while the IRR is 0.5 % and the PP is 24 years and 35 weeks.

The NPV changes from negative to positive at a spot price of 108.7 \$/MWh, and thus this is the price where the IRR equals the discount rate (WACC). With a 20 % increase from the baseline, the investment has an NPV of \$ 289 200 000, and an IRR of 6.2 %, with a PP of 14 years and 50 weeks. If the spot price increases 50 % and averages at 144.2 \$/MWh, the NPV will be \$ 1 565 700 000. The corresponding IRR will be 9.2 % and the PP will be 11 years and 15 weeks, which is over seven years shorter than the baseline PP.

7.6 Innovative Solutions

As shown in Section 7.4, the costs associated with offshore wind energy remain significantly high compared to the electricity prices. To overcome this challenge, researchers and companies have developed innovative solutions as presented in Section 3.4. This section provides estimates for the potential LCOE reduction for different innovative solutions. The LCOE values only provide an approximation and cannot be perceived as the outright correct value since the use of estimates instead of detailed engineering has been utilized.

7.6.1 Shared Substructure

To evaluate the TwinWind concept, a wind farm with half the number of substructures (this affects the array system, mooring, and substructure) has been modeled, and therefore these component costs have been adjusted based on the methods in Section 6.5. This includes increasing the affected costs with an adjustment factor. For the non-affected components, the cost is set to the same as the reference wind farm. With the use of shared substructures, the LCOE is calculated to be 91.11 \$/MWh. These calculations have been exhibited in Table 7.8.

Table 7.8 Calculation of Adjusted Cost for TwinWind

Description	Adjusted Cost	Difference from Baseline	
Array System	\$ 44 550 000	-\$ 24 300 000	35.3 %
Export System	\$ 110 700 000	\$ 0	0 %
Substructure	\$ 991 728 000	-\$ 284 012 000	22.3 %
Mooring System	\$ 147 187 000	-\$ 38 533 000	20.7 %
Offshore Substation	\$ 204 813 000	\$ 0	0 %
Array System Installation	\$ 11 340 000	-\$ 8 910 000	44.0 %
Export System Installation	\$ 195 426 000	\$ 0	0 %
Substructure Installation	\$ 50 490 000	-\$ 6 210 000	11.0 %
Mooring System Installation	\$ 28 080 000	-\$ 4 320 000	13.3 %
Offshore Substation Installation	\$ 5 265 000	\$ 0	0 %
Turbine	\$ 759 000 000	\$ 0	0 %
Soft	\$ 653 400 000	\$ 0	0 %
Project	\$ 204 000 000	\$ 0	0 %
OpEx (annually)	\$ 88 500 000	\$ 0	0.0 %
AEP [MWh]	3 552 317	86 642	2.5 %
LCOE [\$/MWh]	91.11	- 9.58	9.5 %

7.6.2 Shared Mooring Lines

For the new LCOE calculation of the shared mooring lines, there have been performed adjustments of the costs. This is based on decreased mooring line length compared to the reference wind farm. This includes reducing the cost of the mooring system (relating to reducing mooring length) and the mooring installation. For the innovative solution of shared mooring, three estimates are considered: (1) two turbines connected, (2) squared shared lines, and (3) hexagon pattern, all based on concepts from figure 3.11. These adjusted costs are displayed in Table 7.9. The LCOE is estimated to decrease in the span of 99.96 \$/MWh to 98.52 \$/MWh.

Table 7.9 Calculation of Adjusted Cost for Shared Mooring Line Concepts

Description	Adjusted Cost	Difference from Baseline	
Two turbines with shared line			
Mooring System	\$ 154 148 000	-\$ 31 572 000	
Mooring System Installation	\$ 26 892 000	-\$ 5 508 000	
LCOE [\$/MWh]	99.96	- 0.73	
Four turbines with shared lines			
Mooring System	\$ 124 432 000	-\$ 61 288 000	
Mooring System Installation	\$ 21 708 000	-\$ 10 692 000	
LCOE [\$/MWh]	99.26	- 1.43	
Hexagon concept			
Mooring System	\$ 92 860 000	-\$ 92 860 000	
Mooring System Installation	\$ 16 200 000	-\$ 16 200 000	
LCOE [\$/MWh]	98.52	- 2.17	

8. Discussion

8.1 Baseline Trollvind

An initial cost of over \$ 3 770 500 000 is a significant investment decision to make and contains several risks and uncertainties. As the results show, the largest portion of the cost is related to the wind turbines and associated substructures. The two components account for over half of the total costs, which implies that the largest portion of uncertainty is related to these, and hence requires a high degree of consideration. Smaller costs such as the installation of substructure and turbine, mooring line, and project cost, make up a smaller fraction of the total, and variations in these costs will most likely not have as great consequences as variations in i.e., the substructure cost. Soft costs, costs that are not related to one specific component, make up 17 % of the initial cost, which could be considered a noticeable part of the total. These costs, such as insurance and financing of the wind farm, could be difficult to manage, as they are indirect and dependent on many factors. Evaluating and negotiating contracts that regard soft costs could potentially contribute towards reducing the initial cost, and thus, reduce the risk related to the investment.

The baseline LCOE is slightly above 100 \$/MWh, highly driven by the OpEx, comprising over 37 % of the total LCOE. This indicates a potential for reducing the LCOE, by reducing the yearly OpEx. The OpEx is fixed at \$ 88 500 000 every year, however, by identifying and evaluating innovative maintenance strategies, this cost might be possible to reduce. By optimizing a combination of corrective and preventive maintenance, some of the major failures which account for a significant amount of the downtime, could be avoided. As the wind farm is located 65 km from the nearest harbor, and the Trollvind location is exposed to relatively harsh weather conditions, maintenance might be difficult to schedule. This could also lead to extended periods of downtime, thus decreasing the annual energy production, and increasing the OpEx.

The detailed component description in Table 7.3 displays some of the more specific key cost drivers for the Trollvind wind farm. In the context of evaluating costs for the array system, it is noteworthy that the export cable expenditures are nearly twice as high as those incurred for the inter-array cables. This observation emphasizes some of the importance of accounting for the distance to shore when assessing project expenses. The use of a jacket foundation has been assumed for the substation in this case. However, a more comprehensive assessment would entail an evaluation of the feasibility of a floating substation, which could entail a more costly floater and mooring expenses. All turbine floating modules are also assumed as semi-submersible substructures and other concepts such as spar buoy, tension leg platform or barge floater have not been evaluated. Given that the Trollvind project is owned by Equinor and involves deep-water operations, the deployment of the spar buoy technology could prove highly pertinent.

When evaluating the installation phase, the findings underscore the critical role of efficient planning and management during the installation phase of large wind farm projects. Notably, the assembly of turbines and substructures, in conjunction with the offshore installation of the complete structure, represents a substantial proportion of the overall installation duration and costs. To minimize delays and increase efficiency, it is crucial to identify potential time and resource constraints early in the project planning phase and develop contingency plans to mitigate any potential delays. For the Trollvind project, the second assembly lines were crucial for minimizing unnecessary delays by upwards of 70 % based on earlier modeling. Furthermore, effective coordination and communication between all project stakeholders, including vessel operators, construction crews, and engineering teams, are essential to ensure the timely and successful completion of the installation phase. Finally, cost considerations must also be taken into account, as vessel day rates, transit, delays, mobilization, and other expenses can significantly impact project budgets, and strategies to minimize costs should be explored where feasible.

8.2 Sensitivity Analyses

8.2.1 Project Life Span

The analysis shows that the LCOE decreases as the life span increases, thus, a 35-year life span provides the lowest LCOE. As Figure 7.4 and Table 7.5 shows, the LCOE starts to flatten out as the life span increases, however, it is not realistic to have life spans so long that it flattens completely out. Although the longer life spans to provide the lower LCOE, the CapEx cost has not been adjusted according to the different life spans. Materials and installation for a wind farm with longer life spans can be more time-consuming and expensive to install, which the model has not taken into consideration.

Similar to the CapEx, the annual OpEx does not vary even though the life span increases. With an increased life span, the wind farm may require more annual maintenance, which would have a negative impact on the LCOE. This would also influence the cost breakdown, where the OpEx cost has the most prominent change. The CapEx will not vary after its initial expense, but the OpEx will increase as the total energy production rises with a longer life span. Thus, it will impact the total cost more as the lifespan expands.

8.2.2 Scale Effect

It can be expected that an increased number of turbines may lead to a reduced LCOE. At a lower number of turbines, from five to 25, the LCOE decreases drastically. However, the results showed that the LCOE starts to flatten out as the scale of the wind farm increases.

With an increased number of turbines, OpEx will start to constitute more of the total cost. This is seen to happen as the LCOE decreases, but as the graph flattens out the OpEx does not change substantially in terms of the total cost. The cost breakdown shows that the project cost has the most distinguished change. Since the project cost is fixed even though the number of turbines varies, it will naturally make up a larger part of the total cost when there are fewer turbines. The

assumption that the project cost does not vary even though the number of turbines increases can be seen as a limitation as it is reasonable to assume that an increased number of turbines require more costs related to the project.

8.2.3 Turbine Power Rating

As seen in Figure 7.8, when the turbine power rating varies the LCOE drops more in percent per MW at the lower power ratings. This means that the effect on LCOE is more notable when the power rating is increased from 6 MW to 12 MW, rather than from 12 MW to 15 MW. Although the 15 MW turbine has a CapEx that is 90.8 % and 18.5 % higher than the 12 MW and 15 MW wind turbines, respectively, it still provides the lowest LCOE. This is because the annual energy production increases more in percentage than the CapEx cost. Thus, the results show that even though the CapEx is noticeably higher when the power rating increases, it will still provide the lowest LCOE.

The cost breakdown, seen in Figure 7.9, shows that the OpEx cost constitutes a larger part of the total cost as the power rating increases. This could be expected since the CapEx cost does not increase linearly with higher power ratings.

8.2.4 Project Discount Rate

The results from Figure 7.10 show that the projected discount has a significant impact on the LCOE. As the interest rates and debt ratio may vary for every single project, the results show that this is an area that is important for the project owners to focus on. The interest rates are difficult to influence as they are set by the central bank. However, by varying the debt-to-equity ratio it is possible to influence the WACC. As seen in Section 7.1.1, the CapEx cost is a significant expense. Thus, it may be difficult for the project owners to influence it substantially.

8.2.5 Operational Expenditure

Figure 7.11 shows that a change in the OpEx cost has an impact on the LCOE, however, it is not as influential as the project discount rate. From the baseline, the CapEx cost constitutes 63 % of the total. Thus, it is reasonable that the OpEx does not have as immense an impact as the CapEx.

In this thesis, the OpEx cost is not varying over the project's lifespan, which may not be completely realistic. There can occur incidents that force more maintenance, which could increase the OpEx by a variable amount. As well as the possibility for the wind turbines to need more maintenance in the latter years of their lifetime. As described in Section 6.3.2, various sources state a different OpEx cost, i.e., it is feasible to assume that the OpEx cost varies. Figure 7.12 shows that OpEx is the affected factor in the cost breakdown, which is expected. Additionally, it illustrates that with a vast increase in OpEx, it can make up almost half of the total cost.

8.3 Metocean Sensitivity Analysis

8.3.1 Capacity Factor

With varying wind conditions at offshore sites, a change in the capacity factor may occur. The capacity factor, calculated in Section 6.2.4, is based on the power rating graph for the wind turbine, as well as the Weibull distribution of the wind conditions at the site. Although the wind conditions are based on the last nine years and should be representable for the coming years, they can be variable; thus, a sensitivity analysis is conducted. The results show that the LCOE is highly sensitive to a change in the capacity factor. At a lower capacity factor, the effect of an increased capacity factor is more prominent. However, the results show that the LCOE decreases significantly even when the initial capacity factor is high. This implies the importance of considering the wind conditions and the power rating graph when researching potential new offshore wind sites.

8.3.2 Site Conditions

Similar to the wind conditions, the water depth and distance to shore can also vary. Contrary to the wind conditions, these do not have a significant impact on the LCOE. This shows that although they are factors to consider, none of them are areas to highly emphasize. However, there are some shortcomings as only the CapEx cost is influenced in both analyses. The OpEx cost could realistically be influenced in both instances. For the water depth the mooring length would increase which could lead to more maintenance. With an increased distance to shore, the operating time of maintenance can rise as the vessels will take a longer time to reach the site; thus, increasing the OpEx cost.

8.3.3 Key Cost Drivers of the LCOE

The key cost drivers of the LCOE display which of the factors has the most impact on the LCOE. The results show that the lifespan, capacity factor, and project discount rate have the most influence. As seen, a shortened lifespan can increase the LCOE by a substantial amount. A 10-year lifespan would not be a sensible lifespan for a wind farm; however, it shows the potential risk of how high the LCOE can be if the wind farm cannot fulfill its planned life span. The project discount rate, WACC, is also seen to have a considerable effect on the LCOE. It is the factor with the most potential of reducing the LCOE. Although it is possible to influence the WACC by adjusting the debt-to-equity ratio, it is also highly influenced by the national interest rates; thus, it can be difficult to impact. The capacity factor is also an essential cost driver. This shows the importance of choosing wind farm areas and layouts as these impacts the capacity factor.

The diagram shows that the variation in contingency, and steel price has a similar effect on the LCOE, while the OpEx has a slightly higher impact. The OpEx and steel price is set to vary from $\pm 50\%$ since these are seen to be more subject to change than the contingency. Even though they all affect different areas of the total cost, the possible change in LCOE is remarkably similar. The scale effect, distance to shore, water depth, and turbine spacing are the

factors with the least potential to positively impact the LCOE. On the other hand, the scale effect, distance to shore, and water depth may all have a noticeable negative impact.

8.4 Financial Evaluation

As the Trollvind wind farm has a negative NPV of over \$ 500 000 000, it is relatively far from being a profitable investment, and various measures need to be considered. The cost of manufacturing and installing a wind park is quite significant, which results in a large initial cost, and considerable debt. One way of making the investment profitable could be to work towards reducing the CapEx, hence reducing the large portion of expenses at the early point of the investment. This could be executed by renegotiating contracts and considering more suppliers for the different components. An alternative way to reduce the initial cost is to apply for subsidies from the government or non-governmental organizations, hence reducing both debt and initial investment portion.

If it is not achievable to lower the initial cost, another option is to increase the yearly cash flow with two things; (1) increase the revenue, or (2) reduce the current expenses. The revenue of \$ 333 200 000 could be increased by selling the electricity at a higher price or generating more power. Generating more power normally requires more costs, both initially and yearly, which need to be evaluated thoroughly before deciding to invest in greater power capacity. The current spot price of 96.15 \$/MWh is apparently not sufficient to cover the expenses and make the investment profitable, even if the cash flow is positive most years, and the cumulative cash flow turns positive in the year 2042. Predicting the spot price for the next 25 years is difficult and would contain a lot of uncertainty. To reduce this uncertainty, it might be beneficial to identify the spot price that provides an NPV of zero and try to negotiate power purchase agreements (PPA) above this value.

The Trollvind project has two yearly expenses that may be reduced, OpEx and interest payments, as principal payments impact the yearly cash flow but are not considered direct expenses. The OpEx is fixed at \$ 88 500 000 each year, but in practice, it will probably be lower early in the investment period and increase throughout. Floating wind turbines have considerably higher OpEx than land-based ones due to aspects such as availability and vessel requirements. Different maintenance strategies could be contemplated to reduce the yearly OpEx, thus increasing the cash flow and project profitability. The 15-year serial loan has a 4.72 % interest rate, and by evaluating other loan terms, the loan-related expenses might be reduced.

An IRR of 4.0 % is not necessarily an unacceptable yield, but as it is lower than the WACC, it implies that the investment may be reassessed. An IRR lower than the WACC implies that the cost of opportunity may be higher than the considered alternative, thus other investments might be more profitable than the Trollvind wind farm.

8.5 Financial Sensitivity Analyses

As the initial baseline investment provided a negative NPV, analyses of three different parameters were conducted to provide information for evaluating measures toward making the investment profitable.

8.5.1 Project Discount Rate

Results from the discount rate sensitivity implied that a lower discount rate resulted in a higher NPV. This implies that one procedure for making the investment profitable could be to lower the WACC, as this is used for setting the discount rate. The IRR was calculated to approx. 4.0 %, hence this is what the WACC needs to be lowered to for the investment to be economically viable since the WACC controls the discount rate. A WACC of 4.0 % or lower would provide a positive NPV but might be difficult to achieve in practice, as the WACC is impacted by several aspects such as debt/equity ratio, systematic risk, and the expected return of the market. Some of these parameters, like the debt/equity ratio, are possible to determine and adjust individually, but parameters such as the systematic risk apply to the entire market and would therefore be difficult to adjust within a project or company.

8.5.2 Debt Repayment Time

The results from variations in debt repayment time showed that an increase from 10 to 20 years in repayment time increased the NPV, and thus, the profitability of the project. The trend line is nearly linear, but slightly flattened out after 15 years. This implies that the trend is most likely to continue if the sensitivity boundaries are extended, and probably reach a maximum point where the NPV would no longer increase with the extension of repayment time. By increasing the repayment time from the baseline of 15 years to 20 years, the NPV increases by \$ 55 200 000, which is a significant amount if it is compared to the total initial NPV of negative \$ 561 900 000.

One of the primary reasons why the NPV increases with a longer debt repayment time is the delay in payments so that the principal amount is discounted further ahead in time. By carrying forward the debt payments, the cash flow will increase at the beginning of the project, hence the value of the cash flow is larger than at a later point of discount. This implies that to achieve maximum profitability of the investment, it might be reasonable to delay the principal payments as much as possible since a greater cash flow early in the project increases the NPV.

8.5.3 Spot Price

Variations in the spot price are the sensitivity that provided the most significant differences and thus is one of the most important parameters to contemplate. The spot price also contains a lot of uncertainty, and as mentioned earlier, predicting the spot price 25 years ahead is severely challenging. Results from the analysis indicate that the difference between a 50 % reduction and a 50 % increase is over \$ 4 000 000 000 in NPV, which indicates that the profitability of the investment is highly dependent on the spot price. Thus, before making an investment decision, contemplating the uncertainty regarding the spot price systematically appears to be

important. Additionally, identifying and evaluating measures to reduce specific uncertainty could be of interest to investment decision-makers.

In the analysis, a break-even spot price of 108.7 \$/MWh was identified, which implies that if all costs are presumed correctly, this is what the 25-year average needs to be for achieving an NPV of zero. This is noticeably higher than the 96.2 \$/MWh applied in the baseline calculations, and might not be realistic, hence unattainable. As discussed in 8.6.1, a PPA might be beneficial, and with the sensitivity results calculated, the fixed-price needs to be at least 108.7 \$/MWh to break even.

8.6 Innovative Solutions

Results from the innovative solutions of sharing mooring lines and substructures provide an outlook for the opportunities of decreasing the LCOE of offshore wind. Since the calculations are largely based on estimates, all results for the innovative solutions must be understood with caution. Simultaneously, the estimates can demonstrate the significance of further developing the new concepts, and most importantly which concepts have the greatest cost-efficiency.

The results exhibit large differences in the LCOE for different concepts. This is exposed with the largest opportunity of LCOE reduction being concepts that decrease the number of substructures. Correlating to the large percentage of CapEx associated to the substructure fabrication and installation. While cost reductions in the mooring system are important, they may not provide the most significant percentage of change to the overall LCOE of the project. Overall, innovation is important for further LCOE reduction, and optimization of a future wind farm may include multiple concepts, new material technology, and enhanced procedures.

8.7 Limitations

Since the modeling efforts are based on the NREL ORBIT wind farm modeling package there is a margin of error that prevents the cost estimates from achieving 100 % accuracy. This is because of the scaling parameters, unit costs, and lack of detailed engineering design. While these modeling assumptions provide the possibility to perform comprehensive economic evaluations, the margin of error will constantly be present. In a more detailed case for Trollvind, there would be necessary with more specific substructure, mooring, seabed, substation engineering designs, and additional evaluation for soft and project costs based on Norwegian conditions.

With the OpEx being based on a cost per MW of the theoretical power output, it sets a limitation as it generalizes all offshore floating wind farms. The Trollvind area has its own site-specific parameters such as water depth, distance to shore, and wind conditions. All of these factors may have an influence on the OpEx cost, e.g., an increased vessel cost if the offshore site is located further from shore than other areas. Thus, to conduct a more comprehensive assessment of the

Trollvind area, it would be imperative to gather more accurate and detailed data on the OpEx cost for this specific site.

One of the primary limitations is the unpredictability of interest rates, which can change on a daily basis, and the investment proposal would therefore not be valid for a long period. Interest rates play a crucial role in determining the cost of capital for the project, which in turn affects the cash flows and profitability of the investment. The spot price of electricity is a critical determinant of revenue for the project, and any significant fluctuation can significantly impact profitability. In addition, it is essential to consider the volatility and uncertainty associated with spot prices, which is challenging to implement in a conceptual cash flow analysis. Although the assessment may not consider subsidies, it is important to note that in practice, many floating offshore wind farms receive subsidies, which can significantly impact the financial viability of the project.

Several of the implied reductions in costs related to innovative solutions originate from Hexicon, the patent owner of TwinWind. This is a limitation as the information might be biased or affected by the company's intention of promoting their concept. Further, a few simplifications had to be provided, as both TwinWind and shared mooring are relatively new concepts; thus, they have not been researched comprehensively.

9. Conclusion

The purpose of this master's thesis was to sufficiently answer the following research question:

How to estimate the life cycle costs of a floating wind farm off the coast of Norway?

With the partial objectives of:

1. *Identifying and analyzing key cost drivers throughout the life cycle*
2. *Understanding how the different input parameters affect the LCOE*
3. *Assessing the financial metrics of the wind farm investment*

In this thesis, a comprehensive analysis of the total costs of an offshore wind farm located off the coast of Norway was conducted. The key cost drivers were presented before several sensitivity analyses were performed to assess how different parameters affect the LCOE. The economic feasibility of the wind farm was also evaluated, and at last innovative offshore wind solutions were assessed. Based on these results, a few concluding remarks can be drawn:

1. The levelized cost of energy for the Trollvind wind farm is 100.69 \$/MWh. The key cost driver is capital expenditure which constitutes 63.1 % of the total cost, where the wind turbines and associated substructure account for over half of this.
2. The sensitivity analyses show that the primary cost influencers on the levelized cost of energy are the lifespan, capacity factor, and project discount rate. The lifespan has the highest possible increase in cost as it may vary -10.9 \$/MWh to $+64.0$ \$/MWh from the baseline. Further, the capacity factor and project discount rate may increase the cost by 51.1 \$/MWh and 44.8 \$/MWh or reduce it by 24.8 \$/MWh and 25.7 \$/MWh, respectively.
3. Trollvind faces profitability challenges due to a negative NPV and an IRR lower than the WACC, implying that alternative investments might be more profitable. Reducing initial costs, increasing revenue, or reducing expenses could enhance profitability. Predicting the spot price over the next 25 years is uncertain, and PPAs should be negotiated to reduce uncertainty.
4. A lower discount rate and longer debt repayment time increase the NPV and profitability of the investment. However, the spot price is the most important factor affecting the NPV and has a break-even point of 108.7 \$/MWh.
5. The innovative solutions of TwinWind and shared mooring show the potential to reduce the LCOE. Innovation plays a crucial role in achieving further LCOE reduction, and optimizing future wind farms may involve incorporating multiple concepts, utilizing new material technology, and implementing enhanced procedures.

10. Suggestion for Further Work

In this thesis, only one, semisubmersible floating foundation has been considered. For further examination of the Trollvind wind farm, it could be of high interest to evaluate different substructures such as spar or tension-leg platforms. Illustrated in the results, the substructure including installation is one of the most significant costs of a floating wind farm. Thus, providing thorough information regarding which substructure is the most cost-effective could be highly valuable.

As presented in the methodology section, the costs related to operation and maintenance have been calculated with a factor only dependent on the theoretical capacity, hence a simplification. Identifying the actual operation and maintenance costs for the Trollvind wind farm would provide a more accurate estimate of both the levelized cost of energy and the investment proposal.

Several sensitivity analyses have been conducted for the Trollvind location, but to locate the best site for an offshore wind farm, the analysis could be expanded to include several locations. The Norwegian Sea is relatively spacious, thus, initially examining the weather conditions for various locations could be beneficial. With such an approach, it is possible to identify locations with the greatest potential for a wind farm, enabling the opportunity of examining each location more thoroughly.

This thesis assesses the potential of new innovative solutions, but further work should encompass other concepts, alterations to the turbine layout, material choices, and other more cost-effective alternatives. The aforementioned innovative alternatives hold the potential to lower the LCOE. Thus, it could be intriguing to conduct a comprehensive evaluation of other solutions and concepts to further understand their viability and potential for practical implementation.

11. References

- Abed, K. A., & El-Mallah, A. A. (1997, May). Capacity Factor of Wind Turbines. *Energy*, pp. 487-491.
- Accenture. (2017). *Changing the Scale of Offshore Wind - Examining Mega-Projects in the United Kingdom*. Accenture.
- Aker Solutions. (2023, March 07). *Subsea Substation – Unlocking the potential of floating offshore wind*. Retrieved from Aker Solutions: <https://www.akersolutions.com/news/news-archive/2022/subsea-substation--unlocking-the-potential-of-floating-offshore-wind/>
- Aldersey-Williams, J., & Rubert, T. (2019, January). Levelised cost of energy – A theoretical justification and critical assessment. *Energy Policy*, pp. 169-179.
- Aldersey-Williams, J., Broadbent, I. D., & Strachan, P. A. (2019, May). Better estimates of LCOE from audited accounts – A new methodology with examples from United Kingdom offshore wind and CCGT. *Energy Policy*, pp. 25-35.
- Altuzarra, J., Herrera, A., Matías, O., Urbano, J., Romero, C., Wang, S., & Soares, G. (2022). Mooring System Transport and Installation Logistics for a Floating Offshore Wind Farm in Lannion, France. *Journal of Marine Science and Engineering*.
- Anaya-Lara, O. (2016). Offshore wind farm arrays. In C. Ng, & L. Ran, *Offshore Wind Farms: Technologies, Design and Operation* (pp. 389-417). Woodhead Publishing.
- Archer, C. L., Mirzaeifayat, S., & Lee, S. (2013, August). Quantifying the sensitivity of wind farm performance to array layout options using large-eddy simulation. *Geophysical Research Letters*, pp. 4963-4970.
- Asgarpour, M. (2016). Assembly, transportation, installation and commissioning of offshore wind farms. In C. Ng, & L. Ran, *Offshore Wind Farms: Technologies, Design and Operation* (pp. 527-541). Woodhead Publishing.
- Attema, A. E., Brouwer, W., & Claxton, K. (2018, May). Discounting in Economic Evaluations. *Pharmacoeconomics*, pp. 745-758.
- Barooni, M., Ashuri, T., Sogut, D. V., Wood, S., & Taleghani, S. G. (2022, December). Floating Offshore Wind Turbines: Current Status and Future Prospects. *Energies 16*.
- Birkelund, H., Arnesen, F., Hole, J., Spilde, D., Jelsness, S., Aulie, F. H., & Haukeli, I. E. (2021). *Long-term Power Market Analysis 2021*. The Norwegian Water Resources and Energy Directorate.
- Bodie, Z., Kane, A., & Marcus, A. J. (2018). Equilibrium in Capital Markets. In *Investments 11th ed.* (pp. 277-424). McGraw-Hill Education.
- Bosch, J., Staffell, I., & Hawkes, A. D. (2019, December 15). Global levelised cost of electricity from offshore wind. *Energy*.
- Brealey, R. A., Myers, S. C., & Allen, F. (2011). Net Present Value and Other Investment Criteria. In *Principles of Corporate Finance 10th ed.* (pp. 101-126). McGraw-Hill Irwin.
- Brealey, R. A., Myers, S. C., & Allen, F. (2011). Risk and the Cost of Capital. In *Principles of Corporate Finance 10th ed.* (pp. 213-239). McGraw-Hill Irwin.

- Brindley, G., & Fraile, D. (2021). *Financing and Investment Trend - The European Wind Industry in 2020*. WindEurope.
- Bruck, M., Sandborn, P., & Goudarzi, N. (2018, July). A Levelized Cost of Energy (LCOE) model for wind farms that include Power Purchase Agreements (PPAs). *Renewable Energy*, pp. 131-139.
- Cascianelli, S., Astolfi, D., Castellani, F., Cucchiara, R., & Fravolini, M. L. (2021, November). Wind Turbine Power Curve Monitoring Based on Environmental and Operational Data. *IEEE Transactions on Industrial Informatics*, pp. 5209-5218.
- Castro-Santos, L. (2016). Life-Cycle Cost of a Floating Offshore Wind Farm. In L. Castro-Santos, & V. Diaz-Casas, *Floating Offshore Wind Farms* (pp. 23-38). Springer.
- Castro-Santos, L., Filgueira-Vizoso, A., Carral-Couce, L., & Formoso, J. F. (2016, October). Economic feasibility of floating offshore wind farms. *Energy*, pp. 868-882.
- Catapult. (2022). *Floating offshore wind: Cost reduction pathways to subsidy free*. Catapult.
- Collu, M., & Borg, M. (2016). Design of floating offshore wind turbines. In C. Ng, & L. Ran, *Offshore Wind Farms - Technologies, Design and Operation* (pp. 359-382). Woodhead Publishing.
- Cranmer, A., & Baker, E. (2020, April). The global climate value of offshore wind energy. *Environmental Research* 15.
- Damodaran, A. (1994). *Estimating Equity Risk Premiums*. Stern School of Business.
- Damodaran, A. (2005). Valuation Approaches and Metrics: A Survey of the Theory and Evidence. *Foundations and Trends in Finance*, pp. 693-784.
- Damodaran, A. (2008). *What is the riskfree rate? A Search for the Basic Building Block*. Stern School of Business.
- Damodaran, A. (2017). *Equity Risk Premiums (ERP): Determinants, Estimation and Implications*. Stern School of Business.
- Danish Ministry of Energy, Utilities and Climate. (2018). *Note on technology costs for offshore wind farms and the background for updating CAPEX and OPEX in the technology catalogue datasheets*. Danish Energy Agency.
- DHI. (2021, October 19). *Decode offshore wind engineering challenges at every stage*. Retrieved from DHI: <https://blog.dhigroup.com/2021/10/19/decode-offshore-wind-engineering-challenges-at-every-stage/>
- DNV. (2018). *Integrated analysis of floating wind turbines*. DNV.
- DNV. (2020). *Energy Transition Norway 2020*. DNV.
- DNV. (2022). *Energy transition outlook 2022 - A global and regional forecast to 2050*. DNV.
- DNV. (2023, March 07). *Floating Substations: the next challenge on the path to commercial scale floating windfarms*. Retrieved from DNV: <https://www.dnv.com/article/floating-substations-the-next-challenge-on-the-path-to-commercial-scale-floating-windfarms-199213>
- DNV. (2023, April 19). *Offshore wind development*. Retrieved from DNV: <https://www.dnv.com/power-renewables/themes/offshore-wind/offshore-wind-development.html>
- DNV. (2023, April 19). *Offshore Wind Feasibility*. Retrieved from DNV: <https://www.dnv.com/power-renewables/themes/offshore-wind/offshore-wind-feasibility.html>

- DNV. (2023). *Wind energy – going offshore*. DNV.
- Elmakis, D., & Lisnianski, A. (2006, January). Life Cycle Cost Analysis: Actual Problem in Industrial Management. *Journal of Business Economics and Management*, pp. 5-8.
- Elobeid, M., Tao, L., Ingram, D., Pillai, A., Mayorga, P., & Hanssen, J. (2022). Hydrodynamic performance of an innovative semisubmersible platform with twin wind turbines. *Conference on Ocean, Offshore and Arctic Engineering*.
- Emblemsvåg, J. (2020). On the Levelised Cost of Energy of Windfarms. *International Journal of Sustainable Energy* (pp. 700-718). Taylor & Francis Group.
- Equinor. (2023, March 20). *Equinor and partners consider 1 GW offshore wind farm off the coast of Western Norway*. Retrieved from Equinor: <https://www.equinor.com/news/20220617-considering-1gw-offshore-wind-farm-off-western-norway>
- Eriksson, H., & Kullander, T. (2013). *Assessing feasible mooring technologies for a Demonstrator in the Bornholm Basin as restricted to the modes of operation and limitations for the Demonstrator*. Gothenburg: University of Gothenburg.
- European Maritime Spatial Planning Platform. (2022). *North Sea*. Brussels: The European Commission.
- European Union. (2020). *An EU Strategy to harness the potential of offshore renewable energy for a climate neutral future*. European Union.
- European Union. (2022). *REPowerEU Plan*.
- Fama, E., & French, K. (2004). The Capital Asset Pricing Model: Theory and Evidence. *Journal of Economic Perspectives* 18, pp. 25-46.
- Gaertner, E., Rinker, J., Sethuraman, L., Zahle, F., Anderson, B., Barter, G., . . . Viselli, A. (2020). *Definition of the IEA 15-Megawatt Offshore Reference Wind Turbine*. National Renewable Energy Laboratory.
- Gailly, B. (2011). *Developing Innovative Organizations*. Palgrave Macmillan.
- Georgios, S. (2010). Techno-Economical Analysis of DC Collection Grid for Offshore Wind Parks. *Master thesis*, pp. 19-21.
- Graham, J., & Harvey, C. (2001). The theory and practice of corporate finance: evidence from the field. *Journal of Financial Economics* 60, pp. 187-243.
- Greaves, P. (2016). Design of offshore wind turbine blades. In C. Ng, & L. Ran, *Offshore Wind Farms - Technologies, Design and Operation* (pp. 105-136). Woodhead Publishing.
- Guachamin-Acero, W., Jiang, Z., & Li, L. (2020). Numerical study of a concept for major repair and replacement of offshore wind turbine blades. *Wind Energy* 23, pp. 1673-1692.
- Gözcü, O., Kontos, S., & Bredmose, H. (2022). Dynamics of two floating wind turbines with shared anchor and mooring lines. *Journal of Physics: Conference Series* 2265.
- Hall, M., Lozon, E., Housner, S., & Srinivas, S. (2022). Design and analysis of a ten-turbine floating wind farm with shared mooring lines. *Journal of Physics: Conference Series*.
- Heskestad, T. (2002, October). Regnskapsmessige Avskrivinger. *Scandinavian Journal of Business Research*, pp. 37-49.
- Hexicon. (2023, May 03). *Technology*. Retrieved from Hexicon: <https://www.hexicongroup.com/technology/>

- Hexicon. (2023, May 06). *TwinWind*. Retrieved from Hexicon: <https://hexiconpower.com/twinwind/>
- Hiester, T. R., & Pennell, W. (1981, January). Meteorological aspects of siting large wind turbines. *Environmental Science*.
- Hsu, S., Meindl, E., & Gilhousen, D. (1994, June). Determining the power-law wind-profile exponent under near-neutral stability conditions at sea. *Journal of Applied Meteorology*, pp. 757-765.
- International Electrotechnical Commission. (2019, April). IEC 61400-3-1:2019. American National Standards Institute.
- International Energy Agency. (2020). *Global Energy Review 2020*. Paris: International Energy Agency.
- IPCC. (2014). *Energy Systems*. In: *Climate Change 2014: Mitigation of Climate Change*. IPCC.
- Islam, R., Guo, Y., & Zhu, J. (2013). *Materials and Processes for Energy: Communicating Current Research and Technological Developments*. Formatex.
- Jagannathan, R., & Wang, Z. (1996). The Conditional CAPM and the Cross-Section of Expected Returns. *The Journal of Finance* 51, pp. 3-53.
- Jiang, Z. (2021, April). Installation of offshore wind turbines: A technical review. *Renewable and Sustainable Energy Reviews* 139.
- Johannessen, K., Meling, T. S., & Haver, S. (2002, March). Joint Distribution for Wind and Waves in the Northern North Sea. *International Journal of Offshore and Polar Engineering*.
- Jonkman, J., Robertson, A., Masciola, M., Song, H., Goupee, A., Coulling, A., & Luan, C. (2014). *Definition of the Semisubmersible Floating System for Phase II of OC4*. National Renewable Energy Laboratory.
- Jung, C., & Schindler, D. (2019, October). Wind speed distribution selection – A review of recent development and progress. *Renewable and Sustainable Energy Reviews*.
- Kolouchova, P., & Novák, J. (2010, May). Cost of Equity Estimation Techniques Used by Valuation Experts. *Working Papers IES*.
- Kreider, M., Oteri, F., Robertson, A., Constant, C., & Gill, E. (2022). *Offshore Wind Energy: Technology Below Water*. National Renewable Energy Laboratory.
- Lamb, H. H. (1975). *Our Understanding of the Global Wind Circulation and Climatic Variations*. Taylor & Francis.
- Lamb, W. F. (2021). A review of trends and drivers of greenhouse gas emissions by sector from 1990 to 2018. *Environmental Research Letters*.
- Lang, L. H., Litzenberger, R. H., & Liu, A. L. (1998, December). Determinants of interest rate swap spreads. *Journal of Banking and Finance*, pp. 1507-1532.
- Lazard. (2023). *2023 Levelized Cost Of Energy+*. Lazard.
- Lerch, M., De-Prada-Gil, M., Molins, C., & Benveniste, G. (2018, December). Sensitivity analysis on the levelized cost of energy for floating offshore wind. *Sustainable Energy Technologies and Assessments*, pp. 77-90.
- Li, L., Gao, Z., & Moan, T. (2023). Joint Environmental Data at Five European Offshore Sites for Design of Combined Wind and Wave Energy Devices. *International Conference on Ocean, Offshore and Arctic Engineering*. Nantes.

- Liang, G., Jiang, Z., & Merz, K. (2021). Mooring Analysis of a Dual-Spar Floating Wind Farm with a Shared Line. *Journal of Offshore Mechanics and Arctic Engineering*.
- Liang, G., Jiang, Z., & Merz, K. (2023). Dynamic analysis of a dual-spar floating offshore wind farm with shared moorings in extreme environmental conditions. *Marine Structures* 90.
- Liu, Y., Li, S., Yi, Q., & Chen, D. (2016, January). Developments in semi-submersible floating foundations supporting. *Renewable and Sustainable Energy Reviews*, pp. 433-449.
- Lloyd-Smith, P., Adamowicz, W., Entem, A., Fenichel, E. P., & Rad, M. R. (2021, March). The decade after tomorrow: Estimation of discount rates from realistic temporal decisions over long time horizons. *Journal of Economic Behavior and Organization*, pp. 158-174.
- Ma, K.-T., Luo, Y., Kwan, T., & Wu, Y. (2019). Types of Mooring Systems. In *Mooring System Engineering for Offshore Structures* (pp. 19-39). Gulf Professional Publishing.
- Mahmood, F. H., Resen, A. K., & Khamees, A. B. (2020, October). Wind characteristic analysis based on Weibull distribution of Al-Salman site, Iraq. *Energy Reports*, pp. 79-87.
- Maienza, C., Avossa, A. M., Ricciardelli, F., Coiro, D., Troise, G., & Georgakis, C. T. (2020, May). A life cycle cost model for floating offshore wind farms. *Applied Energy*.
- Maness, M., Maples, B., & Smith, A. (2017). *NREL Offshore Balance-of- System Model*. National Renewable Energy Laboratory.
- Manwell, J. F., McGowan, J. G., & Rogers, A. L. (2009). Wind turbine siting, system design and integration. In *Wind Energy Explained: Theory, Design and Application* (pp. 407-448). John Wiley & Sons.
- Manwell, J., McGowan, J., & Rogers, A. (2009). Introduction: Modern Wind Turbines and its Origins. In *Wind Energy Explained: Theory, Design and Application* (pp. 1-22). John Wiley & Sons.
- Manwell, J., McGowan, J., & Rogers, A. (2009). Wind Characteristics and Resources. In *Wind Energy Explained - Theory, Design and Application* (pp. 23-90). John Wiley & Sons.
- Martinez, A., & Iglesias, G. (2022). Mapping of the levelised cost of energy for floating offshore wind in the European Atlantic. *Renewable and Sustainable Energy Reviews* 154.
- Masseran, N. (2015, May). Evaluating wind power density models and their statistical properties. *Energy*, pp. 533-541.
- Masson-Delmotte, V., Portner, H.-O., Skea, J., Zhai, P., Roberts, D., Shukla, P., . . . Waterfield, T. (2018). *Global Warming of 1.5°C*. Intergovernmental Panel on Climate Change.
- Mendoza, V., Katsidoniotaki, E., Florentiades, M., Dot Fraga, J., & Dyachuk, E. (2023, March). Aerodynamic performance of a dual turbine concept characterized by a relatively close distance between rotors. *Wind Energy*, pp. 1-17.
- Microsoft. (2023, March 13). *Microsoft Excel*. Retrieved from <https://www.microsoft.com/en-us/microsoft-365/excel>

- Milan, P., Morales, A., Wächter, M., & Peinke, J. (2014). Wind Energy: A Turbulent, Intermittent Resource. In M. Hölling, J. Peinke, & S. Ivanell, *Wind Energy - Impact of Turbulence* (pp. 73-78). Springer.
- Morthorst, P.-E., & Awerbuch, S. (2009). *The Economics of Wind Energy*. The European Wind Energy Association.
- Multiconsult. (2023). *Mulige nye områder for havvind - Leveranse til Norwegian Offshore Wind*.
- Myhr, A., Bjerkseter, C., Nygaard, T. A., & Ågotnes, A. (2014, June). Levelised cost of energy for offshore floating wind turbines in a life cycle perspective. *Renewable Energy*, pp. 714-728.
- Narakorn, S. (2016). Cabling to connect offshore wind turbines to onshore facilities. In C. Ng, & L. Ran, *Offshore Wind Farms: Technologies, Design and Operation* (pp. 419-440). Woodhead Publishing.
- Normann, S. (2020). Green colonialism in the Nordic context: Exploring Southern Saami representations of wind energy development. *Innovation in community intervention*.
- Norwegian Centre for Climate Services. (2023, March 21). Observations and Weather Statistics. Oslo, Norway.
- Norwegian Environment Agency. (2013). *Scientific basis for an integrated management plan for the north sea and skagerak*.
- NREL. (2016). *The Role of Advancements in Solar Photovoltaic Efficiency, Reliability, and Costs*. National Renewable Energy Laboratory.
- Nunemaker, J., Shields, M., Hammond, R., & Duffy, P. (2020). *ORBIT: Offshore Renewables Balance- of-System and Installation Tool*. National Renewable Energy Laboratory.
- NVE. (2023, April 24). *Kostnader for kraftproduksjon*. Retrieved from NVE: <https://www.nve.no/energi/analyser-og-statistikk/kostnader-for-kraftproduksjon/>
- Nygaard, T. A., & Myhr, A. (2014). *Tension-Leg-Buoy (TLB) Platforms for Offshore Wind Turbines*. Sintef.
- Organisation for Economic Co-operation and Development. (2023, February 15). *OECD*. Retrieved from OECD.stat: <https://stats.oecd.org/>
- Osmundsen, P., Emhjellen-Stendal, M., & Lorentzen, S. (2021). *Project economics of offshore*. Norwegian Research Centre.
- Petersen, C., Plenborg, T., & Kinserdal, F. (2017). *Financial statement analysis*. Fagbokforlaget.
- Petty, T. D., & Chabot, L. G. (1989). *US Patent No. 4850744*.
- Pohjolainen, P., Kukkonen, I., Jokinen, P., Poortinga, W., & Umit, R. (2018). *Public Perceptions on Climate Change and Energy in Europe and Russia*. European Social Survey.
- POOP. (2020). *Definition of the IEA 15-Megawatt Offshore Reference Wind*. National Renewable Energy Laboratory.
- PwC. (2022). *The Risk Premium in the Norwegian Market*. Oslo.
- Ray, M. L., Rogers, A. L., & McGowan, J. G. (2006). *Analysis of wind shear models and trends in different terrains*. University of Massachusetts.
- Reckhaus, N. (2022). *The Ongoing Conflict between Offshore Wind Farms and the Fishing Industry in the North Sea*. University of Groningen.

- Redman, F. Q., & Crepea, A. T. (2006, July). A Basic Primer in Life Cycle Cost Analysis. *INCOSE International Symposium*, pp. 1229-1240.
- Ren, Z., Verma, A. S., Li, Y., Teuwen, J. J., & Jiang, Z. (2021, July). Offshore wind turbine operations and maintenance: A state-of-the-art review. *Renewable and Sustainable Energy Reviews*.
- Rossum, G. v. (2007). Python Programming Language. *USENIX Annual Technical Conference*.
- Ruegg, R. T., & Marshall, H. E. (1990). Internal Rate of Return (IRR). In *Building Economics: Theory and Practice* (pp. 67-78). Springer Science.
- Rystad Energy. (2020, February 5). *Rystad Energy Research and Analysis*. Retrieved from <https://www.rystadenergy.com/>
- Salahshour, S., Ong, M. C., Skaare, B., & Jiang, Z. (2022). A Perspective of Decommissioning Methods for Bottom-Fixed Offshore Wind Turbines. *Offshore and Arctic Engineering* 8.
- Schlichting, H. (1968). *Boundary-Layer Theory (6th Edition)*. New York: McGraw-Hill.
- Scholes, M., & Williams, J. (1977). Estimating betas from nonsynchronous data. *Journal of Financial Economics* 5, pp. 309-327.
- Schwemmer, P., Pederson, R., Haecker, K., Bocher, P., Fort, J., Mercker, M., & Jiguet, F. (2022). Assessing potential conflicts between offshore wind farms and migration patterns of a threatened shorebird species. *Animal conservation*.
- Shafiee, M., Brennan, F., & Espinosa, I. A. (2016, July). A parametric whole life cost model for offshore wind farms. *The International Journal of Life Cycle Assessment*, pp. 961-975.
- Shi, H., Dong, Z., Xiao, N., & Huang, Q. (2021, November). Wind Speed Distributions Used in Wind Energy Assessment: A Review. *Frontiers in Energy Research*.
- Shil, N., & Mahbub, P. (2007, January). Life Cycle Costing: an alternative selection tool. *Journal of Business Research*, pp. 49-68.
- Sintef. (2023, April 26). *Floating offshore wind: Cost reductions will come with deployment*. Retrieved from Sintef: <https://www.sintef.no/en/latest-news/2023/floating-offshore-wind-cost-reductions-will-come-with-deployment/>
- Sohoni, V., Gupta, S. C., & Nema, R. K. (2016). *A Critical Review on Wind Turbine Power Curve Modeling Techniques and Their Applications in Wind Based Energy Systems*. Hindawi Publishing Corporation.
- Statistics Norway. (2023). *Electricity price, grid rent and taxes for households, by contents and year*. Statistics Norway.
- Stehly, T., & Beiter, P. (2019). *2018 Cost of Wind Energy Review*. National Renewable Energy Laboratory.
- Stehly, T., & Duffy, P. (2022). *2021 Cost of Wind Energy Review*. National Renewable Energy Laboratory.
- Stehly, T., Beiter, P., & Duffy, P. (2020). *2019 Cost of Wind Energy Review*. National Renewable Energy Laboratory.
- Svendsen, H., Endegnanew, A., & Torres-Olguin, R. (2013). *Design procedure for inter-array electric design (D2.2)*.

- Swart, C., Gaylard, J. M., & Mulenga Bwalya, M. (2022, October). A Technical and Economic Comparison of Ball Mill Limestone Comminution with a Vertical Roller Mill. *Mineral Processing and Extractive Metallurgy Review*, pp. 275-282.
- The Central Bank of Norway. (2023, April 24). *Statistics*. Retrieved from The Central Bank of Norway: <https://www.norges-bank.no/en/topics/Statistics/norwegian-government-securities/generiske-statsrenter/>
- The Federation of Norwegian Industries. (2022). *Leveransemodeller for havvind – Supply Chain*.
- The Norwegian Ministry of Finance. (1999). LOV-1999-03-26-14. *Norwegian Tax Law*.
- Topham, E., & McMillan, D. (2017). Sustainable decommissioning of an offshore wind farm. *Renewable Energy* 102, pp. 470-480.
- Trinomics. (2020). *Final Report Cost of Energy (LCOE) - Energy costs, taxes and the impact of government interventions on investments*. Trinomics.
- van Binsbergen, J. H., Graham, J. R., & Yang, J. (2010, November). The Cost of Debt. *The Journal of Finance*.
- Vartiainen, E., Masson, G., Breyer, C., Moser, D., & Medina, E. R. (2019, August). Impact of weighted average cost of capital, capital expenditure, and other parameters on future utility-scale PV levelised cost of electricity. *Progress in Photovoltaics: Research and Applications*, pp. 439-453.
- Vrana, V., Kydros, D., Kotzaivazoglou, I., & Pechlivanaki, I. (2023). EU Citizens' Twitter Discussions of the 2022–23 Energy Crisis: A Content and Sentiment Analysis on the Verge of a Daunting Winter. *Sustainability* 15.
- Walday, M., & Kroglund, T. (2020). *The North Sea*. Oslo: Norwegian Institute for Water Research.
- Wang, H., Barthelmie, R. J., Pryor, S. C., & Kim, H. G. (2014, October). A new turbulence model for offshore wind turbine standards. *Wind Energy*, pp. 1587-1604.
- Williams, R., Zhao, F., & Lee, J. (2022). *Global Offshore Wind Report 2022*. Brussel: Global Wind Energy Council.
- Woodward, D. G. (1997, December). Life Cycle Costing - theory, information acquisition and application. *International Journal of Project Management*, pp. 335-344.
- World Wide Fund for Nature. (2011). *The Energy Report: 100% renewable energy by 2050*. Gland: World Wide Fund for Nature.
- Wortman, A. J. (1983). *Introduction to Wind Turbine Engineering*. Boston: Butterworth.
- Yoshimoto, H., Awashima, Y., & Kitakoji, Y. (2013). *Development and construction of floating substation*.
- Yuan, W., Feng, J.-C., Zhang, S., Sun, L., Cai, Y., Yang, Z., & Sheng, S. (2023). Floating wind power in deep-sea area: Life cycle assessment of environmental impacts. *Advances in Applied Energy* 9.
- Zhang, L. (2017, September). The Investment CAPM. *European Financial Management*, pp. 545-603.
- Zizlavsky, O. (2014, April). Net present value approach: method for economic assessment of innovation projects. *Procedia - Social and Behavioral Sciences*, pp. 506-512.

12. Appendices

Appendix A – Sensitivity Analyses Calculation

Appendix B – Effect of Metocean Conditions Calculation

Appendix A

Sensitivity Analysis

Project Lifespan

Component [million \$]	Lifespan (years)									
	5	10	15	18	20	23	25	28	30	35
Array System	69	69	69	69	69	69	69	69	69	69
Export System	111	111	111	111	111	111	111	111	111	111
Substructure	1276	1276	1276	1276	1276	1276	1276	1276	1276	1276
Mooring System	186	186	186	186	186	186	186	186	186	186
Offshore Substation	205	205	205	205	205	205	205	205	205	205
Array System Installation	20	20	20	20	20	20	20	20	20	20
Export System Installation	196	196	196	196	196	196	196	196	196	196
Substructure Installation	57	57	57	57	57	57	57	57	57	57
Mooring System Installation	32	32	32	32	32	32	32	32	32	32
Offshore Substation Installation	5	5	5	5	5	5	5	5	5	5
Turbine	759	759	759	759	759	759	759	759	759	759
Soft	653	653	653	653	653	653	653	653	653	653
Project	204	204	204	204	204	204	204	204	204	204
Sum	3773	3773	3773	3773	3773	3773	3773	3773	3773	3773
OpEx (annual)	89	89	89	89	89	89	89	89	89	89
Annual energy production [MWh]	3 465 675	3 465 675	3 465 675	3 465 675	3 465 675	3 465 675	3 465 675	3 465 675	3 465 675	3 465 675
FCR	22.93 %	12.78 %	9.46 %	8.38 %	7.84 %	7.23 %	6.90 %	6.52 %	6.31 %	5.90 %
LCOE [\$/MWh]	275.09	164.67	128.50	116.70	110.90	104.20	100.69	96.47	94.18	89.77

Wind Farm Scale

Component [million \$]	Number of Turbines									
	5	10	20	35	50	60	75	100	125	150
Array System	5	11	23	45	69	88	120	182	255	340
Export System	19	36	55	74	111	130	147	203	258	294
Substructure	127	255	510	892	1276	1531	1913	2550	3188	3825
Mooring System	19	36	75	130	186	222	278	371	463	557
Offshore Substation	43	57	87	160	205	231	307	373	472	575
Array System Installation	3	4	8	14	20	24	31	42	54	68
Export System Installation	31	51	86	140	196	232	285	377	468	558
Substructure Installation	8	14	24	41	57	68	85	112	139	167
Mooring System Installation	4	7	14	23	32	39	49	65	81	96
Offshore Substation Installation	4	4	4	5	5	5	8	8	11	12
Turbine	76	152	304	531	759	911	1139	1518	1898	2277
Soft	65	131	262	458	653	783	980	1307	1632	1959
Project	204	204	204	204	204	204	204	204	204	204
Sum	608	963	1 656	2 716	3 773	4 467	5 545	7 311	9 124	10 932
OpEx (annual)	8.85	17.7	35.4	61.95	88.5	106.2	132.75	177	221.25	265.5
Annual energy production [MWh]	346 568	693 135	1 386 270	2 425 973	3 465 675	4 158 810	5 198 513	6 931 350	8 664 188	10 397 025
FCR	6.90 %	6.90 %	6.90 %	6.90 %	6.90 %	6.90 %	6.90 %	6.90 %	6.90 %	6.90 %
LCOE [\$ /MWh]	146.68	121.42	108.00	102.85	100.69	99.70	99.18	98.36	98.24	98.13

Turbine Power Rating

Component [million \$]	Turbine Power Rating		
	6MW	12MW	15MW
Array System	41	59	69
Export System	55	92	111
Substructure	783	1095	1276
Mooring System	132	186	186
Offshore Substation	87	172	205
Array System Installation	18	19	20
Export System Installation	86	159	196
Substructure Installation	57	57	57
Mooring System Installation	32	32	32
Offshore Substation Installation	4	5	5
Turbine	218	581	759
Soft	262	522	653
Project	204	204	204
Sum	1978	3183	3773
OPEX [yearly]	35.4	70.8	88.5
Annual energy production [MWh]	1 386 270	2 772 540	3 465 675
FCR	6.9 %	6.9 %	6.9 %
LCOE [\$/MWh]	124.1	104.80	100.70

Project Discount Rate

Component [million \$]	Weighted Average Cost of Capital									
	1 %	2 %	3 %	4 %	5 %	6 %	7 %	8 %	9 %	10 %
Array System	69	69	69	69	69	69	69	69	69	69
Export System	111	111	111	111	111	111	111	111	111	111
Substructure	1276	1276	1276	1276	1276	1276	1276	1276	1276	1276
Mooring System	186	186	186	186	186	186	186	186	186	186
Offshore Substation	205	205	205	205	205	205	205	205	205	205
Array System Installation	20	20	20	20	20	20	20	20	20	20
Export System Installation	196	196	196	196	196	196	196	196	196	196
Substructure Installation	57	57	57	57	57	57	57	57	57	57
Mooring System Installation	32	32	32	32	32	32	32	32	32	32
Offshore Substation Installation	5	5	5	5	5	5	5	5	5	5
Turbine	759	759	759	759	759	759	759	759	759	759
Soft	653	653	653	653	653	653	653	653	653	653
Project	204	204	204	204	204	204	204	204	204	204
Sum	3773	3773	3773	3773	3773	3773	3773	3773	3773	3773
OpEx (annual)	88.5	88.5	88.5	88.5	88.5	88.5	88.5	88.5	88.5	88.5
Annual energy production [MWh]	3 465 675	3 465 675	3 465 675	3 465 675	3 465 675	3 465 675	3 465 675	3 465 675	3 465 675	3 465 675
FCR	4.54 %	5.12 %	5.74 %	6.40 %	7.10 %	7.82 %	8.58 %	9.37 %	10.18 %	11.02 %
LCOE [\$ /MWh]	74.96	81.29	88.05	95.22	102.77	110.69	118.95	127.51	136.36	145.46

Operational Expenditure

Component [million \$]	Operational Expenditure									
	-50.00 %	-40.00 %	-30.00 %	-20.00 %	-10.00 %	10.00 %	20.00 %	30.00 %	40.00 %	50.00 %
Array System	69	69	69	69	69	69	69	69	69	69
Export System	111	111	111	111	111	111	111	111	111	111
Substructure	1276	1276	1276	1276	1276	1276	1276	1276	1276	1276
Mooring System	186	186	186	186	186	186	186	186	186	186
Offshore Substation	205	205	205	205	205	205	205	205	205	205
Array System Installation	20	20	20	20	20	20	20	20	20	20
Export System Installation	196	196	196	196	196	196	196	196	196	196
Substructure Installation	57	57	57	57	57	57	57	57	57	57
Mooring System Installation	32	32	32	32	32	32	32	32	32	32
Offshore Substation Installation	5	5	5	5	5	5	5	5	5	5
Turbine	759	759	759	759	759	759	759	759	759	759
Soft	653	653	653	653	653	653	653	653	653	653
Project	204	204	204	204	204	204	204	204	204	204
Sum	3773	3773	3773	3773	3773	3773	3773	3773	3773	3773
OPEX (annual)	44.25	53.1	61.95	70.8	79.65	97.35	106.2	115.05	123.9	132.75
Annual energy production [MWh]	3 465 675	3 465 675	3 465 675	3 465 675	3 465 675	3 465 675	3 465 675	3 465 675	3 465 675	3 465 675
FCR	6.90 %	6.90 %	6.90 %	6.90 %	6.90 %	6.90 %	6.90 %	6.90 %	6.90 %	6.90 %
LCOE [\$ /MWh]	87.93	90.48	93.03	95.59	98.14	103.25	105.80	108.36	110.91	113.46

Appendix B

Effect of Metocean Conditions

Capacity Factor

Component [million \$]	Capacity Factor										
	20 %	25 %	30 %	35 %	40 %	45 %	50 %	55 %	60 %	65 %	70 %
Array System	69	69	69	69	69	69	69	69	69	69	69
Export System	111	111	111	111	111	111	111	111	111	111	111
Substructure	1276	1276	1276	1276	1276	1276	1276	1276	1276	1276	1276
Mooring System	186	186	186	186	186	186	186	186	186	186	186
Offshore Substation	205	205	205	205	205	205	205	205	205	205	205
Array System Installation	20	20	20	20	20	20	20	20	20	20	20
Export System Installation	196	196	196	196	196	196	196	196	196	196	196
Substructure Installation	57	57	57	57	57	57	57	57	57	57	57
Mooring System Installation	32	32	32	32	32	32	32	32	32	32	32
Offshore Substation Installation	5	5	5	5	5	5	5	5	5	5	5
Turbine	759	759	759	759	759	759	759	759	759	759	759
Soft	653	653	653	653	653	653	653	653	653	653	653
Project	204	204	204	204	204	204	204	204	204	204	204
Sum	3 773	3 773	3 773	3 773	3 773	3 773	3 773	3 773	3 773	3 773	3 773
OpEx (annual)	88.5	88.5	88.5	88.5	88.5	88.5	88.5	88.5	88.5	88.5	88.5
Annual energy production [MWh]	1 314 000	1 642 500	1 971 000	2 299 500	2 628 000	2 956 500	3 285 000	3 613 500	3 942 000	4 270 500	4 599 000
FCR	6.90 %	6.90 %	6.90 %	6.90 %	6.90 %	6.90 %	6.90 %	6.90 %	6.90 %	6.90 %	6.90 %
LCOE [\$/MWh]	265.58	212.47	177.06	151.76	132.79	118.04	106.23	96.58	88.53	81.72	75.88

Water Depth

Components [million \$]	Water Depth [m]										
	50	100	150	200	250	300	350	400	500	600	700
Array System	59	61	62	65	66	69	70	73	76	80	84
Export System	111	111	111	111	111	111	111	111	111	111	111
Substructure	1276	1276	1276	1276	1276	1276	1276	1276	1276	1276	1276
Mooring System	82	99	118	137	156	175	196	215	257	299	342
Offshore Substation	205	205	205	205	205	205	205	205	205	205	205
Array System Installation	19	19	19	19	19	20	20	20	20	20	22
Export System Installation	196	196	196	196	196	196	196	196	196	196	196
Substructure Installation	57	57	57	57	57	57	57	57	57	57	57
Mooring System Installation	28	30	30	31	31	32	34	34	36	38	39
Offshore Substation Installation	5	5	5	5	5	5	5	5	5	7	7
Turbine	759	759	759	759	759	759	759	759	759	759	759
Soft	653	653	653	653	653	653	653	653	653	653	653
Project	204	204	204	204	204	204	204	204	204	204	204
Sum	3654	3674	3694	3717	3738	3762	3786	3807	3855	3903	3953
OpEx (annual)	88.5	88.5	88.5	88.5	88.5	88.5	88.5	88.5	88.5	88.5	88.5
Annual energy production [MWh]	3 465 675	3 465 675	3 465 675	3 465 675	3 465 675	3 465 675	3 465 675	3 465 675	3 465 675	3 465 675	3 465 675
FCR	6.90 %	6.90 %	6.90 %	6.90 %	6.90 %	6.90 %	6.90 %	6.90 %	6.90 %	6.90 %	6.90 %
LCOE [\$/MWh]	98.32	98.72	99.13	99.59	100.00	100.49	100.96	101.39	102.33	103.29	104.29

Distance to Shore

Component [million \$]	Distance to Shore [km]												
	5	10	20	40	60	80	100	125	150	175	200	300	400
Array System	69	69	69	69	69	69	69	69	69	69	69	69	69
Export System	14	22	38	70	103	135	167	208	248	289	329	491	653
Substructure	1276	1276	1276	1276	1276	1276	1276	1276	1276	1276	1276	1276	1276
Mooring System	186	186	186	186	186	186	186	186	186	186	186	186	186
Offshore Substation	205	205	205	205	205	205	205	205	205	205	205	205	205
Array System Installation	19	19	19	20	20	20	20	20	20	20	20	22	23
Export System Installation	182	184	186	190	194	204	208	213	219	230	236	266	308
Substructure Installation	53	53	54	55	57	57	58	63	69	76	81	105	130
Mooring System Installation	31	32	32	32	32	32	34	34	34	34	35	36	38
Offshore Substation Installation	5	5	5	5	5	5	7	7	7	7	7	8	9
Turbine Installation	0	0	0	0	0	0	0	0	0	0	0	0	0
Turbine	759	759	759	759	759	759	759	759	759	759	759	759	759
Soft	653	653	653	653	653	653	653	653	653	653	653	653	653
Project	204	204	204	204	204	204	204	204	204	204	204	204	204
Sum	3655	3666	3686	3725	3763	3805	3845	3897	3948	4006	4060	4280	4512
OpEx (annual)	88.5	88.5	88.5	88.5	88.5	88.5	88.5	88.5	88.5	88.5	88.5	88.5	88.5
Annual energy production [MWh]	3 465 675	3 465 675	3 465 675	3 465 675	3 465 675	3 465 675	3 465 675	3 465 675	3 465 675	3 465 675	3 465 675	3 465 675	3 465 675
FCR	6.90 %	6.90 %	6.90 %	6.90 %	6.90 %	6.90 %	6.90 %	6.90 %	6.90 %	6.90 %	6.90 %	6.90 %	6.90 %
LCOE [\$/MWh]	98.36	98.57	98.97	99.75	100.51	101.34	102.15	103.17	104.19	105.35	106.42	110.81	115.43